

AD-A171 483

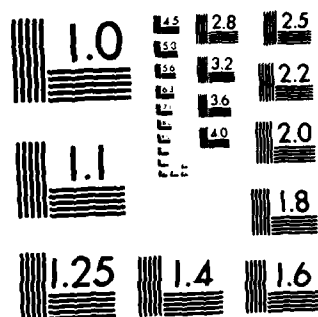
MODELS OF CEREBRAL SYSTEM MECHANICS(U) TECHNION -
ISRAEL INST OF TECH HAIFA S SOREK ET AL 28 JUL 86
SCIENTIFIC-2 BOARD-TR-86-07 AFOSR-85-0233

1/2

UNCLASSIFIED

F/G 6/16

NL



XEROCOPY RESOLUTION TEST CHART
NATIONAL BUREAU OF STANDARDS-1963-A

2

GRANT AFOSR-85-0233

AD-A171 483

MODELS OF CEREBRAL SYSTEM MECHANICS

S. Sorek*, J. Bear**, Z. Karni+, M. Feinsod***

Technion - Israel Institute of Technology, Haifa, 32000, Israel

*Dept. of Biomedical Engineering

**Dept. of Civil Engineering

***Dept. of Neurosurgery

+Deceased

July 1986

SCIENTIFIC REPORT NO. 2

DTIC
ELECTE
SEP 02 1986
S E

Approved for public release, distribution unlimited

Prepared for

UNITED STATES AIR FORCE, AIR FORCE OFFICE OF SCIENTIFIC RESEARCH

AND

EUROPEAN OFFICE OF AEROSPACE RESEARCH AND DEVELOPMENT, London, England

DTIC FILE COPY

86 8 29 018

UNCLASSIFIED

SECURITY CLASSIFICATION OF THIS PAGE (When Data Entered)

REPORT DOCUMENTATION PAGE		READ INSTRUCTIONS BEFORE COMPLETING FORM
1. REPORT NUMBER 2	2. GOVT ACCESSION NO. DA171483	3. RECIPIENT'S CATALOG NUMBER
4. TITLE (and Subtitle) MODELS OF CEREBRAL SYSTEM MECHANICS		5. TYPE OF REPORT & PERIOD COVERED FINAL REP. SCIENTIFIC REP. NO 2
7. AUTHOR(s) S. SOREK, J. BEAR, Z. KARNI, M. FEINSOD		6. PERFORMING ORG. REPORT NUMBER
9. PERFORMING ORGANIZATION NAME AND ADDRESS TECHNION-RESEARCH AND DEVELOPMENT FOUNDATION		8. CONTRACT OR GRANT NUMBER(s) AFOSR-85-0233
11. CONTROLLING OFFICE NAME AND ADDRESS US AIR FORCE OFFICE OF SCIENTIFIC RES.		10. PROGRAM ELEMENT, PROJECT, TASK AREA & WORK UNIT NUMBERS
AND EUROPEAN OFFICE OF AEROSPACE RES. AND DEVELOPMENT		12. REPORT DATE JULY 20, 1986
		13. NUMBER OF PAGES 118
		15. SECURITY CLASS. (of this report) UNCLASSIFIED
		15a. DECLASSIFICATION/DOWNGRADING SCHEDULE
16. DISTRIBUTION STATEMENT (of this Report) APPROVED FOR PUBLIC RELEASE; DISTRIBUTION UNLIMITED		
17. DISTRIBUTION STATEMENT (of the abstract entered in Block 20, if different from Report) AS IN 16.		
18. SUPPLEMENTARY NOTES		
19. KEY WORDS (Continue on reverse side if necessary and identify by block number) Intracranial Fluid Dynamics, Compentmental Flow Model, Kinetics Cerebrovascular System, Brain Mechanics		
20. ABSTRACT (Continue on reverse side if necessary and identify by block number) A lumped parameter, seven-compartmental model for the crebrovascular fluid system is constructed and solved for the quasi-steady state flow. The model predicts the pressure waves in the various compartments of the intracranial region in response to changes in the arterial pressure.		

DD FORM 1 JAN 73 1473

EDITION OF 1 NOV 65 IS OBSOLETE

SECURITY CLASSIFICATION OF THIS PAGE (When Data Entered)

GRANT AFOSR-85-0233

MODELS OF CEREBRAL SYSTEM MECHANICS

S. Sorek*, J. Bear**, Z. Karni+, M. Feinsod***

Technion - Israel Institute of Technology, Haifa, 32000, Israel

*Dept. of Biomedical Engineering

**Dept. of Civil Engineering

***Dept. of Neurosurgery

+Deceased



July 1986

SCIENTIFIC REPORT NO. 2

DTIC	
COPY	
INSPECTED	
1	
X	
By _____	
Distribution _____	
Approved _____	
Date _____	
Dist	Special
A-1	

Approved for public release, distribution unlimited

Prepared for

UNITED STATES AIR FORCE, AIR FORCE OFFICE OF SCIENTIFIC RESEARCH

AND

EUROPEAN OFFICE OF AEROSPACE RESEARCH AND DEVELOPMENT, London, England

TABLE OF CONTENTS

	page
1. Preface-----	3
2. A Quasi-Steady State Compartmental Model of Intracranial Fluid Dynamics.-----	6
2.1: Abstract-----	6
2.2: Introduction-----	7
2.3: The compartmental flow equations-----	9
2.4: The seven-compartmental model with constant resistances and compliances-----	11
2.5: Parameter identification of the seven compartmental systems-----	12
2.5.1: The steady state-----	16
2.5.2: The non-steady state-----	17
2.6. The quasi-steady state pressure waves-----	19
2.7. References-----	24
3. A Non-Steady Compartmental Flow Model of the Cerebrovascular System.-----	30
3.1: Abstract-----	30
3.2: Introduction-----	31
3.3: Compartmental model equations-----	35
3.4: Evaluation of the fluidity matrix-----	39
3.4.1: The steady state-----	40
3.4.2: Non steady flow-----	46
3.5: Evaluation of the compliance matrix-----	46
3.6: Evaluation of the compartmental pulse wave-----	49
3.7: References-----	51

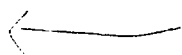
	page
4. Resistances and Compliances of a Compartmental Model of the Cerebrovascular System.-----	56
4.1: Abstract-----	57
4.2: Introduction-----	58
4.3: The compartmental balance equations-----	60
4.4: Parameter estimation-----	62
4.5: Evaluation of model resistances and compliances-----	63
4.6: References-----	69
5. Intracranial Compartmental Pulse Wave Simulation.-----	73
5.1: Abstract-----	73
5.2: Introduction-----	74
5.3: Compartmental pulse wave forms-----	76
5.4: Examples-----	79
5.4.1: Example 1-----	79
5.4.2: Example 2-----	80
5.4.3: Example 3-----	80
5.5: Summary-----	80
5.6: References-----	82
6. Can N.P.H. be caused by Cerebral Small Vessel Disease? A new look based on mathematical model.-----	89
6.1: Abstract-----	89
6.2: Introduction-----	90
6.3: Case report-----	91
6.4: Discussion-----	93
6.5: References-----	98

	page
7. A Simple Continuum Model of Brain Tissue Deformation--	101
7.1: Abstract-----	101
7.2: Introduction-----	102
7.3: Assumptions-----	104
7.4: Force balance equation-----	105
7.5: Implementation-----	110
7.6: Conclusion-----	110
7.7: References-----	112

PREFACE

A model of a system is a simplified version of the real system. The simplification is done by introducing a set of assumptions that express our understanding of the system's behavior. In the process of simplification, we omit non-dominant effects, leaving the main features of the system. The objective of simplification is to obtain a set that can be solved by available tools and still maintain the main characteristics of the real system.

The model is a tool that provides forecasts of the response of the real system to various excitations. Thus it is essential that the model retains those features that are the subject of investigations.

This volume contains 7 papers dealing with models of brain mechanics. The objective of the models is to provide a tool for simulating the mechanical behavior of the cerebral system, as manifested by pressure, velocity, stress and strain variations, in response to changes in input pressures and fluxes. 

At this stage, the models deal only with changes in fluxes pressures, stresses and strains. At a later stage of investigations, the transport, spreading and interactions with the tissue material of chemicals carried with the brain fluids, will be investigated and reported.

In principle, our objective is to develop continuum models of brain mechanics. Such models will provide information on the behavior at every point in space and time of the brain domain, in response to changes in the normal behavior in various parts of the brain (e.g., vessel occlusions). However, at this stage

reported here, only one simplified model that investigates deformation and stress in response to pressure variations, is of the continuum type. All other models are of the multicompartment type.

In a multicompartment model, the entire domain, here the portion of space occupied by the brain, is visualized as comprised of a number of interacting compartments. Each compartment represents the lumped behavior of a certain part of the brain that has distinct features. Fluids move from one compartment to the next under, pressure gradients. In the present investigations, a seven-compartment model was employed to simulate the behavior of the various parts of the brain.

Every model contains a number of parameters that express the excitation response characteristics of elements of the investigated system. In order to make use of a model in specific cases, the values of these parameters must be known. The only way to determine these parameters is to make use of observations in the real cerebral system, and compare them with values predicted by the model. The process of determining model parameters is referred to as the inverse problem.

Accordingly, one of the papers describes how the basic parameters of the model are estimated.

Typically, pressures and fluxes in the brain vary in a cyclic manner, occasionally, especially under pathologic conditions, transient changes may take place. Accordingly, the models presented in the various papers, simulate non-steady and transient flow conditions. In order to enable such conditions, compliances had to be introduced between adjacent compartments

(in addition to resistances that control the pressure flux relations).

Results of model predictions were compared with actual observed data, whenever available.

The results of the comparisons were satisfactory and encouraging.

A QUASI-STEADY STATE COMPARTMENTAL MODEL
OF INTRACRANIAL FLUID DYNAMICS

Z. KARNI^{*}

J. BEAR

S. SOREK

Z. PINCZEWSKI^{**}

*Departments of Bio-Medical Engineering,
and Civil Engineering, Technion -
Israel Institute of Technology,
Haifa 32000, Israel*

*Department of Chemical Engineering,
The University of New South Wales,
Kensington, NSW 2033, Australia*

Abstract - A lumped parameter, seven-compartmental model for the cerebrovascular fluid system is constructed and solved for the quasi-steady state flow. The model predicts the pressure waves in the various compartments of the intracranial region in response to changes in the arterial pressure.

Keywords - Brain tissue, Compartmental model, Intracranial pressure, Pulse wave

^{**} In the spring of 1983, a Visiting Scholar at the Bio-Medical Engineering Department, Technion - Israel Institute of Technology, under the Henry Goldberg Chair.

^{*} Deceased.

INTRODUCTION

Ever since the cerebrovascular fluid system was modelled, the relatively simple compartmental representation has been favoured. MONRO, the younger (1783), the pioneer of intracranial mechanics, characterized the physical forces in the intracranial cavity assuming incompressibility of the fluid; nearly incompressibility of the brain tissue, and zero motion of the boundaries. The intradural space was regarded as bi-compartmental - brain and blood, so that a change in either compartment had to be compensated for by the other.

KELLIE (1824) modified this hypothesis by assuming three instead of two compartments, namely arteries, veins and brain tissue. About the brain tissue, Kellie said: "The brain itself, little compressible is contained within a firm and unyielding case of bone which it exactly fills If these premises be true, it does not then appear very conceivable how any portion of the circulating fluid can ever be withdrawn from within the cranium, without its place being simultaneously occupied by some equivalent or how anything new or exuberant can be intruded, without an equivalent displacement" (*loc. cit.*, p. 102).

The Monro-Kellie doctrine of almost absolute rigidity, prevailed into this century and was only relaxed in stages. The number of fluid compartments was increased to six: artery (*A*), capillary (*C*), venous (*V*), venous sinus (*S*), jugular bulb (*J*) and cerebrospinal fluid (*F*) (AGARWAL, 1971). Yet the fluid itself remained incompressible. More recent approaches relaxed the latter assumption and the fluid was taken as linearly compressible, namely the change in pressure and the change in volume are proportional to each other, and the coefficient of proportionality, the bulk modulus or its inverse - the *compliance*, are constants.

The thick layer of the brain tissue between the ventricles and the sub-arachnoidal space has also undergone various stages of modelling. The buoyancy theory (LIVINGSTON, 1965) regarded the tissue phase submerged in the ideal, incompressible (Pascalian) CSF fluid to which Archimedes law applies. The tissue itself was taken as single-phase and incompressible.

When the incompressibility assumption was abandoned, it paved way to compressible representations for the brain tissue. Numerous experimental studies have been conducted in the past four decades in that direction. The results pointed at the inelasticity of the tissue or, alternatively, the non-linearity of the compliance (RYDER *et al.*, 1953; MILLER and GARIBI, 1972; LUNDBERG *et al.*, 1974; MARMAROU *et al.*, 1975; MILLER, 1975; HAKIM *et al.*, 1976; LEWER ALLEN and BUNT, 1977; GRIFFITH *et al.*, 1978; BRUCE, 1978; CHOPP and PORTNOY, 1980). To overcome the "non-linearity" of a single coefficient, more complex models of single-phased, multi-parameter viscoelastic materials were introduced such as the one consisting of four viscoelastic coefficients known as the "three-parameter solid", coupled dynamically with another elastic element (PAMIDI and ADVANI, 1978).

In the literature on the mechanics of head impacts, the skull was idealized to be a rigid sphere with an opening that simulated the foramen magnum, and the spinal dura mater was idealized as a cylindrical membrane fitted to the foramen magnum (LIU, 1978). The intradural content of the central nervous system (CNS) fluid-filled continuum was regarded by some as a single-phase incompressible fluid in a two-compartment (skull and spinal dura mater) structure; or else as a single-phase compressible *elastic* fluid (later, also a *viscoelastic* fluid) possessing a single averaged "elastance" (strictly, a bulk modulus - inverse of compliance) along with a shear modulus (POLLACK and BOSHES, 1936; OMMAYA and HIRSCH, 1971; LÖFGREN and ZWETNOW, 1973; GOLDSMITH, 1972; MARMAROU, 1973; KING and CHOU, 1976).

Here, we extend the discussion to the n -compartmental model and present the methods how to solve it for the general non-steady state flow with constant resistances and compliances. An explicit numerical solution is given for the case $n=7$. It is also shown that for the slow mode, compartmental pressure waves, solutions for the more simplified quasi-steady state flow are already in good agreement with some clinical measurements.

1. The Compartmental Flow Equation

By its nature, the compartmental modelling of any hydraulic system is a lumped-parameter modelling. Thus, the resistance to flow due to a particular vessel type is lumped at the outflow of the compartment. Likewise, the integrated change in volume of each compartment is representable as an overall compartmental property. Furthermore, if there is a production or a drainage of fluid in a compartment, the source-sink function is attributed to the entire compartment. Finally, the functional interaction between the components of a lumped parameter model is assumed to be at the interface between adjacent compartments.

The general compartmental flow problem is that of the *non-steady* state. Here, all parameters are functions of time and the deformability of the compartments is taken into account. Fluxes are composed of two terms: (i) Flow rate of fluid as result of pressure difference (transmural) between two compartments, expressible as

$$Q' = Z\Delta P = \frac{\Delta P}{R} \quad (P = \text{pressure, } R = \text{resistance,} \quad (1) \\ Z = \text{fluidance})$$

(ii) Flow rate from the deformational volume change which, in turn, relates to the change in pressure by a functional relation of the type

$$Q'' = \frac{dV}{dt} = C \frac{dP}{dt} \quad (C = \text{compliance}) \quad (2)$$

The governing equations for the compartmental flow problem are the balances of mass and of linear momentum. We do not consider high-speed turbulent motions (vanishing of the angular momentum) and the system is assumed isothermal and thermodynamically stable (identical vanishing of the energy balance). Under these assumptions, the mass and linear-momentum balance conditions for the n -compartmental flow model are grouped into a single matrix equation of the type (KARNI *et al.*, 1985)

$$\underline{C} \frac{d\underline{P}}{dt} + \underline{Z} \underline{P} = \underline{Q} + \underline{S} \quad (3)$$

Here, \underline{P} is the n -column pressure vector, \underline{Z} is the symmetric $n \times n$ fluidity (inverse of resistivity) matrix, \underline{C} is the symmetric $n \times n$ compliance matrix, \underline{Q} is the n -column flux vector, and \underline{S} - the n -column source/sink vector which either adds or drains out fluid from the compartmental domains. If $\underline{S} = 0$, the system is *conserved*, and equation (3) reduces to the conservation of mass, also known as the continuity equation. The numerical solution presented here is for a conservative system. Solutions for non-conservative systems are discussed elsewhere (SOREK *et al.*, 1985).

In general, equation (3) is an inhomogeneous, ordinary differential matrix equation of the first rank with respect to time (t). It is also non-linear, since, if homeostasis is taken into account, the sensory and endocrinological biofeedback control mechanisms turn the coefficient matrices \underline{C} and \underline{Z} functions of the dependent vector \underline{P} and of the independent scalar t . Thus, in the general case,

$$\underline{\underline{C}} = \underline{\underline{C}} [\underline{P}(t), t] ; \quad \underline{\underline{Z}} = \underline{\underline{Z}} [\underline{P}(t), t]$$

There are, however, some passive cases that can be approximated by the linear problem, i.e. when $\underline{\underline{C}}$ and $\underline{\underline{Z}}$ assume constant values. Moreover, even if the problem is non-linear we have to pass through the linear case and proceed to the non-linear case by applying incremental perturbation techniques. The rest of the discussion, therefore, focuses on the linear case.

The procedure for solving the linear problem is as follows:

- (a) Given information about fluxes and pressures, equation (3) can be solved to yield the resistances and compliances. This is often referred to as *parameter identification or model calibration*.
- (b) When the elements of $\underline{\underline{Z}}$ and $\underline{\underline{C}}$ have been evaluated, the pressure waves $\underline{P} = \underline{P}(t)$ or the fluxes $\underline{Q} = \underline{Q}(t)$ can be determined.
- (c) With the pressures and the compliances solved, information about the volume changes and, under certain assumptions, also of the compartmental displacements can be obtained.

We shall next apply this to the case of a seven-compartmental ($n=7$) model that represents the intracranial cerebrovascular fluid system.

2. The Seven-Compartmental Model with Constant Resistances and Compliances

The numerical example that we chose to calculate is based on AGARWAL'S six-compartmental model (*loc. cit.*, 1971), for which no numerical results were given, with the addition of the brain tissue (B) compartment; seven altogether (Fig. 1).

Fig. 1

The lumped resistances are: between the artery and capillary compartments (R_{AC}), the capillary and cerebrospinal fluid compartments (R_{CF}), the capillary and brain tissue compartments (R_{CB}), the capillary and vein compartments (R_{CV}), the brain tissue and vein compartments (R_{BV}), the cerebrospinal fluid and brain tissue compartments (R_{FB}), the vein and venous sinus compartments (R_{VS}), the cerebrospinal fluid and the venous sinus compartments (R_{FS}), and between the venous sinus and the jugular bulb compartments (R_{VJ}); altogether nine resistances. In the figure, the capillary compartment, likewise the R_{AC} resistance, are divided into: the choroid plexuses - those tufts of small capillary vessels inside each of the four ventricles, and the capillary system outside the ventricles. However, in the equations to follow, only the combinations in parallel of the resistances, namely $(R'_{AC})^{-1} + (R''_{AC})^{-1} = (R_{AC})^{-1}$ and $(R'_{CV})^{-1} + (R''_{CV})^{-1} = (R_{CV})^{-1}$ appear, so that the combined lumped resistances R_{AC} and R_{CV} , into and out of the capillaries, suffice for our purposes.

The resistances R_{CB} , R_{CF} and R_{FB} are identified as the lumped blood-brain barrier; the lumped blood-cerebrospinal fluid barrier, and the lumped cerebrospinal fluid-brain barrier, respectively. Quantitative studies of these barriers indicate that on the gross compartmental level they assume large values, yet they cannot be regarded infinite (DAVSON, 1960).

The compliance elements C_{ij} indicate that an increase in volume of one of the compartments equals the volume of the "cup" formed by the deformed membrane. This volume, in turn, equals the volume displaced from the neighbouring compartments, all within the rigid container of the skull bones.

First, a compliance element C_{AB} is introduced between the artery and the brain tissue compartments. This element represents the overall pulsatory effect of the arteries on the brain tissue. Next, a compliance element C_{CF} is inserted between the choroid plexuses and the cerebrospinal fluid compartment. The CSF system and the brain tissue share common boundaries - at the ventricles and along the subarachnoidal space - which are deformable, so that a compliance element C_{FB} is introduced between them. Finally, as result of the sharp drop in pressure along the cardiovascular passage, from the artery to the jugular compartments, additional compliance elements C_{BV} and C_{FS} are added between the brain tissue and the venous compartments, and between the cerebrospinal fluid and the venous sinus compartments, respectively (there is no compliance element between the sinuses and the large jugular veins because the pressure there is very small). Altogether, the seven-compartmental model for the cerebrospinal fluid system described above assumes five compliance elements of the type C_{ij} .

The mechanical properties of 'resistances' and 'compliances' are "symmetric" with respect to the interchange of direction between one compartment and its neighbour. This is the outcome of the law of action and reaction. In formulae

$$R_{AC} = R_{CA} \quad R_{CF} = R_{FC} \quad etc.$$

$$C_{AB} = C_{BA} \quad C_{CF} = C_{FC} \quad etc.$$

The chart of mean pressure variations along the cerebrovascular fluid conforms with the pressure profile of the cardiovascular system cited in the

literature (e.g., GUYTON, 1969, Ch. 14). In the arteries, the average pressure between systole and diastole is 100 mm Hg. It drops to 30 mm Hg in the capillaries including the choroid plexuses; 10 mm Hg in the CSF system, 9.5 mm Hg in the brain tissue, 9 mm Hg in the venous system, 8 mm Hg in the sinuses and 1-2 mm in the large veins - jugular and spinal - leading to the vena cava (Fig. 1). Volumes of the compartments are also recorded in the figure as much as they are documented in the literature.

For the flux matrix \underline{Q} , we assume the following:

The heart pumps blood into the artery compartment (arteries and arterioles) at the rate of approximately 750 ml/min. The larger amount of blood flows into the capillaries branching outside the cerebral ventricles, while a small amount reaches the choroid plexuses which are the capillary zones inside the ventricles. No definite information is available about the partition ratio between the flows through the capillary section and through the choroid plexuses. In our scheme, the ratio of $\lambda=250:1$ has been postulated, namely 747 ml/min of blood being carried into the capillaries against 3 ml/min entering the choroid plexuses in all the four ventricles. However, as mentioned before, only the compound resistances R_{AC} and R_{CV} ; so also the fluxes Q_C , Q_V , enter the calculations and no use is made of the ratio λ later on.

The ultrafiltration of the blood at the choroid plexuses diverts a flow of 0.3 ml/min to the CSF compartment. This is a figure extensively quoted in the literature. From the capillaries, blood is recollected into the venous system (venules and veins). A minute fraction escapes as interstitial fluid to the extracellular region of the brain tissue but because of the blood-brain barrier, it is hardly measurable in a tenth of ml/min. It is therefore marked as 0.0 ml/min in Figure 1, likewise with the flow from the cerebrospinal fluid

compartment to the brain tissue compartment. The venous compartment also regains the $3.0 - 0.3 = 2.7$ ml/min of blood which does not escape from the choroid plexuses into the CSF system, thus totalling, with the flow from the CSF system into the brain tissue, 749.7 ml/min that proceed to the venous sinus compartment. The drainage of the CSF into the sinuses adds the 0.3 ml/min which closes the loop flow of the CSF from the choroid plexuses to the sinuses. The rejoining of the CSF drives the original flow of 750.0 ml/min back to the heart through the jugular and the spinal veins. This scheme implicitly assumes no gains or losses in the flow from one compartment to the other, namely the source/sink matrix $\underline{S} = 0$.

3. Parameter Identification of the Seven-Compartmental Model

Given the above data, the explicit expressions for the fluidity \underline{Z} matrix and the compliance \underline{C} matrix are:

$$\underline{Z} = [z_{i,j}] = \left[\frac{1}{R_{i,j}} \right] = \begin{bmatrix} z_{AC} & 0 & -z_{AC} & 0 & 0 & 0 \\ 0 & [z_{CR} + z_{FR} + z_{BV}] & -z_{CB} & -z_{FB} & -z_{BV} & 0 \\ -z_{AC} & -z_{CB} & [z_{AC} + z_{CF} + z_{CB} + z_{CF}] & -z_{CF} & -z_{CV} & 0 \\ 0 & -z_{FB} & -z_{CF} & [z_{CF} + z_{FS} + z_{FB}] & 0 & -z_{FS} \\ 0 & -z_{BV} & -z_{CV} & 0 & [z_{CV} + z_{VS} + z_{BV}] & -z_{VS} \\ 0 & 0 & 0 & -z_{FS} & -z_{VS} & [z_{VS} + z_{FS}] \end{bmatrix} \quad (4)$$

$$\underline{\underline{C}} = [C_{ij}] = [C_{ji}] = \begin{bmatrix} C_{AB} & -C_{AB} & 0 & 0 & 0 & 0 \\ -C_{AB} & [C_{AB} + C_{FB} + C_{BV}] & 0 & -C_{FB} & -C_{BV} & 0 \\ 0 & 0 & C_{CF} & -C_{CF} & 0 & 0 \\ 0 & -C_{FB} & -C_{CF} & [C_{CF} + C_{FS} + C_{FB}] & 0 & -C_{FS} \\ 0 & -C_{BV} & 0 & 0 & C_{BV} & 0 \\ 0 & 0 & 0 & -C_{FS} & 0 & C_{FS} \end{bmatrix} \quad (5)$$

The pressure \underline{P} vector has the following elements

$$\underline{P} = \{P_A, P_B, P_C, P_F, P_V, P_S\} \quad (6)$$

and the flux \underline{Q} vector reads:

$$\underline{Q} = \{Q_A, 0, 0, 0, 0, -Q_j\} \quad (7)$$

The parameter identification is performed in two stages:

I. The *steady* state. For constant pressures, the matrix equation to be solved is the particular integral of the differential matrix equation (3), namely

$$\underline{\underline{Z}} \underline{P}^* = \underline{Q}^* \quad (8)$$

Hence, \underline{P}^* and \underline{Q}^* indicate the average, time-independent compartmental pressure and flux vectors, respectively, the values of which are given in Figure 1. For the linear problem, equation (8) is a solution of the steady state; it is, by the uniqueness theorem, also the solution.

II. The *non-steady* state. Once the matrix \underline{Z} is determined from the steady state, we insert it into equation (3) rearranged to read

$$\underline{C} \frac{d\underline{P}(t)}{dt} = \underline{Q}(t) - \underline{Z} \underline{P}(t) \quad (\underline{C}, \underline{Z} = \text{const.}) \quad (3')$$

The solution for \underline{C} depends on the availability of information about the time dependency of both the flux vector $\underline{Q}(t)$ and of the pressure vector $\underline{P}(t)$. In addition, the boundary conditions have to be in the form of pressure variation with time in order to solve uniquely for the compliances.

To proceed with the numerical solution of these equations, we replace the partial derivatives by implicit, backwards time difference quotients:

$$\frac{dP_A(t)}{dt} \approx \frac{P_A^{n+1}(t) - P_A^n(t)}{\Delta t} \quad (P_A^k(t) \equiv P_A(t_0 + k\Delta t)) \quad (9)$$

At the same time, we express all the space derivatives at the new time, namely at $n+1$. For example

$$\frac{P_A(t) - P_C(t)}{R_{AC}} = \frac{P_A^{n+1}(t) - P_C^{n+1}(t)}{R_{AC}} \quad \text{etc.}$$

The differential matrix equation now turns into a system of six sets of algebraic equations, each having the form

$$a_i Q_A^{n+1} + b_i P_B^{n+1} + c_i P_C^{n+1} + d_i P_F^{n+1} + e_i P_S^{n+1} + f_i P_V^{n+1} = g_i \quad (i = 1 \dots 6) \quad (10)$$

For example, for the artery chamber ($i=1$), we have

$$a_1 = 1; \quad b_1 = \frac{C_{AB}}{\Delta t}; \quad c_1 = \frac{1}{R_{AC}}; \quad d_1 = e_1 = f_1 = 0;$$

$$g_1 = P_A^{n+1} \left(\frac{1}{R_{AC}} + \frac{C_{AB}}{\Delta t} \right) - P_A^n \frac{C_{AB}}{\Delta t} + P_B^n \frac{C_{AB}}{\Delta t}$$

In this system of equations we have pressure values at times n and $n+1$ (namely, at times $t_0 + n\Delta t$ and $t_0 + (n+1)\Delta t$ respectively), values of resistances R_{ij} which we already know from the inverse solution of the steady state, and the values of the five compliances as unknowns. Given the values of pressures at times n and $(n+1)$, we can explicitly solve these equations for the five compliances C_{AB} , C_{CF} , C_{FB} , C_{FV} , and C_{BV} .

Using the data base of Figure 1, the compartmental resistances turn out to be:

R_{AC}	=	0.0933 mmHg/ml/min	
R_{CF}	=	66.67	" (lumped blood-cerebrospinal fluid barrier)
R_{CB}	=	13,300.0	" (lumped blood-brain barrier)
R_{CV}	=	0.0280	"
R_{FB}	=	13.30	" (lumped cerebrospinal fluid-brain barrier)
R_{FS}	=	7.62	"
R_{BV}	=	12.77	"
R_{VS}	=	0.0013	"
R_{SJ}	=	0.0080	"

To solve numerically for the compliances, the time-dependent compartmental pressures have to be taken from clinical measurements. For our solution, we chose those of HAMIT *et al.* (1965) discussed below. Solving equations (10) leads to the following values:

$$C_{AB} = 0.0012 \text{ ml/mmHg}$$

$$C_{CF} = 0.0357 \quad "$$

$$C_{BV} = 0.3750 \quad "$$

$$C_{FS} = 0.0494 \quad "$$

$$C_{FB} = 0.2090 \quad "$$

This concludes the calibration of the seven-compartmental model of the cerebrovascular fluid system with constant resistances and compliances.

4. The Quasi-Steady State Pressure Waves

Once the linear model has been calibrated, it is possible to obtain solutions for the pressure waves in all the compartments.

The solution of the inhomogeneous differential matrix equation for \underline{P} in incremental form is

$$\underline{P}(t+\Delta t) = \exp(-\underline{\kappa}) \left[\underline{P}(t) - \underline{Z}^{-1} \underline{Q}(t) \right] + \underline{Z}^{-1} \underline{Q}(t) \quad (11)$$

Here, $\Delta t = t_{k+1} - t_k$ denotes a time step between the frontier time level t_{k+1} and backtime level t_k . The matrix $\underline{\kappa}$ equals

$$\underline{\kappa} = \Delta t \cdot \underline{C}^{-1} \underline{Z} \quad (12)$$

The rational expansion of $\exp(-\underline{\kappa})$ leads to the following formula

$$\exp(-\underline{\kappa}) \cong \frac{\underline{I} - (1-\theta)\underline{\kappa}}{\underline{I} + \theta\underline{\kappa}} \quad (0 \leq \theta \leq 1) \quad (13)$$

in which \underline{I} is the $n \times n$ unit matrix. A substitution of equations (12), (13) into equation (11) yields

$$\underline{P}_{(t+\Delta t)} = (\underline{I} + \theta\underline{\kappa})^{-1} [\underline{I} - (1-\theta)\underline{\kappa}] [\underline{P}_{(t)} - \underline{Z}^{-1}\underline{Q}_{(t)}] + \underline{Z}^{-1}\underline{Q}_{(t)} \quad (14)$$

The coefficient θ controls the type of solution which evolves in time. When $\theta=0$, we have an explicit scheme; $\theta=1$, an implicit scheme, and $0 < \theta < 1$ is the mixed scheme. Thus, with the choice of θ , the pressure waves in the various compartments can be calculated from equation (14).

Yet there is another state between the steady state and the non-steady state. If we consider the contribution of the compliance term to be *negligible*, $\underline{C} \frac{d\underline{P}}{dt} \approx 0$ (which, in effect, is the case once we insert the numerical values of C_{ij} into equation (3')), we obtain the relation

$$\underline{Z} \underline{P}(t) \cong \underline{Q}(t) \quad (15)$$

Equation (15) "looks" like equation (8) - the condition for the steady state flow - but, this time, neither the pressure \underline{P} nor the flux \underline{Q} assume constant values; rather, each of them is a function of time. This is the *quasi-steady* state and the pressure waves can be calculated from a simplified formula, namely

$$\underline{P}_{(t+\Delta t)} = \underline{Z}^{-1} \underline{Q}_{(t)} \quad (14')$$

HAMIT *et al.* (*loc. cit.*) performed simultaneous recordings of ECG, PCG, arterial, brain, cisternal and venous (strictly, venous-sinus) pressure waves in anesthetized dogs (Fig. 2b). The recorded waves were in the 6-8 cycle-per-

Fig. 2

minute (c.p.m.) range upon which the faster cardiac waves - also termed "pulse waves" - were superimposed. In the classification of the intracranial pressure waves, the slow ones correspond to the Lundberg B-waves (LUNDBERG *et al.*, *loc. cit.*, 1974) and the faster pulse waves to the Lundberg A-waves.

The arterial B-wave shows an almost ideal sine wave pattern varying between 110-140 mmHg. We took it as the excitation pressure wave in the artery compartment $P_A(t)$, at frequency 0.144 Hz or a 7 second period, and calculated, by means of equation (14'), the rest of the compartmental pressure waves. The computer plotting of the venous-sinus pressure wave $P_S(t)$ shows a sine pattern of the same frequency at amplitudes varying between 2.8 - 7.2 mmHg (Fig. 2a) which is in excellent agreement with the P_S - wave measured by HAMIT *et al.*

The compartmental analysis also allows estimates about some kinematical changes which take place with the pressure waves. On the lumped-compartmental scale, the volumetric deformation of the brain tissue (β) compartment is representable by the compliance coefficient C_{FB} . As listed above,

$$C_{FB} = 0.2090 \text{ ml/mmHg}$$

The pressure difference (cf. Fig. 1) $P_{FB} = P_F - P_B = 0.5$ mmHg. Following HAKIM *et al.* (*loc. cit.*, 1976) we assume the brain tissue to lie in a spherical layer between the inner radius of the ventricles r_i and the outer radius of the subarachnoidal space r_o ; the ratio of the radii to be $\frac{r_o}{r_i} = 4$, and the volume $V_o = 600/2\pi$ mm. Thus, the radial displacement of the ventricles is found to be

$$\Delta r_i = 0.128 \times 10^{-4} \text{ mm}$$

HEIFETZ and WEISS (1981) have shown in two patients that after raising the cerebrospinal fluid pressure by 15-20 mmHg (namely, increasing 30-40 times the value of P_{FB} cited before), measurable changes occurred on electrical capacitance strain gauges fastened to the skull. Converting their results to displacements, the movements of the skull in response to the pressure elevation was 0.00078 mm in one case and 0.00372 mm in the other. Multiplying the above calculated value of Δr_i and $P_{FB} = 0.5$ mmHg by the factor 30-40, we find a very good agreement with the measurements of HEIFETZ and WEISS.

A lateral skull motion of the order of a few microns was also recorded by IVAN *et al.* (1983) using electrical resistance, high extension rubber strain gauges (Peekel type 20S) placed over the skull sutures. Earlier, FRYMAN (1971), who used spring dial gauges, recorded lateral motion of the temporal bones in the order of 10-18 microns (μ). ALLEN *et al.* (1983), who analyzed cine-CT scans, reported slow rhythmical deformations of the ventricles - the third ventricle in particular - of the order of 0.1 - 1.0 μ , in conformity with the above data at least to the order of magnitude.

The compartmental approach is a useful tool in the modelling of intracranial fluid dynamics as far as the time dependency is concerned. Its major

drawback is that it does not relate events to their spatial configuration since, by definition, the lumping of the parameters is space-independent. For the space-time modelling of brain tissue mechanics, we have to revert to the continuum or *distributed parameter* modelling which, on the macroscale, considers the brain tissue single phased possessing the averaged property of viscoelasticity, and on the microscale, analyzes it as a multiphasic system - three at least - of neurons, glia and interstitial fluid. Here, much more data is needed to calibrate the models and before this is reached, the continuum modelling will have to stall.

Finally, the illustrated example of the compartmental modelling here is seven-compartmental. If, in view of additional data, a model of more compartments is favoured; or the choice of resistances and compliances altered, nothing changes in the methodology described above or in the computer programme which, anyway, was programmed for $n \times n$ matrices. The authors will be grateful if information about other data bases be brought to their attention.

Acknowledgements - This research has been supported in part by the United States Air Force, Air Force Office of Scientific Research and European Office of Aerospace Research and Development, London, England, under Grant AFOSR-85-0233. Prof. Bear's contribution has been supported in part by the Fund for Promotion of Research at the Technion - Israel Institute of Technology.

References

- AGARWAL, G. C. (1971) Fluid flow - a special case. In *Biomedical Engineering*, BROWN, J. H. V., JACOBS, J. E. and STARK, L. (Eds.), F. A. Davis Co., Philadelphia, 69-81.
- ALLEN, L. K. and BUNT, E. A. (1978) Dysfunction of the fluid mechanical cranio-spinal systems as revealed by stress/strain diagrams. *S. Afr. Mech. Eng.*, 28, 159-166.
- ALLEN, L. K., BUNT, E. A. and POLDAS, H. (1983) Slow rhythmic ventricular oscillations and parenchymal density variations shown by sequential CT scanning. School of Mechanical Engineering, University of Witwatersrand, Johannesburg, South Africa, Research Report #83, 36 pp.
- BRUCE, D. A. (1973) *The Pathophysiology of Increased Intracranial Pressure*. Upjohn Co., Philadelphia.
- CHOPP, M. and PORTNOY, H. D. (1980) Systems analysis of intracranial pressure. *J. Neurosurg.*, 53, 516-527.
- DAVSON, H. (1960) Intracranial and intraocular fluids. In *Handbook of Physiology; Sec. 1 - Neurophysiology, Vol. III*, HAMILTON, W. F. (Ed.). American Physiological Society, Washington, D. C.
- FRYMAN, V. M. (1971) A study of the rhythmic motions of the living cranium. *J. Amer. Osteo. Assoc.*, 70, 928-945.
- GOLDSMITH, W. (1972) Biomechanics of head injuries. In *Biomechanics: Its Foundations and Objectives*, FUNG, Y. C., PERRONE, W. and ANLIKER, M. (Eds.). Prentice-Hall, Eaglewood Cliffs, N.J., 585-634.

- GRIFFITH, R. L., SULLIVAN, H. G. and MILLER, J. D. (1978) Modeling of Intracranial pressure dynamics. *Proc. 2nd Ann. IEEE Symp. on Computer Applications in Medical Care*, 244-253.
- GUYTON, A. C. (1969) *Function of the Human Body*, 3rd Ed., W. B. Saunders, Philadelphia.
- HAKIM, S., VENEGAS, J. G. and BURTON, J. D. (1976) The physics of the cranial cavity, hydrocephalus and normal pressure: mechanical interpretation and mathematical models. *Surg. Neurol.*, 5, 187-210.
- HAMIT, H. F., BEAL, A. C. Jr. and DE BAKEY, M. E. (1965) Hemodynamic influences upon brain and cerebrospinal fluid pulsations and pressures. *J. Trauma*, 5, 174-184.
- HEIFETZ, M. D. and WEISS, M. (1981) Detection of skull expansion with increased intracranial pressure. *J. Neurosurgery*, 55, 811-812.
- IVAN, L. P., BADEJO, A., ASFORA, W. and KARNI, Z. (1983) A correlation of intracranial pressure with suture and dural strain. *Proc. Sci. Conf. of the Inter. Soc. for Pediatric Neurosurgery*, Gothenburg, Sweden, August 23-26.
- KARNI, Z., SOREK, S. and BEAR, J., in collaboration with ALLEN, K. L. (1985) Models of brain tissue mechanics. United States Air Force, Air Force Office of Scientific Research and European Office of Aerospace Research and Development, London, England, Grant AFOSR-85-0233, Scientific Report #1, 71 pp.
- KELLIE, G. (1824) An account ..., with some reflections on the pathology of the brain. *Edinb. Med. Chir. Soc. Trans.*, 1, 34-169.

- KING, A. I. and CHOU, C. C. (1976) Mathematical modelling, simulation and experimental testing of biomechanical system crash response. *J. Biomech.*, 9, 301-317.
- LIU, Y. K. (1978) Biomechanics of closed head impact. *J. Eng. Mech. Div., Proc. ASCE*, 104, 131-152.
- LIVINGSTON, R. B., WOODBURY, D. M. and PATTERSON, J. L. Jr. (1965) Fluid compartments of the brain, cerebral circulation. In *Physiology and Biophysics*. (19th edition), RUCH, T. C. and PATTON, H. D. (Eds.), W. B. Saunders, Philadelphia, 935-958.
- LÖFGREN, J. and ZWETNOW, N. N. (1973) Cranial and spinal components of the cerebrovascular fluid pressure-volume curve. *Acta Neurol. Scandinavia*, 49, 575-585.
- LUNDBERG, N., KJÄLLQUIST, A., KULLBERG, G., PONTÉN, V. and SUNDBÄRG, G. (1974) Non-operative management of intracranial hypertension. In *Advances and Technical Standards in Neurosurgery* Vol. 1, KRAYENBÜHL, H. (Managing Ed.), Springer-Verlag, Wien, 3-59.
- MARMAROU, A. (1973) *A Theoretical Model and Experimental Evaluation of the Cerebrospinal Fluid System*. Ph.D. dissertation presented to Drexel University, Philadelphia, PA.
- MARMAROU, A., SHULMAN, K. and LAMORGESE, J. (1975) Compartmental analysis of compliance and outflow resistance of the cerebrospinal fluid system. *J. Neurosurg.*, 43, 523-534.
- MILLER, J. D. (1975) Volume and pressure in the craniospinal axis. *Clin. Neurosurg.*, 22, 76-105.

- MILLER, J. D. and GARIBI, J. (1972) Intracranial volume/pressure relationships during continuous monitoring of ventricular fluid pressure. In *Intracranial Pressure: experimental and clinical aspects*, BROCK, M. and DIETZ, H. (Eds.), Springer-Verlag, Berlin, 270-274.
- MONRO, J. (1783) *Observations on the Structure and Functions of the Nervous System*. W. CREECH *et al.*, Edinburgh.
- PAMIDI, M. R. and ADVANI, S. H. (1978) Nonlinear constitutive relations for human brain tissue. *Trans. ASME*, 100, 44-48.
- POLLACK, K. J. and BOSHES, B. (1936) Cerebrospinal fluid pressure. *Arch. Neurol. & Psycho.*, 36, 931-974.
- OMMAYA, A. K. and HIRSCH, A. E. (1971) Tolerances for cerebral concussion from head impact and whiplash in primates. *J. Biomech.*, 4, 13-21.
- RYDER, H. W., ESPEY, F. F., KIMBELL, F. D., PENKA, E. J., ROSENAUER, A., PODOLSKY, B. and EVANS, J. P. (1953) The mechanism of the change in cerebrospinal fluid pressure following an induced change in the volume of the fluid space. *J. Lab. Clin. Med.*, 41, 428-435.
- SOREK, S., BEAR, J. and KARNI, Z. (1985) Intracranial compartmental pulse wave simulation, *submitted for publication*.

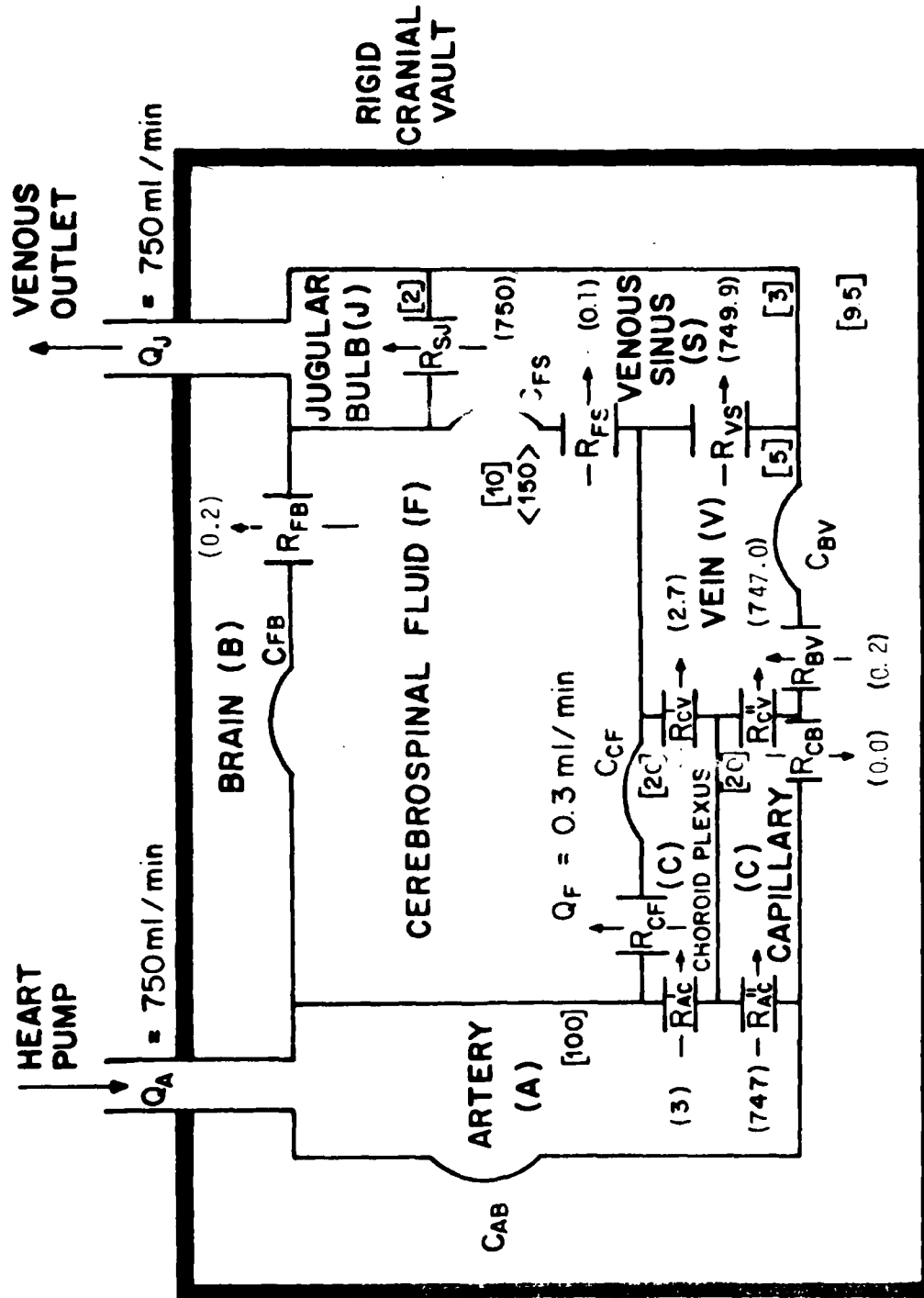


Fig. 1 Lumped-parameter compartmental model of the cerebrovascular system

([] pressure (mm Hg); () flow (ml/min); < > volume (ml)).

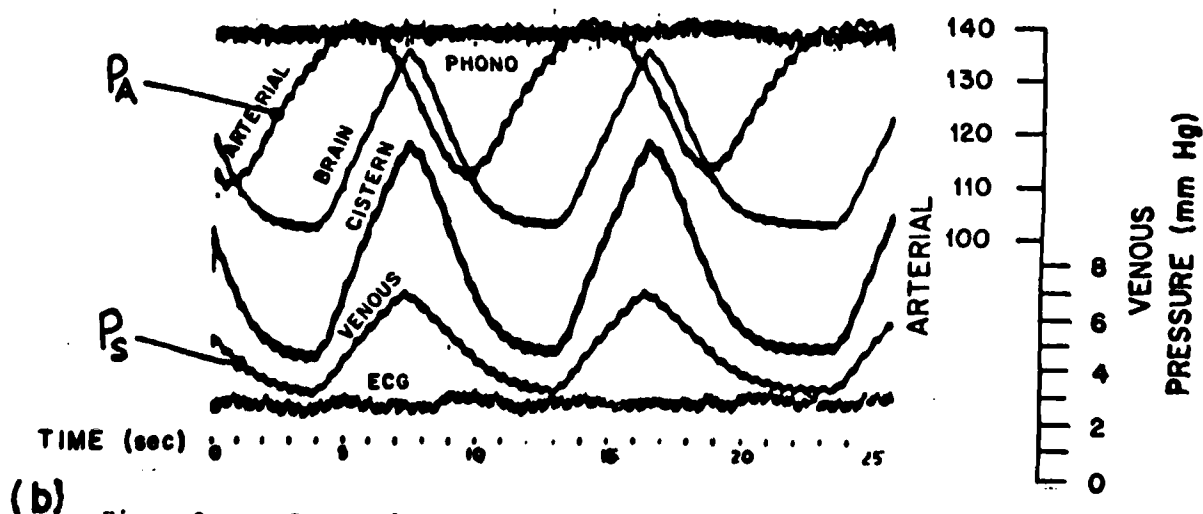
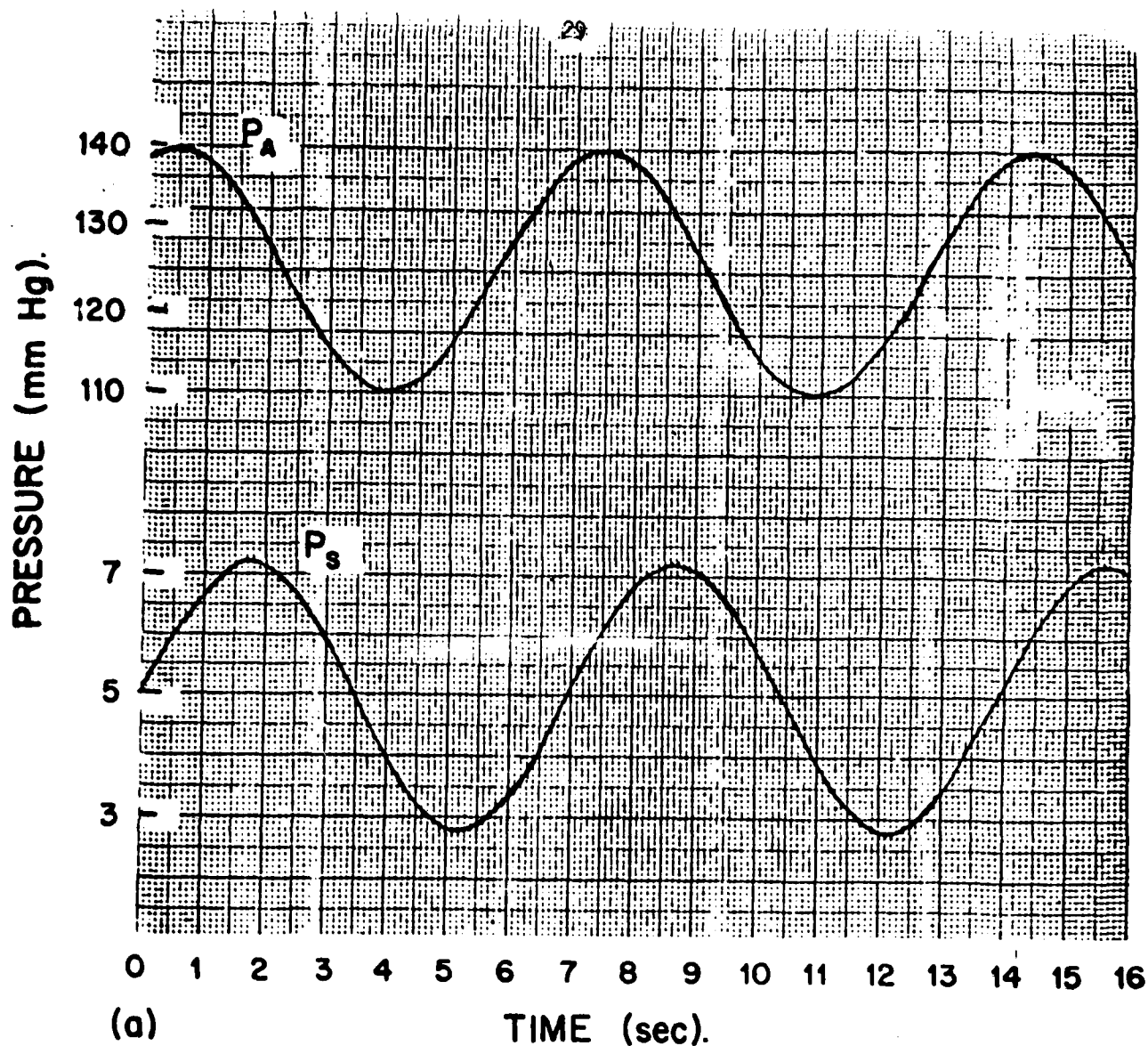


Fig. 2. a. Computed P_S wave from a P_A excitation wave (0.144 Hz, 110-140 mm Hg).

b. Simultaneous recording of ECG, PCG, arterial, brain cisternal and venous pressure waves (Hamit et. al.).

A NON-STEADY COMPARTMENTAL FLOW MODEL OF THE CEREBROVASCULAR SYSTEM

SHAUL SOREK, JACOB BEAR and ZVI KARNI**

Department of Biomedical Engineering, and Civil Engineering, Technion -
Israel Institute of Technology, Haifa 32000, Israel

Abstract - A lumped parameter compartmental model for the cerebrovascular fluid system is constructed and solved for the general linear problem of a nonsteady flow with constant resistances and compliances. The model predicts the intracranial pressure waves in the various compartments of the brain in response to pressure changes in the vascular system.

NOMENCLATURE

<u>A</u> ^(*)	sensitivity matrix	() ^T	transpose
<u>A</u>	arterial	<u>t</u>	time
<u>B</u>	deformational flow	<u>V</u>	venous, volume
<u>B</u>	brain	<u>Z</u>	fluidity matrix
<u>C</u>	compliance matrix	α	ratio of CSF-brain resistance to vein-venous sinus resistance
<u>C</u>	capillary	β	ratio of CSF-brain resistance to capillary-brain resistance
<u>D</u>	difference vector	γ	ratio of capillary-vein resistance to brain-vein resistance
<u>F</u>	cerebrospinal fluid (CSF)	θ	coefficient
<u>J</u>	jugular bulb	$\frac{\Delta t \cdot C^{-1} Z}{\Delta t}$	
<u>P</u>	pressure	<u>II</u>	n-set pressure matrix
<u>Q</u>	flux vector		
<u>R</u>	resistance		
<u>S</u>	venous sinus		

*In print, letters underlined once or twice - boldface type

**Deceased

INTRODUCTION

This paper summarizes the first stage of a research aimed at modelling the movement of fluids and chemicals in the cerebrovascular system. Here, we present the solution of the non-steady flow with constant resistances and compliances; namely, the general linear problem - in its entirety.

The lumped-parameter compartmental model of the cerebrovascular system is the first step towards a more comprehensive modelling of the cerebral content considered as a material continuum both on the macro and on the micro-scales. By the compartmental approach, the intracranial content is divided into a number of subunit compartments the behavior of each of which is represented by a single pressure parameter and by a single fluid discharge, both functions of time but not of space. The resistance to flow due to a particular vessel type is lumped at the outflow of its compartment. Likewise, the integrated change in volume of each compartment of the system is representable as an overall compartmental property and the functional interaction between the components of the lumped parameter system is assumed to be at the interfaces between adjacent compartments.

Monro's (1783) first model of the intracranial cavity was bi-compartmental: brain and blood as two almost-incompressible phases. Kellie (1824), Monro's pupil, modified this hypothesis by assuming three instead of two material compartments, namely arteries, veins and brain tissue. The Monro-Kellie doctrine prevailed to this century and was only relaxed in stages. The number of fluid compartments was increased to six: arterial, capillary, venous, venous sinus, jugular bulb and cerebrospinal (CSF) (Agarwal, 1971). Yet, the fluid itself remained incompressible. More recent approaches relaxed the latter assumption and the fluid was taken as linearly compressible, namely the change in pressure and the change in volume are proportional to

each other, and the coefficient of proportionality, the bulk modulus or its inverse - the *compliance*, are constants. As to the brain tissue, in essence - a multiphasic material continuum, the experimental results pointed at non-linear elasticity of the tissue or, alternatively, the nonlinearity of the compliance (Marmarou *et al.*, 1975; Miller, 1975; Hakim *et al.*, 1976; Lewer Allen and Bunt, 1978; Chopp and Portnoy, 1980). To overcome the "non-linearity" of a single coefficient, more complex models of single-phased, multi-parameter viscoelastic materials were introduced such as the one consisting of four viscoelastic coefficients known as the "three-parameter solid", coupled dynamically with another elastic element (Pamidi and Advani, 1978).

Our model consists of seven compartments, namely the six compartments listed above and the brain tissue compartment (Fig. 1). The lumped resistances are: between the Artery (A) and

Fig. 1

Capillary (C) compartments (R_{AC}), the Capillary (C) and Cerebrospinal Fluid (F) compartments (R_{CF}), the Capillary (C) and Brain Tissue (B) compartments (R_{CB}), the Capillary (C) and Vein (V) compartments (R_{CV}), the Brain tissue (B) and Vein (V) compartments (R_{BV}), the Cerebrospinal Fluid (F) and the Brain (B) compartments (R_{FB}), the Vein (V) and Venous Sinus (S) compartments (R_{VS}), the Cerebrospinal Fluid (F) and the Venous Sinus (S) compartments (R_{FS}), and between the Venous Sinus (S) and Jugular Bulb (J) compartments (R_{SJ}); altogether nine resistances. In the Figure, the Capillary compartment, likewise the R_{AC} resistance, are subdivided into the chambers of: the choroid plexuses - those tufts of small capillary vessels inside each of the four cerebral ventricles, and the capillary system outside the ventricles. However, in the equations to follow, only the

combinations of $R_{AC}^{-1} + R_{AC}^{n-1} = R_{AC}^{-1}$ and $R_{CV}^{-1} + R_{CV}^{n-1} = R_{CV}^{-1}$ appear so that the lumped resistances R_{AC} and R_{CV} , into and out of the capillary compartment, prevail. Nevertheless, it is justified to conserve the individual components of R_{AC}^{-1} and R_{CV}^{-1} because the latter relate to anatomically distinct features through which different flows take place. We note that the lumping is a consequence of the fact that the pressure difference across the components is the same.

The resistances R_{CB} , R_{CF} and R_{FB} are identified as the blood-brain barrier; the blood-cerebrospinal fluid barrier and the cerebrospinal fluid-brain barrier, respectively.

The compliance elements C_{ij} indicate that an increase in volume of one compartment equals the volume of the cup formed by the deformed membrane. This volume, in turn, equals the volume displaced from the neighboring compartments, all this within the overall rigid container of the skull (the Monro-Kellie doctrine).

In the non-steady state, the deformability of the compartments due to the pulsatory motion of the arteries is taken into account. Thus, first, we introduce a compliance element C_{AB} between the artery and the brain tissue compartments. Next, the capillary system is considered non-deformable so we do not insert compliances between this compartment and any of its neighbors. The choroid plexuses, however, although being capillary in character, possess other material properties and can - and in fact, do - convey pulsations to the CSF system (Bering (1955)) so that a compliance element C_{CT} is introduced between them. Further, the CSF system and the brain tissue share common boundaries, at the ventricles and along the sub-arachnoidal space, which are mechanically deformable. A compliance element C_{BT} is, therefore, inserted between the two. Finally, additional

compliance elements C_{BV} and C_{FS} are introduced, respectively, between the brain tissue and venous compartments, and between the CSF and venous sinus compartments to account for possible changes in fluid accumulation between the considered compartments, and in order to reduce the high pressure in the cardiovascular passage. There is no compliance element between the sinuses and the large jugular veins because the jugular bulb is assumed rigid, with very small storage changes. Altogether, in our presentation, we assume five compliance elements between the cerebrovascular elements.

The mechanical properties of 'resistances' and 'compliances' are "symmetric" with respect to the interchange of direction between one compartment and another. These are outcomes of the law of action and reaction. In general formulae,

$$\begin{array}{lll} R_{AC} = R_{CA} & R_{CF} = R_{FC} & \text{etc.} \\ C_{AB} = C_{BA} & C_{CF} = C_{FC} & \text{etc.} \end{array} \quad (1)$$

Three results, obtained by running the model presented here for cases of interest, indicate that the model, even in its present form, can simulate certain features actually observed clinically. The first relates to the observed displacement of the main ventricle peripheral boundary. By computing the value of the compliance between the F-compartment and the Brain Tissue one, approximating the configuration of the F-compartment to a sphere, Karni et al. (1986) showed that this displacement is of the order of magnitude actually observed by Lewer and Bunt (1978).

The second indication relates to the pressure variations in the jugular bulb. Sorek et al. (1986a), by employing the model presented here, predict that a negative pressure appears during certain portions of the pressure cycle in the jugular bulb compartment. Such negative pressure is indeed observed in reality. Also, the model predicts, during certain portions of the cycle, zero pressure in the sinus, a fact that is also accounted for the action of the heart.

Finally, as shown in this paper, the model predicts the excessive accumulation of CSF in the F-compartment (known as Normal Pressure Hydrocephalus), as a result of clogging of the passage between the capillaries and the Brain Tissue compartments. Sorek et al. (1986c) report observing this relation and discuss the use of it in relieving the pressure by transplanting a shunt.

COMPARTMENTAL MODEL EQUATIONS

The assumptions underlying the hydrodynamical model of the circulatory cerebrovascular system may now be summarized as follows:

- (i) Functional brain elements, represented by compartments, are characterized by 'mean' or 'lumped parameter' quantities, of interest to us here are pressure and fluid flux.
- (ii) The fluid is single phased, incompressible and Newtonian. From the physical point of view, there is no differentiation between blood and CSF.
- (iii) The flow is laminar and the relation between the flow rate and pressure drop is linear, i.e.

$$Q = \frac{\Delta P}{R} \quad (2)$$

where R is the resistance.

(iv) For the distensibility (elasticity) of the element of brain, a linear function holds between the volume change ΔV and the pressure drop ΔP namely

$$\Delta V = C \cdot \Delta P \quad (3)$$

where the coefficient of proportionality, C , is the compliance.

(v) The system is isothermal and thermodynamically stable.

The explicit continuity equations for the balance of mass for the various compartments now read:

For the Artery (A) compartment:

$$Q_A = \frac{P_A - P_C}{R_{AC}} + C_{AB} \frac{d}{dt} (P_A - P_B) \quad (4)$$

For the Brain Tissue (B) compartment:

$$\frac{P_C - P_B}{R_{CB}} + \frac{P_F - P_B}{R_{FB}} = \frac{P_B - P_V}{R_{BV}} + C_{BA} \frac{d}{dt} (P_B - P_A) + C_{BV} \frac{d}{dt} (P_B - P_V) + C_{BF} \frac{d}{dt} (P_B - P_F) \quad (5)$$

For the Capillary (C) compartment:

$$\frac{P_A - P_C}{R_{AC}} = \frac{P_C - P_F}{R_{CF}} + \frac{P_C - P_B}{R_{CB}} + \frac{P_C - P_V}{R_{CV}} + C_{CF} \frac{d}{dt} (P_C - P_F) \quad (6)$$

For the Cerebrospinal Fluid (F) compartment:

$$\frac{P_C - P_F}{R_{CF}} = \frac{P_F - P_S}{R_{FS}} + \frac{P_F - P_B}{R_{FB}} + C_{FB} \frac{d}{dt} (P_F - P_B) + C_{FS} \frac{d}{dt} (P_F - P_S) + C_{FC} \frac{d}{dt} (P_F - P_C) \quad (7)$$

For the Vein (V) compartment:

$$\frac{P_C - P_V}{R_{CV}} + \frac{P_B - P_V}{R_{BV}} = \frac{P_V - P_S}{R_{VS}} + C_{VB} \frac{d}{dt} (P_V - P_B) \quad (8)$$

For the Venous Sinus (S) compartment:

$$\frac{P_V - P_S}{R_{VS}} + \frac{P_F - P_S}{R_{FS}} = \frac{P_S - P_J}{R_{SJ}} + C_{SF} \frac{d}{dt} (P_S - P_F) \quad (9)$$

For the Jugular Bulb (J) compartment:

$$\frac{P_S - P_J}{R_{SJ}} = Q_J \quad (10)$$

Adding (4) through (10), making use of (1), yields

$$Q_A = Q_J \quad (11)$$

which is a remanifestation of the Monro-Kellie doctrine.

Equations (4)-(10) can be grouped into a single matrix equation of the form

$$\underline{C} \frac{d\underline{P}}{dt} + \underline{Z} \underline{P} = \underline{Q} \quad (12)$$

where \underline{P} is the pressure column vector:

$$\underline{P} = \{P_A, P_B, P_C, P_F, P_V, P_S\} \quad (13)$$

\underline{Z} is the fluidity (inverse of resistivity) matrix

$$\underline{Z} = [Z_{ij}] = \left[\frac{1}{R_{ij}} \right] = \begin{bmatrix} Z_{AC} & 0 & -Z_{AC} & 0 & 0 & 0 \\ 0 & [Z_{CB} + Z_{FB} + Z_{BV}] & -Z_{CB} & -Z_{FB} & -Z_{BV} & 0 \\ -Z_{AC} & -Z_{CB} & [Z_{AC} + Z_{CF} + Z_{CB} + Z_{CV}] & -Z_{CF} & -Z_{CV} & 0 \\ 0 & -Z_{FB} & -Z_{CF} & [Z_{CF} + Z_{FS} + Z_{FB}] & 0 & -Z_{FS} \\ 0 & -Z_{BV} & -Z_{CV} & 0 & [Z_{CV} + Z_{VS} + Z_{BV}] & -Z_{VS} \\ 0 & 0 & 0 & -Z_{FS} & -Z_{VS} & [Z_{VS} + Z_{FS}] \end{bmatrix} \quad (14)$$

\underline{C} - the symmetric compliance matrix

$$\underline{C} = [C_{ij}] = [C_{ji}] = \begin{bmatrix} C_{AB} & -C_{AB} & 0 & 0 & 0 & 0 \\ -C_{AB} & [C_{AB} + C_{FB} + C_{BV}] & 0 & -C_{FB} & -C_{BV} & 0 \\ 0 & 0 & C_{CF} & -C_{CF} & 0 & 0 \\ 0 & -C_{FB} & -C_{CF} & [C_{CF} + C_{FS} + C_{FB}] & 0 & -C_{FS} \\ 0 & -C_{BV} & 0 & 0 & C_{BV} & 0 \\ 0 & 0 & 0 & -C_{FS} & 0 & C_{FS} \end{bmatrix} \quad (15)$$

and \underline{Q} is the flux column vector

$$\underline{Q} = \{Q_A, 0, 0, 0, 0, -Q_j\} \quad (16)$$

The resistance R_{SS} does not appear in equation (14) as it is readily obtainable from equation (10).

The matrix equation (12) comprises nine resistances and five compliances listed in equation (1). Even for the steady state, whereby all the derivatives with respect to time vanish identically, and equation (12) reduces to

$$\underline{Z} \underline{P} = \underline{Q} \quad (17)$$

we are left with the eight resistances (as R_{SJ} is determined separately) against six independent balance conditions for the various compartments of the cerebrovascular model, excluding the jugular bulb. However, by virtue of the Monro-Kellie doctrine which assumes an absolute rigidity of the cranial vault, actually only five equations of the six are independent. Thus, the redundancy of the system (17) is three, and three additional conditions are needed to solve the set. One of them is the flux $Q_P = 0.3$ ml/min which can be taken as pivot value with high credibility from the literature (Cutalar, 1968). Two more conditions have to be stipulated by physiological data. They, however, do not assume specific values; instead they are known to be within certain limits. We shall have, therefore, to accompany their determination by a sensitivity analysis, sweeping the entire range of variation of possible values, as discussed in the following Section.

EVALUATION OF THE FLUIDITY MATRIX

The intracranial, compartmental flow problem of the cerebrovascular system lies in the solution of the set (12) in its entirety. This is an inhomogeneous, first-order, ordinary differential matrix equation with respect to time. In the previous Section, we chose to refer to the matrices \underline{C} and \underline{Z} as constant, a fact that made (12) a set of linear equations. The respective mean values were taken as these constants, as a first approximation. However, in principle, the coefficient matrices \underline{C} and \underline{Z} could be functions of the dependent vector parameter \underline{P} which,

in turn depend on the time, t . Thus, basically the problem is non-linear. There are, however, some passive cases which can be approximated by the linear problem namely, when \underline{C} and \underline{Z} assume constant values. At any event, even while dealing with the non-linear problem, we shall have to pass through the linear case. To the latter, therefore, our attention is now focused.

The procedure of solution of the linear case is as follows:

- (a) Given information about fluxes and pressures, equation (12) can be solved to yield values for resistances and compliances. This is often referred to as *parameter identification* or *model calibration*.
- (b) When the R_{ij} s and C_{ij} s have been evaluated, the changes in pressures and rates of fluid flow can be determined for variations in the rate of fluid discharge from the heart pump and from the venous outlet.
- (c) With the pressures and compliances already solved, information about the volume changes and, under certain assumption, also of the displacements of the compartments can be obtained.

Here, we confine the attention to the parameter identification and proceed in two stages:

- I. *The steady state*. For constant pressures, the governing equation is the particular integral of (12). The matrix equation to be solved is (17).

The chart of mean pressure variations along the cerebrovascular fluid system conforms with the pressure profile of the cardiovascular system cited in the literature (e.g., in Guyton, 1969, Ch.14). In the arteries, the average pressure - between systole and diastole - is 100 mm Hg. It drops to 20 mm Hg in the capillaries including the choroid plexuses; 10 mm Hg in the CSF system, 9.5 mm Hg in the brain tissue, 5 mm Hg in the

venous system, 2 mm Hg in the sinuses and 1-2 mm Hg in the larger veins - jugular and spinal - leading into the vena cava (Fig.1). Volumes of the compartments are also recorded in the Figure as much as they are documented in the literature.

Given the compartmental mean pressures P_i^* ($i=A, B, C, F, V, S, J$), also introducing the abbreviations P_{ij}^* for the difference in mean pressure between two adjacent interacting compartments, $P_{ij}^* = P_i^* - P_j^*$; similarly, $Q_{ij} = Q_i^* - Q_j^*$ represents the difference between the mean fluxes in compartments i and j . Because Q_A^* , Q_J^* and Q_F^* are a-priori known, and the mean pressure values P_{AC}^* , P_{CF}^* and P_{SJ}^* (as all other mean pressures) are also known, the following elements of \underline{Z} are immediately solved:

$$Z_{AC} = \frac{Q_A^*}{P_{AC}^*} \quad Z_{CF} = \frac{Q_F^*}{P_{CF}^*} \quad Z_{SJ} = \frac{Q_J^*}{P_{SJ}^*} \quad (18)$$

This leaves us with six elements of \underline{Z} against five equations for the remaining compartments, four of which are independent.

To account for the double redundancy, we introduce the scalar coefficients

$$\alpha \quad \frac{R_{FB}}{R_{VS}} = \frac{Z_{VS}}{Z_{FB}} \quad (0 \leq \alpha) \quad (19)$$

$$\beta \quad \frac{R_{FB}}{R_{CB}} = \frac{Z_{CB}}{Z_{FB}} \quad (0 \leq \beta \leq \infty) \quad (20)$$

Here, α indicates the ratio of the cerebrospinal fluid-brain barrier to the vein-venous sinus resistance, whereas β is the ratio of the cerebrospinal fluid-brain barrier to the blood-brain barrier.

Let us now examine the following cases:

(i) $0 \leq \beta < \infty$. Based on equation (20), solution of equation (17) leads to:

$$Z_{AC} = \frac{Q_A^*}{P_{AC}^*} \quad Z_{CF} = \frac{Q_F^*}{P_{CF}^*} \quad Z_{SJ} = \frac{Q_J^*}{P_{SJ}^*} \quad (21.1)$$

$$Z_{FB} = \frac{1}{\alpha P_{VS}^* - P_{FB}^*} Q_{AF}^* \quad (21.2)$$

$$Z_{VS} = \frac{\alpha}{\alpha P_{VS}^* - P_{FB}^*} Q_{AF}^* \quad (21.3)$$

$$Z_{FS} = \frac{1}{\alpha P_{VS}^* - P_{FB}^*} \cdot \frac{1}{P_{FS}^*} (\alpha P_{VS}^* Q_F^* - P_{FB}^* Q_A^*) \quad (21.4)$$

$$Z_{CV} = \frac{\alpha P_{VS}^* - P_{FB}^* - \beta P_{CB}^*}{\alpha P_{VS}^* - P_{FB}^*} \cdot \frac{1}{P_{CV}^*} Q_{AF}^* \quad (21.5)$$

$$Z_{CB} = \frac{\beta}{\alpha P_{VS}^* - P_{FB}^*} Q_{AF}^* \quad (21.6)$$

$$Z_{BV} = \frac{1+\beta}{\alpha P_{VS}^* - P_{FB}^*} \cdot \frac{P_{FB}^*}{P_{BV}^*} Q_{AF}^* \quad (21.7)$$

The lower extreme value of $\beta=0$ is noteworthy of mention. From the definition of β (Eq. (20)), it can assume a zero value in two cases. First, $R_{FB}=0$, indicating a complete rupture of the cerebrospinal-brain barrier. Here, $\alpha=0$ also prevails and the only consistent condition for equation (21.3) to exist is $P_F^*=P_B^*$, which means that there is hydrodynamical equilibrium and absolute stagnancy of flow between the CSF compartment and the brain tissue compartment. To avoid this, the pressures at the CSF compartment and the brain tissue compartment ought to differ by some

amount, $P_F^* \neq P_B^*$. In the literature, it is customary to assume that both are in the order of 10 mm Hg. In our calculations, we arbitrarily used the mean values of $P_F^* = 10$ mm Hg and $P_B^* = 9.5$ mm Hg (Fig.1) to enable flow from the F to the B compartment.

The second possibility for the vanishing of β is $R_{CB} \rightarrow \infty$. Physiologically, this means that there is a complete blockage of the blood-brain barrier; there is no transmission of blood nutrients from the capillaries to the interstitial fluid of the brain tissue, in short - a total collapse of the brain. We, therefore, rule this case out.

There is, however, one more case of an admissible non-singular solution of the hydrodynamical problem for $\beta=0$. It occurs when $Z_{FS}=1/R_{FS}=0$ or, alternatively, from equation (21.4), when $\alpha = Q_A^* \cdot P_{FB}^* / Q_F^* \cdot P_{VS}^*$. This (if $P_F > P_B$) indicates that there is no direct drainage of the CSF into the sinuses through the arachnoidal granulations (the pacchionian bodies), the CSF compartment considerably increases its size and the symptoms are those of hydrocephalus.

There is little, almost no data about the physiological or pathological ranges of α and β . By trial and error, however, we could assume β to be in the range of 1/1000. This value led to results that have actually been observed in the clinic. At the same time, the values of the compliances and resistances obtained were found to be insensitive to the value of β , (see Sorek et al. 1986b). To convert this into corresponding ratios of fluxes, designated by a bar, instead of ratios of resistances, we have by definition,

$$\bar{\beta} \equiv \frac{Q_{CB}}{Q_{FB}} \quad \bar{\alpha} \equiv \frac{Q_{VS}}{Q_{FB}} \quad (22)$$

so that

$$\begin{aligned} \bar{\alpha} &= \frac{P_{VS} Z_{VS}}{P_{FB} Z_{FB}} = \frac{P_{VS}}{P_{FB}} \frac{R_{FB}}{R_{VS}} = \frac{P_{VS}}{P_{FB}} \alpha \\ \bar{\beta} &= \frac{P_{CB}}{P_{FB}} \frac{Z_{CB}}{Z_{FB}} = \frac{P_{CB}}{P_{FB}} \frac{R_{FB}}{R_{CB}} = \frac{P_{CB}}{P_{FB}} \beta \end{aligned} \quad (23)$$

For our choice of $\beta = 1/1000$, $\bar{\beta} = 0.021$ (cf. Fig. 1). As illustrations, Figures 2 and 3 present the computer solution of the set (21) for $R_{CB}(\alpha)$ and $R_{FS}(\alpha)$ respectively in the particular case of $\bar{\beta} = 0.021$

Fig. 2, 3

($\beta = 1/1000$). The functional dependence of R_{CB} on α is linear, whereas that of $R_{FS}(\alpha)$ is hyperbolic.

A general sensitivity analysis for the variation of the resistances R_{ij} in the present case (i) of $0 \leq \beta < \infty$ may follow the same procedure as for case (ii) ($\beta \rightarrow \infty$) discussed below. This was not carried out numerically because, at a later stage, due to the vagueness of the assumptions about β , the complete solution for the resistances $R_{ij}(\alpha, \beta)$, rather than the limited solution of $R_{ij}(\alpha)$ for the above values of β , has been obtained. The three-dimensional plottings for the compartmental resistances $R_{ij}(\alpha, \beta)$; later also those for the compliances $C_{ij}(\alpha, \beta)$, will be reported separately.

We now turn to case:

(ii) $\beta \rightarrow \infty$. In addition to equation (18), the remaining elements of the matrix \underline{Z} read

$$\begin{aligned} Z_{FB} &= 0 \quad ; \quad Z_{FS} = \frac{Q_F^*}{P_{FS}^*} \quad ; \quad Z_{VS} = \frac{Q_{AF}^*}{P_{VS}^*} \\ Z_{CV} &= \frac{1}{P_{CV}^* + \gamma P_{BV}^*} Q_{AF}^* \quad ; \quad Z_{BV} = \gamma Z_{CV} \\ Z_{CB} &= \frac{\gamma}{P_{CV}^* + \gamma P_{BV}^*} \frac{P_{BV}^*}{P_{CH}^*} Q_{AF}^* \end{aligned} \quad (24)$$

Here, for the sake of a smoother solution, a new parameter γ instead of α has been introduced as the ratio of the resistances R_{CV} and R_{BV} , namely

$$\gamma \equiv \frac{R_{CV}}{R_{BV}} \quad (25)$$

Strictly, the exact value of the ratio γ , as much as those of α and β , is not known. However, we can still pursue with the sensitivity assessment of the \underline{z} elements against a variation in γ , P_{CV}^* and P_{BV}^* . Let Δ denote a deviation from the mean value, then

$$\Delta P_{CV}^* = \Delta P_{BV}^* + \Delta P_{CB}^* \quad (26)$$

It follows from equations (24), (25) that

$$\underline{D}_Z = \underline{A} \underline{D}_F \quad (27)$$

where

$$\begin{aligned} \underline{D}_Z &= [\Delta z_{CV}, \Delta z_{CB}, \Delta z_{BV}] \\ \underline{D}_F &= [\Delta \gamma, \Delta P_{CB}^*, \Delta P_{BV}^*] \end{aligned} \quad (28)$$

are the difference vectors of the \underline{z} elements and of their arguments respectively, and \underline{A} is the square matrix

$$\underline{A} = \frac{Q_{AF}^*}{(P_{CV}^* \gamma P_{BV}^*)^2} \times \begin{bmatrix} -P_{BV}^* & -1 & -(1+\gamma) \\ \frac{P_{BV}^*}{P_{CB}^*} P_{CV}^* & -\frac{P_{BV}^*}{P_{CB}^*} \left(\frac{P_{CV}^*}{P_{CB}^*} + \gamma \frac{P_{BV}^*}{P_{CB}^*} + 1 \right) \gamma & \gamma \\ P_{CV}^* & -\gamma & -\gamma(1+\gamma) \end{bmatrix} \quad (29)$$

The extreme case of $\beta \rightarrow \infty$ corresponds to a complete rupture of the blood-brain barrier ($R_{CB}=0$) causing haemorrhage to the entire brain tissue. This is bound to change the compartmental pressure distribution contrary to our assumption of a steady state. Use of equations (27), (28), (29) is, therefore, confined to the onset of the occurrence only.

II. *Non steady flow.* An interim solution of the matrix equation (12) for $\underline{P}=\underline{P}(t)$ and $\underline{Q}=\underline{Q}(t)$ when the effect of \underline{C} is negligible but not zero, has been discussed elsewhere (Karni *et al.*, 1986). As an example, for a given arterial excitation wave $P_A=P_A(t)$, the venous-sinus wave $P_S(t)$ was calculated and checked against the measured $P_S(t)$ wave recorded by Hamit *et al.*, 1965, showing a good matching in wave form, amplitude and frequency. In this way, after the model is calibrated and the resistances R_{ij} solved, the complete evaluation of the pulse wave vector $\underline{P}(t)$ can be obtained.

EVALUATION OF THE COMPLIANCE MATRIX

We now proceed to the complete solution of the non-steady flow problem for the compartmental model with constant coefficients, namely the general linear problem.

Equation (12) is rearranged to read

$$\underline{C} \frac{d\underline{P}(t)}{dt} = \underline{Q}(t) - \underline{Z} \underline{P}(t) = \underline{B}(t) \quad (\underline{C}, \underline{Z} = \text{const.}) \quad (30)$$

Information scarcely exists about the time dependency of the vector $\underline{Q}(t)$ at all compartments. We, therefore, begin with the average pressure vector \underline{P}^* and the average flux vector \underline{Q}^* and solve for the matrix \underline{Z} ,

which by our assumption is now time-independent, from equation (30), namely

$$\underline{B}^* = \underline{Q}^* - \underline{Z}^* \underline{P} = 0$$

That describes the steady state flow discussed above. We then derive information about the values of $\underline{P}(t)$ and $\dot{\underline{P}}(t) \equiv \frac{d\underline{P}(t)}{dt}$ at various times t from clinical data of simultaneous pulse wave recordings at the different compartments (such as from Hamit *et al.*, *loc cit.*).

Equation (30) now yields a n-set of relations for the compliances for each time value t which is of the form

$$\underline{n}_{\underline{P}} \underline{C} = \underline{n}_{\underline{B}} \quad (31)$$

$$\frac{d\underline{n}_{\underline{P}}}{dt} \equiv \underline{n}_{\underline{P}} = \begin{bmatrix} \dot{n}_{P_{AB}} \\ \dot{n}_{P_{CF}} \\ \dot{n}_{P_{BV}} \\ \dot{n}_{P_{FS}} \\ \dot{n}_{P_{FB}} \end{bmatrix} \quad 5 \times 1 \quad (32)$$

$$\underline{C} = \{C_{AB}, C_{CF}, C_{BV}, C_{FS}, C_{FB}\} \quad 5 \times 1 \quad (33)$$

$$\underline{n}_{\underline{B}} = \begin{bmatrix} Z_{SJ} n_{P_{SH}} - Z_{AC} n_{P_{AC}} \\ Z_{AC} n_{P_{AC}} - Z_{CV} n_{P_{CV}} - Z_{CF} n_{P_{CF}} - Z_{CB} n_{P_{CB}} \\ Z_{VS} n_{P_{VS}} - Z_{CV} n_{P_{CV}} - Z_{BV} n_{P_{BV}} \\ Z_{SJ} n_{P_{SJ}} - Z_{VS} n_{P_{VS}} - Z_{FS} n_{P_{FS}} \\ -Z_{SJ} n_{P_{SJ}} + Z_{AC} n_{P_{AC}} + Z_{VS} n_{P_{VS}} - Z_{CV} n_{P_{CV}} - Z_{CB} n_{P_{CB}} - Z_{FB} n_{P_{FB}} \end{bmatrix} \quad 5 \times 1 \quad (34)$$

Applying the Gauss-Markov theorem, the \underline{C} values are obtained by an assortment of the set of informations at all (n) given time observations, namely

$$\underline{C} = (\dot{\Pi}^T \dot{\Pi})^{-1} \dot{\Pi}^T \underline{B} \quad (35)$$

$$\dot{\Pi} = \begin{bmatrix} 1 \cdot \dot{\underline{p}} \\ - \dot{\underline{p}} \\ 2 \cdot \dot{\underline{p}} \\ - \dot{\underline{p}} \\ \vdots \\ n \cdot \dot{\underline{p}} \end{bmatrix} \quad n \times 5 \quad (36)$$

$$\underline{B} = [\underline{1} \cdot \underline{b}, \underline{2} \cdot \underline{b}, \dots, \underline{n} \cdot \underline{b}]_{n \times 1} \quad (37)$$

$$C_{AB} = \frac{\sum_{k=1}^n k \dot{P}_{AB} (Z_{SJ} k_P k_{P_{SJ}} - Z_{AC} k_{P_{AC}})}{\sum_{k=1}^n (k \dot{P}_{AB})^2} \quad (38.1)$$

$$C_{CF} = \frac{\sum_{k=1}^n k \dot{P}_{CF} (Z_{AC} k_P k_{P_{AC}} - Z_{CV} k_{P_{CV}} - Z_{CF} k_{P_{CF}} - Z_{CB} k_{P_{CB}})}{\sum_{k=1}^n (k \dot{P}_{CF})^2} \quad (38.2)$$

$$C_{BV} = \frac{\sum_{k=1}^n k \dot{P}_{BV} (Z_{VS} k_P k_{P_{VS}} - Z_{CV} k_{P_{CV}} - Z_{BV} k_{P_{BV}})}{\sum_{k=1}^n (k \dot{P}_{BV})^2} \quad (38.3)$$

$$C_{FS} = \frac{\sum_{k=1}^n k \dot{P}_{FS} (Z_{SJ} k_P k_{P_{SJ}} - Z_{VS} k_{P_{VS}} - Z_{FS} k_{P_{FS}})}{\sum_{k=1}^n (k \dot{P}_{FS})^2} \quad (38.4)$$

$$C_{FB} = \frac{\sum_{k=1}^n k \dot{P}_{FB} (Z_{AC} k_P k_{P_{AC}} + Z_{VS} k_{P_{VS}} - Z_{SJ} k_{P_{SJ}} - Z_{CV} k_{P_{CV}} - Z_{CB} k_{P_{CB}} - Z_{FB} k_{P_{FB}})}{\sum_{k=1}^n (k \dot{P}_{FB})^2} \quad (38.5)$$

From the clinical measurements of Hamit *et al.*, (1965), the five compartmental compliances listed in equation (33) have been calculated for the values $\alpha = 1000$, $\beta = 1/1000$. They are

$$\begin{aligned} C_{AB} &= 0.0155 \text{ ml/mm Hg} && (\text{const. for } \alpha, \beta) \\ C_{CF} &= 0.0364 && " \\ C_{BV} &= 0.3180 && " \\ C_{FS} &= 0.0334 && (\text{const. for } \beta) \\ C_{FB} &= 0.1830 && " \end{aligned}$$

At a later stage, the numerical solution has been extended to include the general case of $C_{ij} = C_{ij}(\alpha, \beta)$. The three dimensional $C_{ij}(\alpha, \beta)$ plottings will be reported separately. This concludes the calibration of the compartmental model for the cerebrovascular flow system.

EVALUATION OF THE COMPARTMENTAL PULSE WAVE FORMS

Within the framework of this work, which discusses the compartmental cerebrovascular flow problem with constant resistance R_{ij} and compliances C_{ij} namely, the general linear problem, once the model has been calibrated, it is possible to obtain solutions for the pressure-time variations $\underline{P}(t)$ at all the compartments.

Solution of the matrix equation (12) in incremental form is given by

$$\underline{P}_{(t+\Delta t)} = \exp(-\underline{\kappa}) [\underline{P}_{(t)} - \underline{Z}^{-1} \underline{Q}] + \underline{Z}^{-1} \underline{Q} \quad (39)$$

Here, $\Delta t = t_{k+1} - t_k$ denotes a time step between the frontier time level t_{k+1} and backtime level t_k . The matrix $\underline{\kappa}$ equals

$$\underline{\kappa} = \Delta t \cdot \underline{C}^{-1} \underline{Z} \quad (40)$$

The rational expansion of $\exp(-\underline{\kappa})$ leads to the following formula

$$\exp(-\underline{\kappa}) \approx \frac{\underline{I} - (1-\theta)\underline{\kappa}}{\underline{I} - \theta\underline{\kappa}} \quad (0 \leq \theta \leq 1) \quad (41)$$

where \underline{I} is the 6×6 unit matrix. A substitution of equation (41) into equation (40) now reads

$$\underline{P}_{(t+\Delta t)} \approx (\underline{I} + \theta\underline{\kappa})^{-1} [\underline{I} - (1-\theta)\underline{\kappa}] [\underline{P}_{(t)} - \underline{Z}^{-1}\underline{Q}] + \underline{Z}^{-1}\underline{Q} \quad (42)$$

The coefficient θ controls the type of solution which evolves in time. When $\theta = 0$, we have an explicit scheme; $\theta = 1$ — an implicit scheme, and $0 < \theta < 1$ — a mixed scheme. Thus, with the choice of θ , equations (18), (21) or (24), (38) and (42) constitute the complete solution of the non-steady, compartmental cerebrovascular flow problem with constant resistances and compliances. In addition, being phrased as a first-order differential matrix equation — Eq.(12) — sufficient boundary conditions ought to be given to enable us derive complete expressions for the compartmental pressure waves. Unfortunately, because of lack of clinical data, rigour has to give way to speculations from this stage onward. We can only express the hope that the information gap will close itself before long.

ACKNOWLEDGEMENT

This paper describes research on Modelling Brain Mechanics and Chemical Processes, conducted in the Dept. of Biomedical Engineering, Technion, Israel Institute of Technology, Haifa, Israel. The research is sponsored in part by the U.S. Air Force (grant AFOSR-85-0233). The authors wish to thank the U.S.A.F., the Technion and the Fund for the Promotion of Research at the Technion for their financial support.

- Agarwal, C.G. (1971) Fluid flow - a special case. Biomedical Engineering (Edited by Brown, J.H.V., Jacobs, J.E. and Stark, L.). F.A. Davis, Philadelphia.
- Bering, E.A. Jr (1955) Choroid plexus and arterial pulsation of cerebrospinal fluid. Demonstration of the choroid plexus as a cerebrospinal fluid pump. Arch. Neurol. Psychiatry, 73, 165-172.
- Cutalar, R.W.P. (1968) Formation and observation of CSF in man, Brain, 9, 70.
- Chopp, M. and Portnoy, H.D. (1980) System analysis of intracranial pressure. J. Neurosurg. 516-527.
- Davson, H. (1960) Intracranial and intraocular fluids. Handbook of Physiology - 1. Neurophysiology Vol. III. American Physiological Society, Washington.
- Guyton, A.C. (1969) Function of the Human Body, 3rd Ed. W.B. Saunders, Philadelphia.
- Hakim, S., Venegas, J.G. and Burton, J.D. (1976) The physics of the cranial cavity, hydrocephalus and normal pressure: mechanical interpretation and mathematical models. Surg. Neurol. 5, 187-210.
- Hamit, H.F., Beall, A.C. Jr. and DeBaKey, M.E. (1965) Hemodynamic influences upon brain and cerebrospinal fluid pulsations and pressures. J. Trauma 5, 174-184.
- Karni, Z., Bear, J., Sorek, S. and Pinczewski, Z. (1986) A quasi-steady state compartmental model of intracranial fluid dynamics. Submitted for publication.
- Kellie, G. (1824) An account ..., with some reflections on the pathology of the brain. Edin. Med. Chir. Soc. Trans. 1, 84-169.

- Lewer Allen, K. and Bunt, E.A. (1978) Dysfunction of the fluid mechanical cerebrospinal systems as revealed by stress/strain diagrams. S. Afr. Mech. Eng. 28, 159-166.
- Marmarou, A., Shulman, K. and LaMorgese, J. (1975) Compartmental analysis of compliance and outflow resistance of the cerebrospinal fluid system. J. Neurosurg. 43, 523-534.
- Miller, J.D. (1975) Volume and pressure in the craniospinal axis. Clin. Neurosurg. 22, 76-105.
- Monro, J. (1783) Observations on the Structure and Functions of the Nervous System. W. Creech. Edinburgh.
- Pamidi, M.R. and Advani, S.H. (1978) Nonlinear constitutive relations for human brain tissue. Trans. ASME 100, 44-48.
- Rashevsky, N. (1963) Mathematical theory of the effects of cell structure and of diffusion processes on the homeostasis and kinetics of the endocrine system with special reference to some periodic psychoses. Progress in Brain Research, Vol. 2 - Nerve, Brain and Memory Models. (Edited by Wiener, N. and Schafer, J.P.). Elsevier, Amsterdam.
- Sorek, S., Bear, J. and Karni, Z. (1986a) Intracranial compartmental pulse wave simulation, (Submitted for publication).
- Sorek, S., Bear, J. and Karni, Z. (1986b) Compartmental resistances and compliances of the cerebrovascular fluid system, (Submitted for publication).
- Sorek, S., Feinsod, M. and Bear, J. (1986c) Can N.P.H. be caused by cerebral small vessel disease? A new look based on a mathematical model, (Submitted for publication).

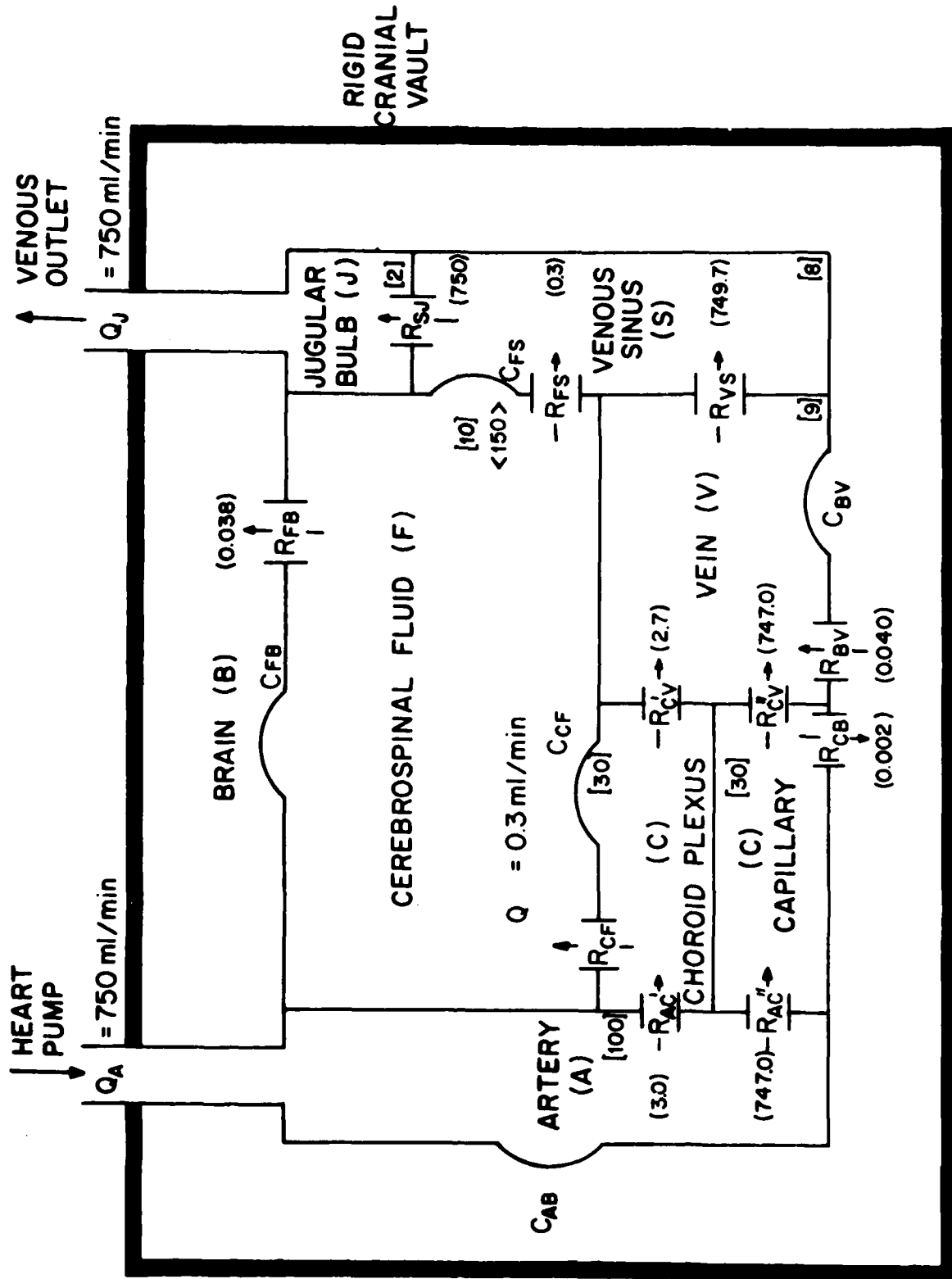


Fig. . Lumped-parameter, seven-compartment model of the intracranial cerebrovascular fluid system (R -resistance, C -compliance; [] pressure (mm Hg); () flow (ml/min); < > volume (ml)).

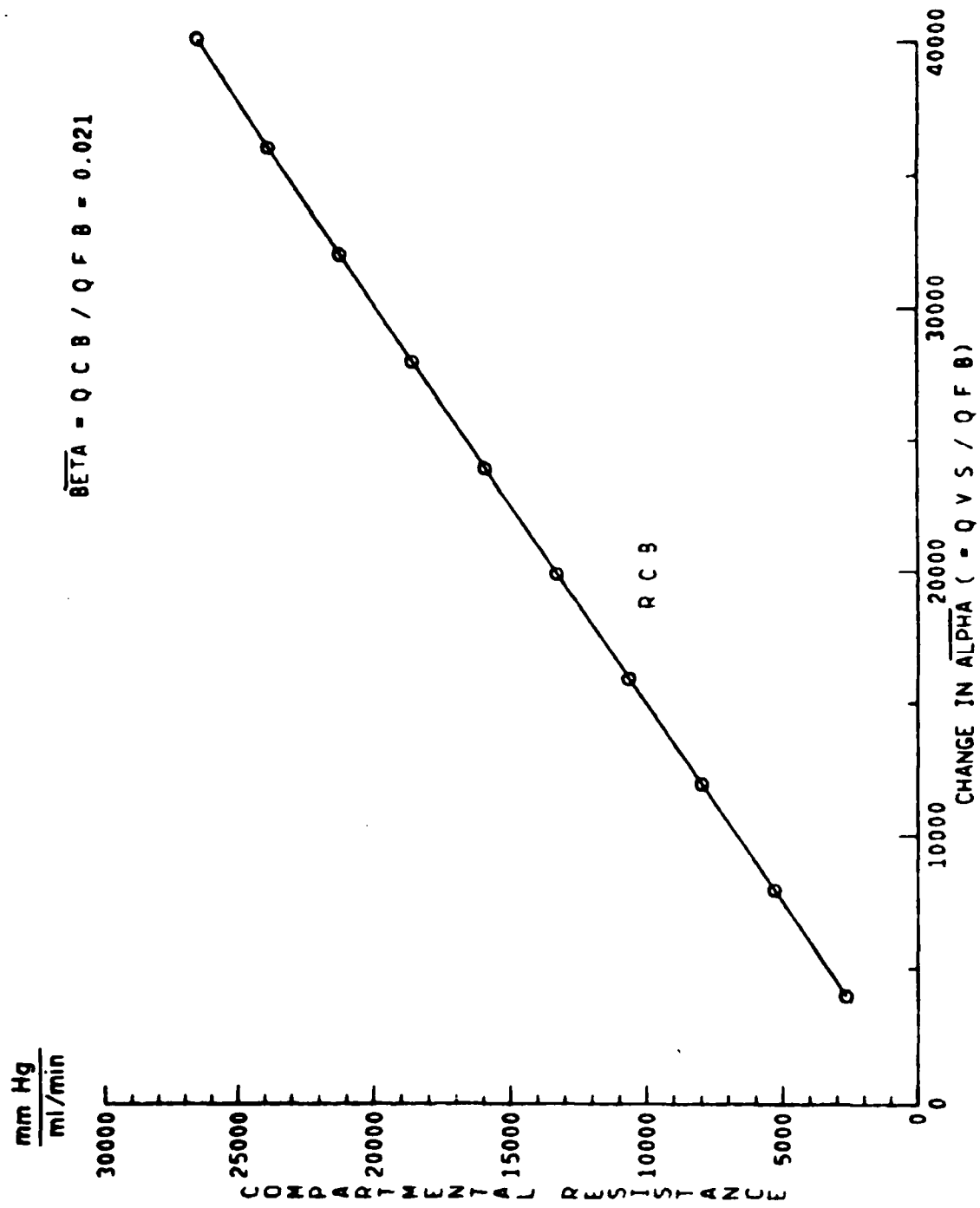


Fig. 2 The lumped blood-brain barrier R_{CB} .

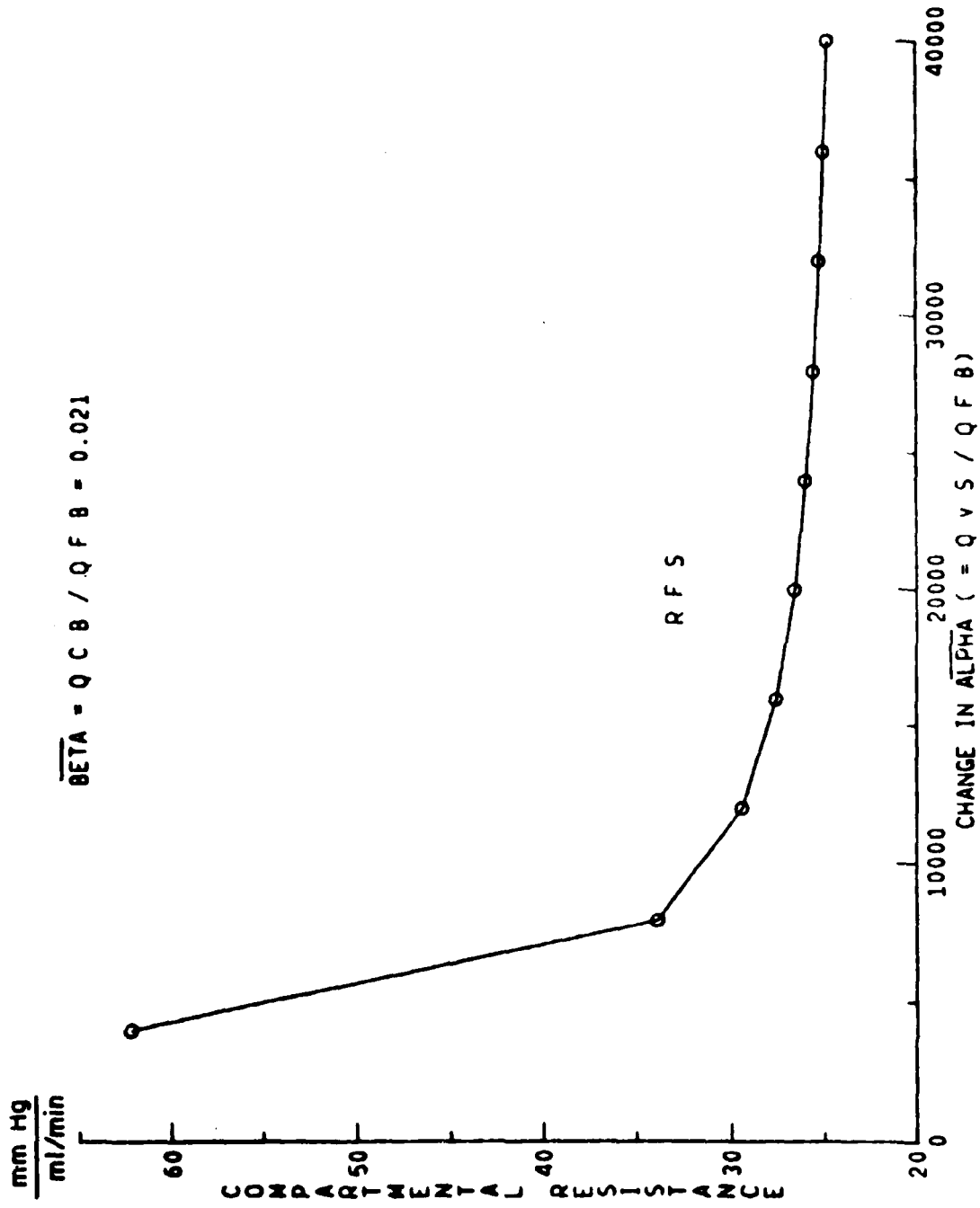


Fig. 3 The lumped cerebrospinal fluid-venous sinus barrier R_{FS} .

RESISTANCES AND COMPLIANCES OF A COMPARTMENTAL MODEL OF THE
CEREBROVASCULAR SYSTEM

Shaul Sorek, Ph.D., Jacob Bear, Ph.D. & Zvi Karni*, Ph.D.

Departments of Biomedical Engineering & Civil Engineering
Technion- Israel Institute of Technology, Haifa 32000, Israel

Keywords: Brain tissue, compartmental model, cerebrovascular
fluid, intracranial pressure, compliance resistance.

*Deceased

ABSTRACT

A lumped parameter compartmental model for the non-steady flow of the cerebrovascular fluid is constructed. The model assumes constant resistances that relate fluid flux to pressure gradients, and compliances between compartments that relate fluid accumulation to rate of pressure changes. Resistences are evaluated by using mean values of artery and cerebrospinal fluid (CSF) fluxes and mean compartmental pressures. Compliances are then evaluated from clinical data of simultaneous pulse wave recordings in the different compartments. Estimate of the average CSF compartmental deformation, based on the compliance between the CSF and brain tissue compartments, proves to be of the order of magnitude of actual experimental measurements.

INTRODUCTION

The lumped-parameter compartmental model of the cerebrovascular system is the first step towards the construction of a more comprehensive model of the intracranial fluid system. The compartmental approach assumes that the intracranial content may be divided into a number of units, or compartments, the behavior of each of which is represented by a single value of pressure and by values of flux exchanged with adjacent compartments. All these values may be time dependent, but they don't vary in space. The resistance to the flow from a compartment to an adjacent one is lumped at the boundary between the two compartments. Likewise, the integrated change in volume of two adjacent compartments due to the movement of their common boundary in response to a pressure difference, is represented as a property called compliance that is assigned to the boundary between two adjacent interacting compartments.

Monro's (1783) first model of the intracranial cavity was bi-compartmental: Brain fluid and blood, as two almost-incompressible fluid phases. Kellie (1824) modified this model by assuming three, instead of two, material compartments: arteries, veins and brain tissue. The Monro-Kellie models prevailed to this century and were modified in stages only in recent years. The number of compartments was increased to six: arteries, capillaries, venous, venous sinus, jugular bulb and cerebrospinal (CSF) (Agarwal, 1971).

Yet, in all these models, the fluid itself remained incompressible. More recent approaches relaxed the latter constraint and the fluid was taken as (linearly) compressible.

As to the brain tissue, it is essentially a multiphasic material (e.g., brain tissue, blood and CSF) continuum. Experimental results show that its behavior is inelastic or, alternatively, that the corresponding compliance is non-linear. To overcome the "non-linearity" of a single coefficient, the tissue is assumed to be a rather complex, single-phase, multi-parameter viscoelastic material e.g., one, whose constitutive relation involves four viscoelastic coefficients. (Panidi and Advam 1978). In the reports of these investigations, although not explicitly stated, the model of the intracranial content returned to be bi-compartmental: The CSF compartment and "all the rest", or the vascular compartment and the rest, etc. In most cases, even for the multicompartmental model of the cerebrovascular fluid system (e.g., Agarwal, 1971), no numerical calculations were presented and the exposition of the subject remained theoretical.

Our first objective, therefore, was to develop an N-compartmental model that can yield numerical values of the various state variables (e.g., pressure). So far, we have successfully achieved (Sorek et al. 1986a) this objective for the general linear problem, assuming constant compliances and resistances. Physiologically, the assumption of linearity corresponds to passive states in which the sensory and endocrinological biocontrol mechanisms have but little effect on the resistances and the compliances. Basically, homeostasis is non-linear by virtue of the feedback mechanism which senses the deviations in the values of resistances and compliances and acts

to restore them to normal values. Nevertheless, one must first construct and solve a linear model and employ perturbation techniques in order to derive solutions for the generalized non-linear problem. Accordingly, we have first constructed and solved a linear model that described non-steady flow in a lumped-parameter N-compartmental model of the cerebrovascular fluid system with constant resistances and compliances.

The compartmental model involves a number of resistances and compliances, the values of which must be known before the model can be employed in predicting pressure and flux changes. In the first paper (Sorek et al. 1986a) it was indeed assumed that the values compliance and resistances including, as we shall see also here, certain ratios between pairs of resistances were known. The objective of the present paper is to present a methodology for estimating the values of the various compliances and resistances and the above mentioned ratios.

1. THE COMPARTMENTAL BALANCE EQUATION

The governing equation for the lumped-parameter compartmental model describe the balance of mass and the balance of linear momentum for each compartment. Essentially, each such equation states that the temporal rate of change of either the fluid mass, or its momentum in a compartment, is equal to the amount of net influx of that quantity through the compartmental boundaries plus the external sources. The mass balance of the n -th compartment, surrounded by a numbr of compartments denoted by $m=1,2,\dots$, can, therefore, be written in the form

$$\frac{dV_n}{dt} = \sum_{(m)} q_{mn} + Q_n \quad (1)$$

where $q_{nm} = (-q_{mn})$ denotes the flux from compartment n to m , Q_n denotes external sources in the n -th compartment and V_n is its volume.

The flux q_{nm} can be expressed in terms of the difference in pressure, $P_{nm} (=P_n - P_m)$ between the n and the m compartment, and a conductance Z_{nm} (reciprocal of the resistance R_{nm}), in the form

$$q_{nm} = \frac{P_{nm}}{R_{nm}} = Z_{nm} P_{nm} \quad (2)$$

The change in volume, ΔV_n is produced by the change in the pressure differences, ΔP_{nm} , in adjacent compartments, taking into account the presence of compliances, C_{nm} , between these cells

$$\Delta V_n = \sum_{(m)} C_{nm} \Delta P_{nm} \quad (3)$$

Together, we obtain for the n -th compartment, a mass balance of the form

$$\sum_{(m)} C_{nm} \frac{dP_{nm}}{dt} + \sum_{(m)} Z_{nm} P_{nm} = Q_n \quad (4)$$

Another compact form of this equation for all cells simultaneously is

$$\underline{C} \frac{d\underline{P}}{dt} + \underline{Z} \underline{P} = \underline{Q} \quad (5)$$

where $\underline{P}(t)$ is the time-dependent ($N \times 1$) pressure vector; $\underline{Q}(t)$ the source ($N \times 1$) flux vector, and \underline{Z} and \underline{C} are the ($N \times N$) conductance and the compliance matrices, respectively.

2. PARAMETER ESTIMATION

The compartmental balance equations for fluid mass, written in the compact form of (5), involve conductivities and compliances, expressed by the matrices \underline{Z} and \underline{C} . In the present work, these parameters are assumed to be constant.

To predict the pressure (and flux) response of the model to external changes, the values of the parameters \underline{C} and \underline{Z} must be known. In order to estimate them, we need measured values of pressure in the various compartments at a sufficient number of points in time.

Because \underline{C} and \underline{Z} are constant, and $p(t)$ is cyclic, by taking a temporal average of (5), (i.e., integration over a period of time divided by the period), we obtain,

$$\underline{\bar{P}}^* \underline{Z} = \underline{Q}^* \quad (6)$$

where $(\dot{})$ denotes a temporal rate of change, $(\bar{})$ denotes the difference between adjacent compartments and p^* and Q^* denote mean values of pressure differences and source fluxes, respectively. We note that (6) is a quasi-steady state equation. With known values of P^* and Q^* , we solve (6) for \underline{Z} .

Given further information from clinical data e.g., Hamit et al. 1965), of simultaneous pulse wave recordings $P(t)$ and $\dot{P}(t)$ ($\equiv dP(t)/dt$), at the different compartments and at various times, t^k , $k=1,2,\dots,K$, equations (3) and (4) now yield a K -set of

relations for the compliances.

$$\dot{\underline{\bar{P}}}^k \underline{C} = \underline{Q}^k - \underline{Z} \underline{\bar{P}}^k \quad (7)$$

By the Gauss-Markov theorem, the C values are derived as an assortment of the set of informations at all K time observations (Sorek et al., 1986a).

This concludes, at least formally, the (inverse) process for identifying parameters appearing in equation (5) for a N-compartment model.

3. EVALUATION OF MODEL RESISTANCES AND COMPLIANCES

Let us determine the values of C and Z in the case of a seven-compartment model, namely for N=7.

Figure 1 shows the model consisting of the following compartments:

Fig. 1

arterial (A), capillary (C), cerebrospinal fluid (F), brain tissue (B), venous (V), venous sinus (S) and the jugular bulb (J). The (lumped) resistances are: between the artery and capillary compartments (R_{AC}); the capillary and cerebrospinal fluid compartments (R_{CF}), the capillary and brain tissue compartments (R_{CB}), the capillary and vein compartments (R_{CV}), the brain tissue and vein compartments (R_{BV}), the cerebrospinal fluid and brain compartments (R_{FB}), the vein and venous sinus compartments (R_{VS}), the cerebrospinal fluid and the venous sinus compartments (R_{FS}), between the venous sinus and the jugular bulb compartments (R_{VI}); altogether nine resistances. In Figure 1,

the capillary compartment, is divided into: the choroid plexuses - those tufts of small capillary vessels inside each of the four ventricles - and the capillary system outside the ventricles. However, in the equations, only the combination in parallel of the conductances $Z'_{AC} + Z''_{AC} = Z_{AC}$ and $Z'_{CV} + Z''_{CV} = Z_{CV}$ appear, so that only the combined resistances R_{AC} and R_{CV} - into and out of the capillaries - are included in the model.

The resistances R_{CB} , R_{CF} and R_{FB} are identified as the lumped blood-brain barrier; the lumped blood-cerebrospinal fluid barrier, and the lumped cerebrospinal fluid - brain barrier, respectively.

We recall that the compliance elements, C_{nm} , indicate that an increase in volume of one compartment equals the volume of the "cup" formed by the deformed membrane. This volume, in turn, equals the volume displaced from the neighboring compartments, all this within the rigid container of the skull bones (the Monro-Kellie doctrine).

In the non-steady state, which takes into account the deformability of the compartments, we first introduce a compliance element C_{AB} between the artery and the brain tissue compartments it represents the overall pulsatory effect of the arteries on the brain tissue. Next, the capillary system is considered non-deformable, so that no compliance is introduced between this compartment and any of its neighbors. The choroid plexuses, however, although capillary in nature, possess other material properties. Hence, they can, and in fact do, convey pulsations to the CSF system (Bering, 1955). Accordingly, a

compliance C_{CF} is introduced between them. Furthermore, the CSF system and the brain tissue share common boundaries - at the ventricles and along the subarachnoidal space - which are deformable. A compliance element C_{FB} is, therefore, inserted between the two. Finally, to account for observed sharp drop in pressure along the cardiovascular passage, additional compliances C_{BV} and C_{FS} are inserted between the brain tissue and venous compartments and between the CSF and venous sinus compartments, respectively. Altogether, in our presentation, we assume five compliances between adjacent elements of the cerebrovascular fluid system.

The mechanical properties of resistances and compliances are symmetric with respect to the change of direction between one compartment and its neighbor, i.e., in formulae

$$\begin{aligned} R_{AC} &= R_{CA}, & R_{CF} &= R_{FC} & \text{etc.} \\ C_{AB} &= C_{BA}, & C_{CF} &= C_{FC} & \text{etc.} \end{aligned}$$

All R_{nm} 's and C_{nm} 's are positive.

We adopt the value of mean pressures along the cerebrovascular fluid system according to the pressure profile of the cardiovascular system cited in the literature (e.g. in Guyton, Ch. 14, 1969). In the arteries, the average pressure - between systole and diastole - is $P_A^* = 100\text{mmHg}$. It drops to $P_C^* = 30\text{mmHg}$ in the capillaries, including the choroid plexuses; $P_F^* = 10\text{mmHg}$ in the CSF system, $P_B^* = 9.5\text{mmHg}$ in the brain tissue, $P_V^* = 9\text{mmHg}$ in the venous system, $P_S^* = 8\text{mmHg}$ in the sinuses and $P_J^* = 2\text{mmHg}$ in the larger juglar veins and in the spinal leading into the vena cava (Fig. 1). The mean values of the injected and

ejected fluxs at the artery and jugular bulb are $Q^*_A = Q^*_J = 750 \text{ ml/min}$.

Altogether, nine values have to be determined. However, the matrix equation (6) comprises only six independent balance equations for the various compartments of the cerebrovascular model. Thus, the redundancy of the system is three, and three additional conditions are needed to solve the set. One of them is the mean flux (from choroid plexus to the CSF ventricles) $Q^*_F = 0.3 \text{ ml/min}$, which can be taken as pivot value with high credibility from the literature, (Cutaler, 1968).

Thus, the Z_{CF} value can be evaluated from the expression

$$Q^*_F = Z_{CF} P^*_{CF} \quad (8)$$

Two more conditions have to be stipulated for resistences, based on the existing physiological data. We now introduce the scalar coefficients.

$$\alpha = \frac{R_{FB}}{R_{VS}} = \frac{Z_{VS}}{Z_{FB}} \quad (9)$$

$$\beta = \frac{R_{FB}}{R_{CB}} = \frac{Z_{CB}}{Z_{FB}} \quad (10)$$

Here, α indicates the ratio of the resistance of the cerebrospinal fluid-brain barrier to the vein-venous sinus resistance, whereas β is the ratio of resistance of the cerebrospinal fluid-brain barrier to that of the blood-brain barrier. Thus, equations (6) to (10) allow a complete solution for the resistences $R_{nm}(\alpha, \beta)$ and compliances $C_{nm}(\alpha, \beta)$ with the

values of α and β . Figures 2 and 3 describe an example of the surfaces $R_{CV}(\alpha, \beta)$ and $C_{BV}(\alpha, \beta)$ respectively

Figs. 2,3

The figures demonstrate zones of α and β that generate unacceptable values (e.g. negative Z's as in Fig. 2) of resistances and compliances and zones of high sensitivity of the resulting Z's and C's to small changes of α and β . Our choice is, therefore, to rely on α and β values that generate stable Z's and C's.

There are almost no data about the physiological, or pathological, ranges of α and β . It was found that when α and β are in the range of 1/1,000 and 10,000, respectively the resistances and compliances meet the desired aforementioned criteria. Hence for $\beta=10^{-3}$ and $\alpha=10^{+4}$, equations (4) to (8) result in the following values

$R_{AC}=0.0933\text{mmHg/ml/min.}$	$R_{VS}=0.0013 \text{ mmHg/ml/min.}$
$R_{CF}=66.667\text{mmHg/ml/min.}$	$R_{FS}=7.6187\text{mmHg/ml/min.}$
$R_{CV}=0.028\text{mmHg/ml/min.}$	$R_{SJ}=0.0080\text{mmHg/ml/min.}$
$R_{CB}=13338.0\text{mmHg/ml/min.}$	$R_{FB}=13.338\text{mmHg/ml/min.}$
$R_{BV}=3.33\text{mmHg/ml/min.}$	

and

$C_{AB}=0.0012\text{ml/mmHg}$	$C_{FS}=0.0494\text{ml/mmHg}$
$C_{CF}=0.0357\text{ml/mmHg}$	$C_{FB}=0.2093\text{ml/mmHg}$
$C_{BV}=0.3746\text{ml/mmHg}$	

With the above value of C_{FB} , we can now assess the average deformation of the CSF compartment. Let us assume a spherical configuration of this compartment, with a mean diameter r_F . Its volume, V_F , and surface area, S_F , are given by $V_F = \frac{4}{3}\pi r_F^3$ and $S_F = 4\pi r_F^2$. By virtue of equation (2), we may thus express the change in V_F by

$$\Delta V_F = S_F \Delta r_F = C_{FB} P_{FB}^* \quad (11)$$

According to Hakim et al. (1976), the mean diameter of the CSF compartment is $r_F = \frac{1}{4} \cdot \frac{600}{2\pi}$ mm. Thus, in view of the mean pressure difference $P_{FB}^* = 0.5$ mmHg, the compliance value $C_{FB} = 0.2093$ ml/mmHg, and from equation (11), we obtain

$$r_F = 16.07 \cdot 10^{-5} \text{ mm.}$$

This estimate of displacement of the CSF compartment boundaries is consistent with measurements done by Allen et al. (1983).

Finally, we wish to emphasize that the model approach presented here (see also Sorek et al., 1986b, Karni et al., 1986) constitutes a methodology that can be implemented to various compartmental schemes representing different aspects of clinical data.

ACKNOWLEDGEMENT

This paper describes research on Modelling Brain Mechanics and Chemical Processes, conducted in the Dept. of Biomedical Engineering, Technion, Israel Institute of Technology, Haifa, Israel. The research is sponsored in part by the U.S. Air Force (grant AFOSR-85-0233). The authors wish to thank the U.S.A.F., the Technion and the Fund for the Promotion of Research at the Technion for their financial support.

REFERENCES

- Agarwal, G.C. (1971) Fluid-flow a special case. In Biomedical Engineering, Brow, J.H.V. Jacobs, J.E. and Stark, L. (Eds.). F.A. Davis Co., Philadelphia, 69-81.
- Allen, K.L., Bunt, E.A. and Poldas, H. (1983) Slow rhythmic ventricular oscillations and parenchymal density variations shown by sequential CT scanning. School of Mechanical Engineering, University of Witwatersand, Johannesburg, South Africa, Research Report #83, p. 36.
- Bering, E.A. Jr. (1955) Choroid plexus and arterial pulsation of cerebrospinal fluid. Demonstration of the choroid plexuses as a cerebrospinal fluid pump. Arch. Neuro Psychiatry V.73, 167-172.
- Cutler, R.W.P., (1968) Formation and observation of CSF in man, Brain 9, 70.
- Davson, H. (1960) Intracranial and intravascular fluids. In Handbook of Physiology; Sect. 1 - Neurophysiology, Vol. 111, Hamilton, W.F. (Ed.). American Physiological Society, Washington, D.C.
- Guyton, A.C. (1969) Function of the human body. 3rd Ed. W.B. Saunders, Philadelphia.
- Hamit, H.F., Beal, A.C., Jr., and DeBaakey, M.E. (1965) Hemodynamic influences upon brain and cerebrospinal fluid pulsations and pressures. J. Trauma, 5:174-184.
- Karni, Z., Sorek, S. and Bear, J. (1986) Models of brain tissue mechanics, Technion, I.I.T., Scientific Report #1. p.73.
- Kellie, G. (1824) An account... with some reflections on the pathology of the brain. Edin. Med. Chir. Soc. Trans., 1:84-169.
- Hakim, S., Venegas, J.G. and Burton, J.D. (1976) The physics of the cranial cavity, hydrocephalus and normal pressure: mechanical interpretation and mathematical models. Surg. Neurol. 5:187-210.
- Monro, J. (1783) Observations of the structure and functions of the nervous system. W. Creech, et al., Edinburgh, pp. 176.
- Pamidi, M.R. and Advani, S.H. (1978) Nonlinear constitutive relations for human brain tissue. Trans. ASME, 100:44-48.
- Sorek, S., Bear, J. and Karni, Z. (1986a) A non-steady compartmental flow model of the cerebrovascular system. Submitted for publication.
- Sorek, S., Bear, J. and Karni, Z. (1986b) Intracranial compartmental pulse wave simulation. Submitted for publication.

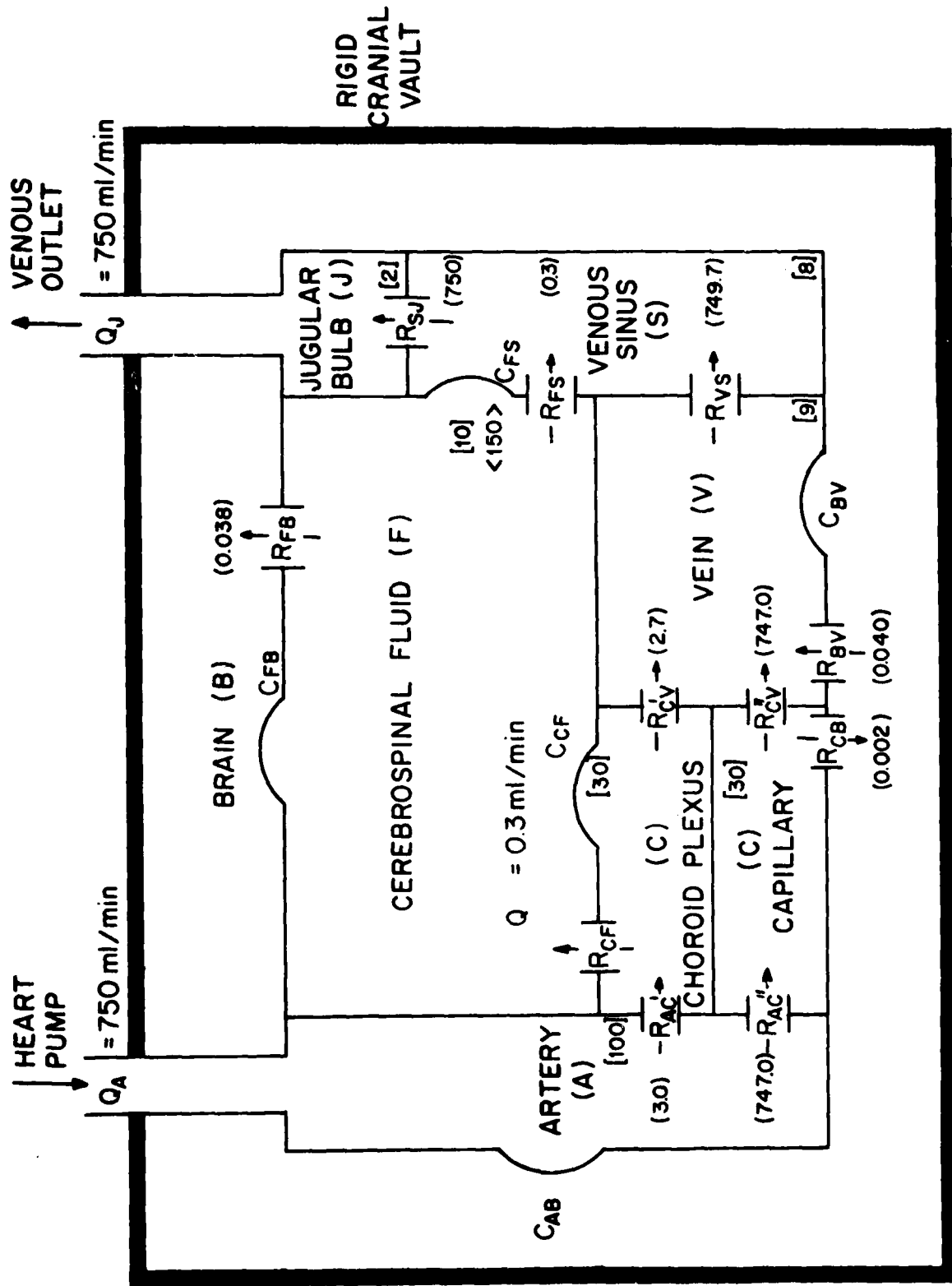


Fig. 1. Lumped-parameter, seven-compartmental model of the intracranial cerebrovascular fluid system (R -resistance, C -compliance; [] pressure (mm Hg); () flow (ml/min); < > volume (ml)).

RESISTANCE $R(CV)$ - VS - BETA & ALPHA
INCREMENTS: $INBETA=2100$ $INALPHA=4000$

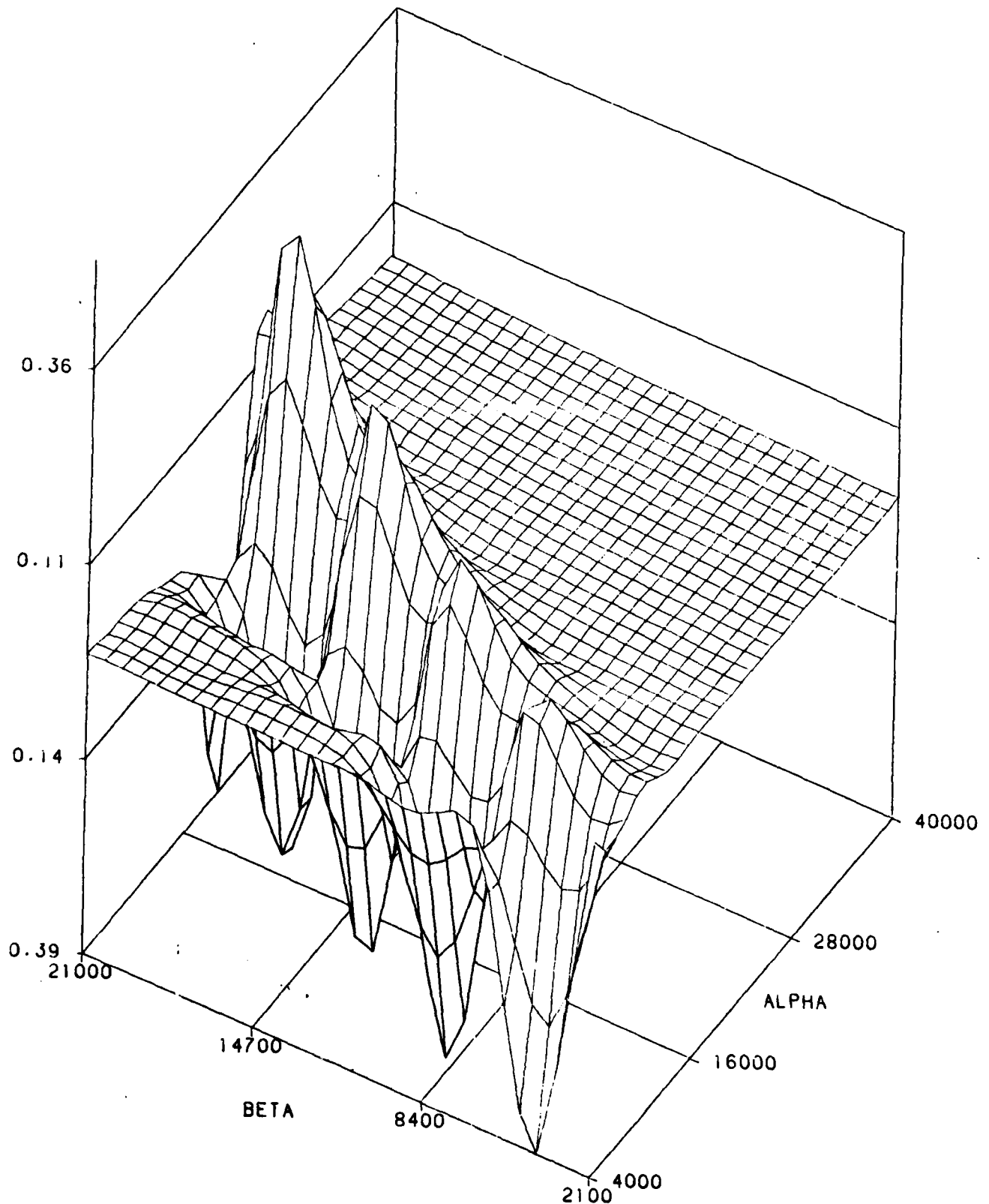


Fig. 2: SURFACE OF $R_{CV}(\alpha, \beta)$

COMPLIANCE $C(BV)$ - VS - BETA & ALPHA

INCREMENTS: $INBETA=1000$ $INALPHA=1000$

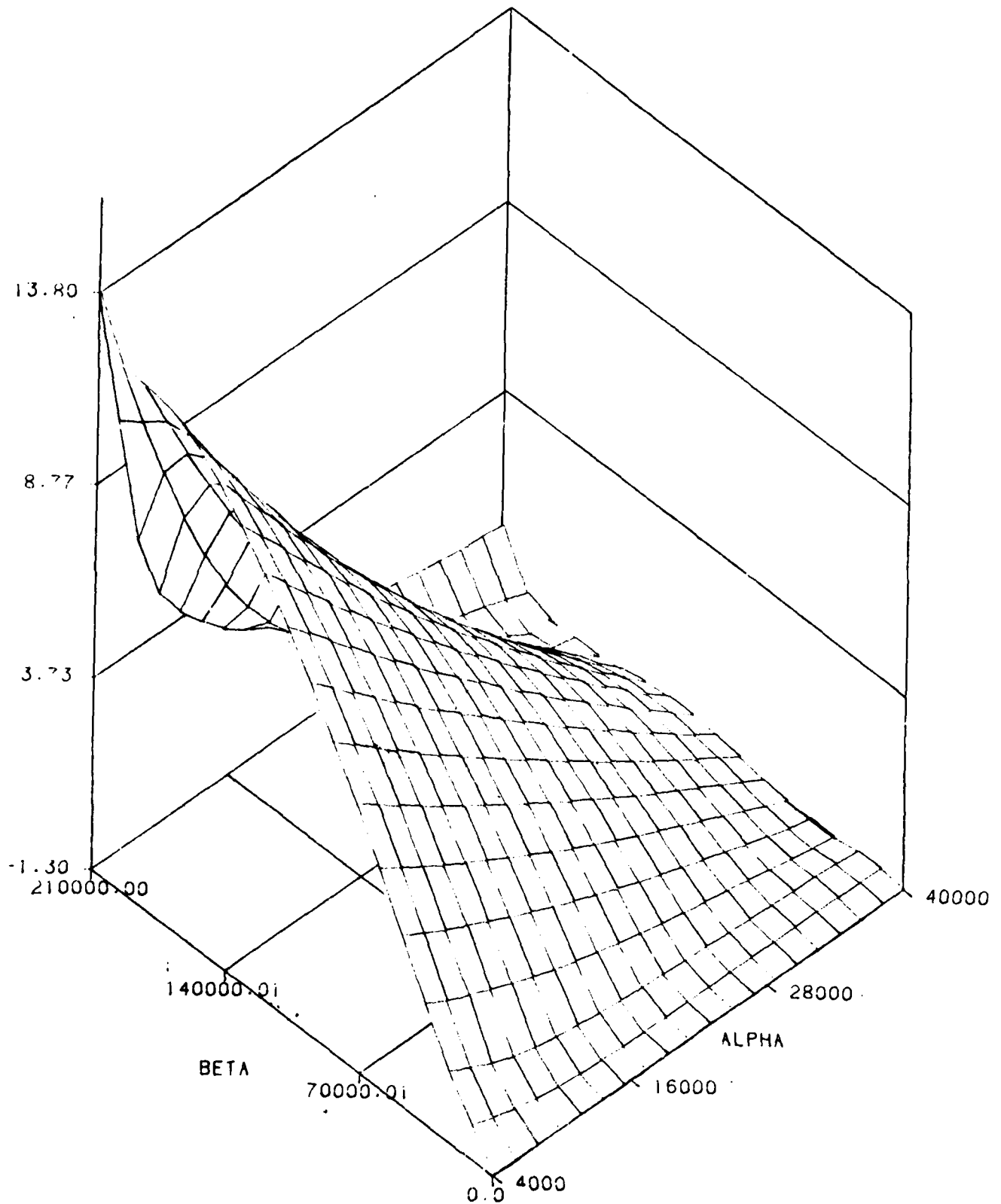


Fig. 3: SURFACE OF $C_{BV}(\alpha, \beta)$

INTRACRANIAL COMPARTMENTAL PULSE WAVE SIMULATION

Shaul Sorek, Ph.D., Jacob Bear, Ph.D. and Zvi Karni, Ph.D, D.Sc.*

Department of Biomedical Engineering and Department of Civil
Engineering, Technion - Israel Institute of Technology
Haifa, 32000, Israel

Abstract

The general solution of the linear compartmental model for the cerebrovascular fluid system with constant resistances and compliances, predicts the pressure waves in the compartments in response to an input pulse wave-arterial and/or jugular. Results are shown for a seven-compartment model and for a sinusoidal arterial pulse wave at a frequency of 1 Hz, with and without fluid drainage from the CSF-compartment.

Keywords: Brain tissue, Compartmental model, Intracranial pressure, Pulse wave.

*Deceased

INTRODUCTION

We chose to simulate the fluid regime in the brain by a seven-compartment model ($N=7$) shown in Figure 1. It is based on Agarwal's (1971) six-compartment model: artery (A), capillary (C), cerebrospinal fluid (F), vein (V), venous sinus (S) and jugular bulb (J), to which we added the brain tissue compartment (B). The model assumes nine resistances and five compliances as shown (Sorek et al, 1986a and b) in the figure (note that the capillary compartment is divided into two parallel one, the choroid plexuses inside the cerebral ventricles and the rest of the capillary system outside the ventricles. Thus, the combined resistances R_{AC} and R_{CV} enter into the calculations).

The mean compartmental pressures are also shown on Fig. 1
 P_A^* (average between systole and diastole) = 100mmHg, $P_C^* = 30$ mmHg,
 $P_F^* = 10$ mmHg, $P_B^* = 9.5$ mmHg, $P_V^* = 9$ mmHg, $P_S^* = 8$ mmHg and $P_J^* = 2$ mmHg.
 The mean arterial flux is $Q_A^* = 750$ ml/min.

The intracranial, compartmental fluid flow of the cerebrovascular system, is governed by the fluid balance equation (Sorek et al. 1986a).

$$\underline{C} \frac{d\underline{P}}{dt} + \underline{Z} \underline{P} = \underline{Q} \quad (1)$$

This is an inhomogeneous, ordinary differential matrix equation of the first rank with respect to time (t). Here, \underline{C} is the $N \times N$ matrix of the intercompartmental compliances; \underline{Z} is the $N \times N$ matrix of the reciprocal intercompartmental resistances, \underline{P} is the $N \times 1$ matrix of the compartmental pressures, \underline{Q} - the $N \times 1$ matrix of the compartmental sources which add fluids to the

intracranial domain from outside. The fluid density is assumed constant.

Equation (1) represents here six linear balance equations, one for each compartment, except the Jugular bulb, in the six variables ($P_A, P_B, P_C, P_F, P_V, P_S$).

The components of the Q matrix are: $Q_A, 0, 0, 0, 0, -Q_J$ where Q_A is the flux input to the artery and Q_J is the flux outflow from the Jugular bulb.

Equation (1) is subject to initial pressure values

$$\underline{P}_{(t=0)} = \underline{P}_0 \quad (2)$$

Basically, the problem is non-linear. By virtue of the homeostatic biocontrol (sensory and endocrinological) feedback mechanisms, the coefficient matrices \underline{C} and \underline{Z} can, and in fact are functions of the pressure vector P and of time, t . There are, however, some passive cases which can be approximated by the linear problem, namely when \underline{C} and \underline{Z} assume constant values. Moreover, even if we deal with the non-linear problem, the solution passes through the linear case. In what follows we will concentrate on the solution of the linear problem, i.e., with constant \underline{C} and \underline{Z} .

In what follows, we assume that the actual values of the \underline{Z} and \underline{C} components are known. These are obtained by solving the appropriate parameter estimation, or inverse, problem (Sorek et al., 1986b).

Actually, in view of the Monro-Kellie doctrine which states that the sum of all compartmental volume changes equals zero,

$$\sum_{n=1}^N \Delta V_n = 0 \quad (3)$$

Only five independent algebraic equations are represented by (1).

In other words, if one compartment changes volume, it has to be at the expense of the volume of its neighbors, all within the cranial vault assumed to be absolutely rigid. This intercompartmental relation is reflected in the expressions for \underline{Z} and \underline{C} .

$$\sum_j C_{ij} = \sum_i C_{ij} = 0 \quad (4)$$

$$\sum_j Z_{ij} = \sum_i Z_{ij} = 0$$

This means that we need external information on the pressure in one of the compartments. Because the pressure artery can be measured, (perhaps in the future by non-invasive methods), we choose to specify it as the additional information.

In the following sections, we bring the numerical results for the compartmental pressure waves that result from an input arterial sine wave with and without a sink (drainage) in the Cerebrospinal Fluid (F) compartment. We will also discuss the physiological and clinical significance of some of these results.

2. COMPARTMENTAL PULSE WAVE FORMS

The choice of a sine wave as the input function Q_A was made for two reasons. First, some of the observed pressure wave forms are indeed close to the sine waves. Secondly, if they do

not correspond to sine waves, but are still periodical, then by Fourier's analysis they can be described as linear combinations of sine waves of different frequency, but of the same periodicity. We also choose the frequency of 1 Hz (1 cycle per second), as base frequency for the calculations. This frequency is close to the cardiac frequency. In the classification of the intracranial pressure wave forms, it corresponds to the Lundberg A-wave (1974), also termed "pulse wave".

$$P_A = P_A^* + P_A' \sin(\omega t) \quad (5)$$

Where $P_A^* = 100\text{mmHg}$ is the average arterial pressure,

$P_A' = 20\text{mmHg}$ is the amplitude of the arterial pulse wave between systole and diastole, and $\omega = 2\pi\text{Hz}$, namely the period of the wave is one second upper part of Fig. 2.

Based on the above considerations on $P_A(t)$, the arterial fluctuating flux was chosen

$$Q_A = Q_A^* + Q_A' \sin(\omega t) \quad (6)$$

where $Q_A^* = 750\text{ml/min}$, and $Q_A' = 125\text{ml/min}$ for $0 < \omega t \leq \pi$ and $Q_A' = 100\text{ml/min}$ for $\pi < \omega t \leq 2\pi$.

Jagular bulb involves no compliance (i.e., its walls are practically non-deformable). Hence the fluid mass balance equation for it is

$$Z_{SJ}(P_S - P_J) = Q_J \quad (7)$$

Due to the absence of compliances in the Jugular bulb, we assume that the pressure in it under unsteady conditions (i.e., in reality) is the same as under quasi steady conditions. The latter are defined by

$$\sum P(t) = Q(t) \quad (8)$$

i.e., deleting the effect of cell compliances. Under quasi steady state conditions

$$Q_A(t) = Q_J(t) \quad (9)$$

We take advantage of this conclusion by combining (7) through (9) to yield the pressure, $P_J(t)$, in the Jugular bulb compartment. Furthermore, knowing the pressure, P_J , we employ (7) to express Q_J in terms of P_J and substitute this expression into $Q_J(t)$ given in (1) and solve for the pressure variations $P(t)$ in the non-steady case.

We should emphasize that (9) is valid only for a quasi-steady state. Under unsteady state conditions, $Q_A(t) \neq Q_J(t)$.

Once a solution for $P_S(t)$, among other pressure values, is obtained one may insert it into (7), which is valid also for unsteady state, to obtain $Q_J(t)$ under unsteady flow conditions. It is also possible to calculate the arterial flux by (eqs. (1), (5))

$$Q_A = Z_{AC}(P_A^* - P_C) + P_A' [Z_{AC} \sin(\omega t) + C_{AB} \omega \cos(\omega t)] + C_{AB} \frac{dP_B}{dt} \quad (10)$$

obtained from (1), that also takes into account the compliances in all of the compartments.

3. EXAMPLES

A number of computer solutions were derived for cases of interest. In all cases, the following values of resistances and compliances were employed (Sorek et al. 1986b).

$R_{AC} = 0.0933 \text{ mmHg/ml/min.}$	$R_{VS} = 0.0013 \text{ mmHg/ml/min.}$
$R_{CF} = 66.667 \text{ mmHg/ml/min.}$	$R_{FS} = 7.6187 \text{ mmHg/ml/min.}$
$R_{CV} = 0.028 \text{ mmHg/ml/min.}$	$R_{SI} = 0.0080 \text{ mmHg/ml/min.}$
$R_{CB} = 13338.0 \text{ mmHg/ml/min.}$	$R_{FB} = 13.338 \text{ mmHg/ml/min.}$
$R_{BV} = 3.33 \text{ mmHg/ml/min}$	
and	
$C_{AB} = 0.0012 \text{ ml/mmHg}$	$C_{FS} = 0.0494 \text{ ml/mmHg}$
$C_{CF} = 0.0357 \text{ ml/mmHg}$	$C_{FB} = 0.02093 \text{ ml/mmHg}$
$C_{BV} = 0.3746 \text{ ml/mmHg}$	

EXAMPLE 1:

Given the phasic pressure $P_A(t)$, as expressed by eqn. (5), and the arterial flux, $Q_A(t)$, as expressed by eqn. (6), the Jugular phasic pressure, $P_J(t)$ and the corresponding pressures $P_C(t)$, $P_B(t)$, $P_F(t)$, $P_S(t)$ and $P_V(t)$ were determined. The results for $P_C(t)$ are shown in Fig. 2. The other pressures are shown in Fig. 3.

It is of interest to note (in Fig. 3) the negative values of $p_j(t)$ during part of the cycle, as a result of the suction action of the cardiac system. This is consistent with clinical observations.

Figure 4 shows the calculated Jugular outflow and arterial inflow. As may be seen from the figure, the two fluxes are equal to each other. The time integrated difference over half a cycle indicates no fluid quantity stored and then released from storage during each cycle.

EXAMPLE 2:

By introducing a shunt into the CSF ventricles (F compartment), CSF can be drained out. We impose drainage rates of .2, .8, 1.4ml/min. Figure 5 shows the resulting pressure, $P_F(t)$. As can be seen, an excessive drainage will lead to a strong distortion of the sinusoidal wave configuration.

EXAMPLE 3:

Upon imposing a constant pressure on the brain tissue, $P_B = 9.5\text{mmHg}$, Figure 6 shows that the pressure curve in the F-compartment will be highly decayed. This fact emphasizes the importance of the pulsational behavior of the pressure within each compartment of the cerebral system.

SUMMARY

The interaction of the various components of the cerebrovascular fluid system is representable by a lumped-parameter compartmental model which takes into account the pressure and volume changes between the compartments.

Presently, only the linear problem is discussed for which the resistances and compliances are assumed constant. The general solution of the linear problem enables us to derive the

non steady pressure waves in all the compartments, also with sink (drainage) function systems.

The computer has been programmed for the general case of an N-compartmental model. The results brought here are for a seven-compartmental (N=7) model: arterial, capillary (including the choroid plexuses), cerebrospinal fluid, brain-tissue, venous-sinus and jugular bulb.

The simulation of the compartmental pressure waves is for an input sinusoidal arterial pressure wave, also termed "pulse wave", of 1 Hz frequency.

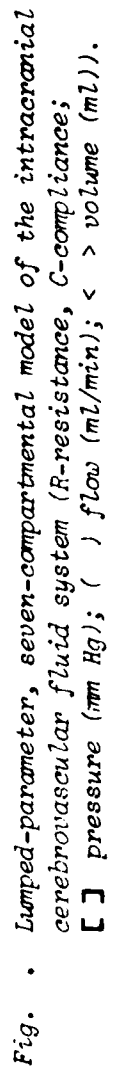
The linear assumptions correspond fairly well to some passive states of long-standing coma and chronic neurologic cases. Even when the problem becomes non-linear and the feedback effects of the bio-control mechanisms - sensory and endocrinological - have to be incorporated into the model, the linear solution will again be the first stage upon which the nonlinear effects are then superimposed. We thus have at our disposal, at least as a first step a method of "computerized simulation" for the intracranial fluid dynamic system the use of which, particularly in cerebral intensive care unit, is self-evident:

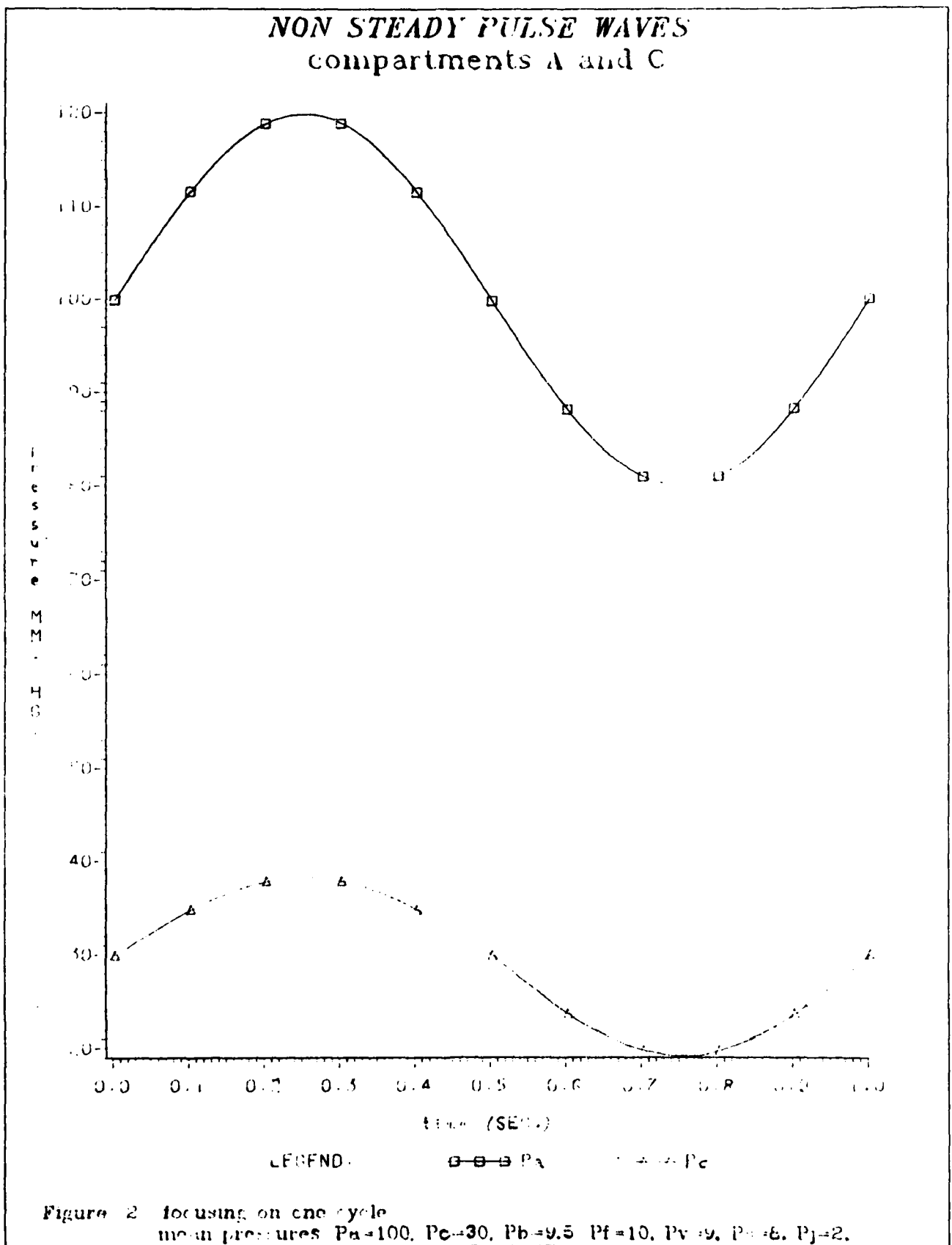
ACKNOWLEDGEMENT

This paper describes research on Modelling Brain Mechanics and Chemical Processes, conducted in the Dept. of Biomedical Engineering, Technion, Israel Institute of Technology, Haifa, Israel. The research is sponsored in part by the U.S. Air Force (grant AFOSR-85-0233). The authors wish to thank the U.S.A.F., the Technion and the Fund for the Promotion of Research at the Technion for their financial support.

REFERENCES

- Agarwal GC: Fluid flow - a special case, in Brown JHV, Jacobs JG and Stark L (eds): Biomedical Engineering. Philadelphia: FA David, 1971, pp. 69-81.
- Hamit HF, et al: Hemodynamic influences upon brain and cerebrospinal fluid pulsations and pressures. J. Trauma 5:174-184, 1965.
- Lundberg N, et al: Non-operative management of intracranial hypertension, in Krayenbuhl H (managing ed): Advances and Technical Standards in Neurosurgery, Vol. 1. Wien: Springer, 1974, pp. 3-59.
- Sorek S, et al: A non-steady compartmental flow model of the cerebrovascular system, 1986a. Submitted for publication.
- Sorek S, et al: Resistances and compliances of a compartmental model of the cerebrovascular system 1986b. Submitted for publication.





NON STEADY PULSE WAVES compartments B, F, S, V and J

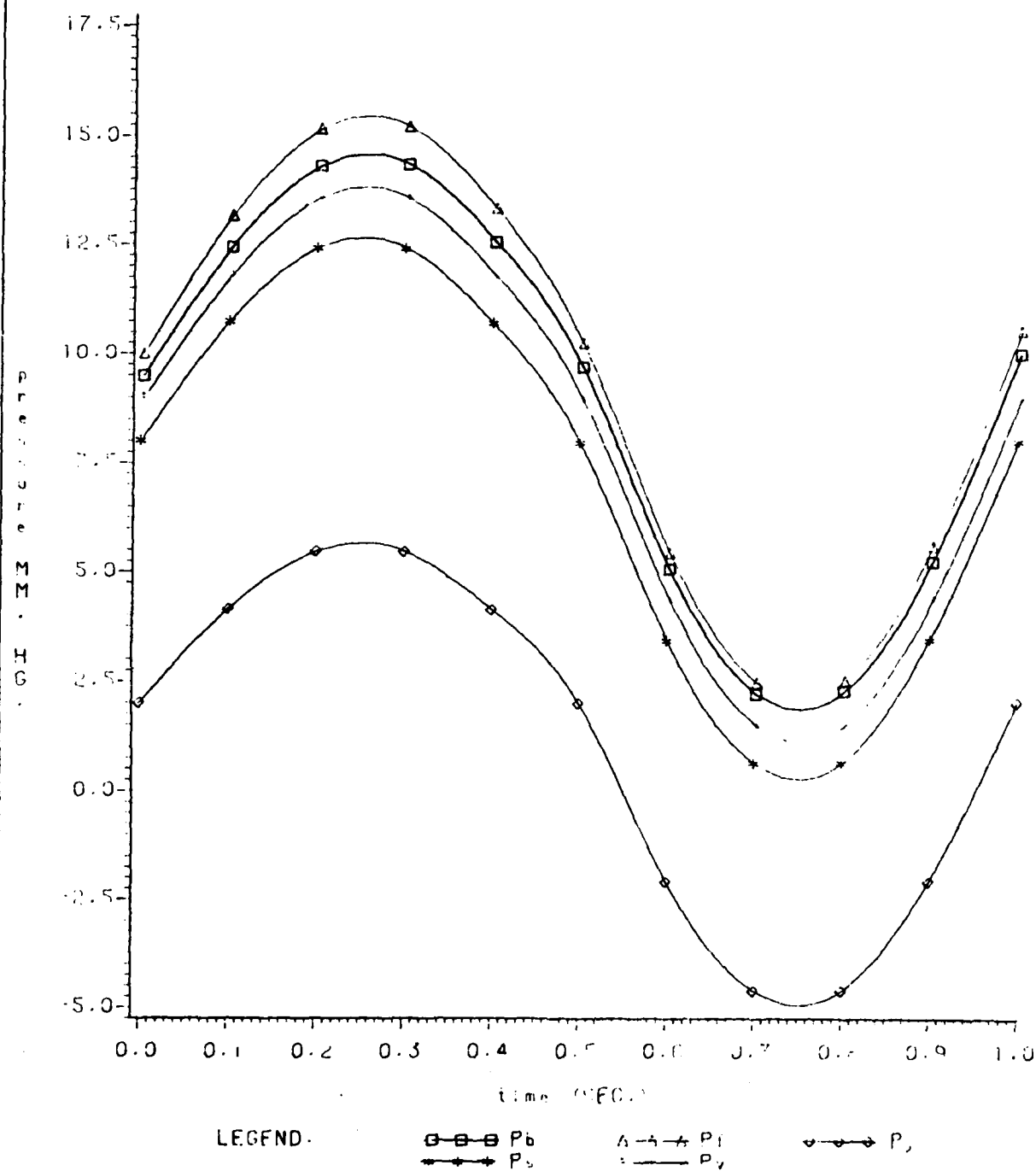
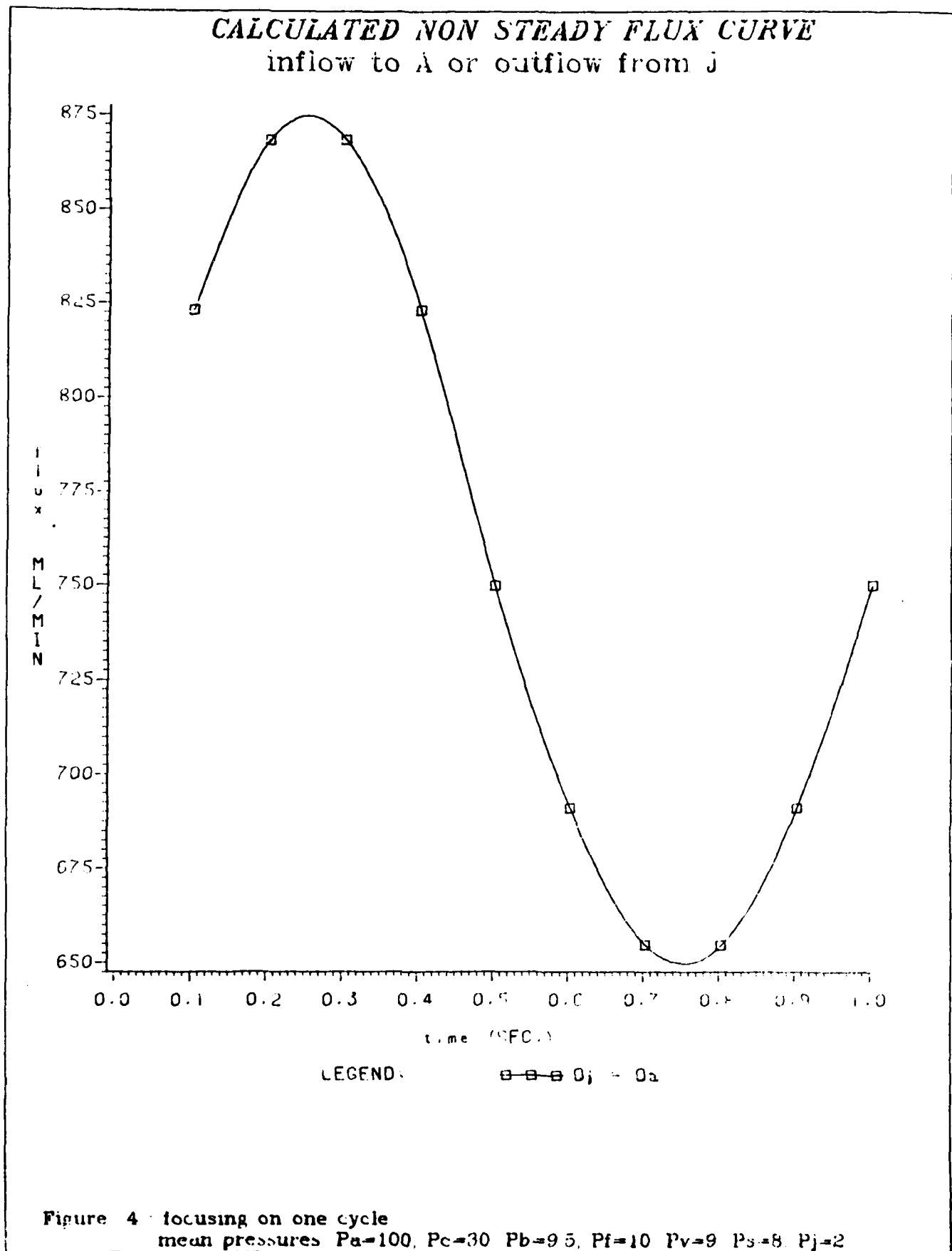


Figure 3 focusing on one cycle
mean pressures $P_a=100$ $P_c=30$ $P_b=9.5$ $P_f=10$ $P_v=9$ $P_s=8$ $P_j=2$



NON STEADY P_f PULSE WAVE with various shunt drainage rates

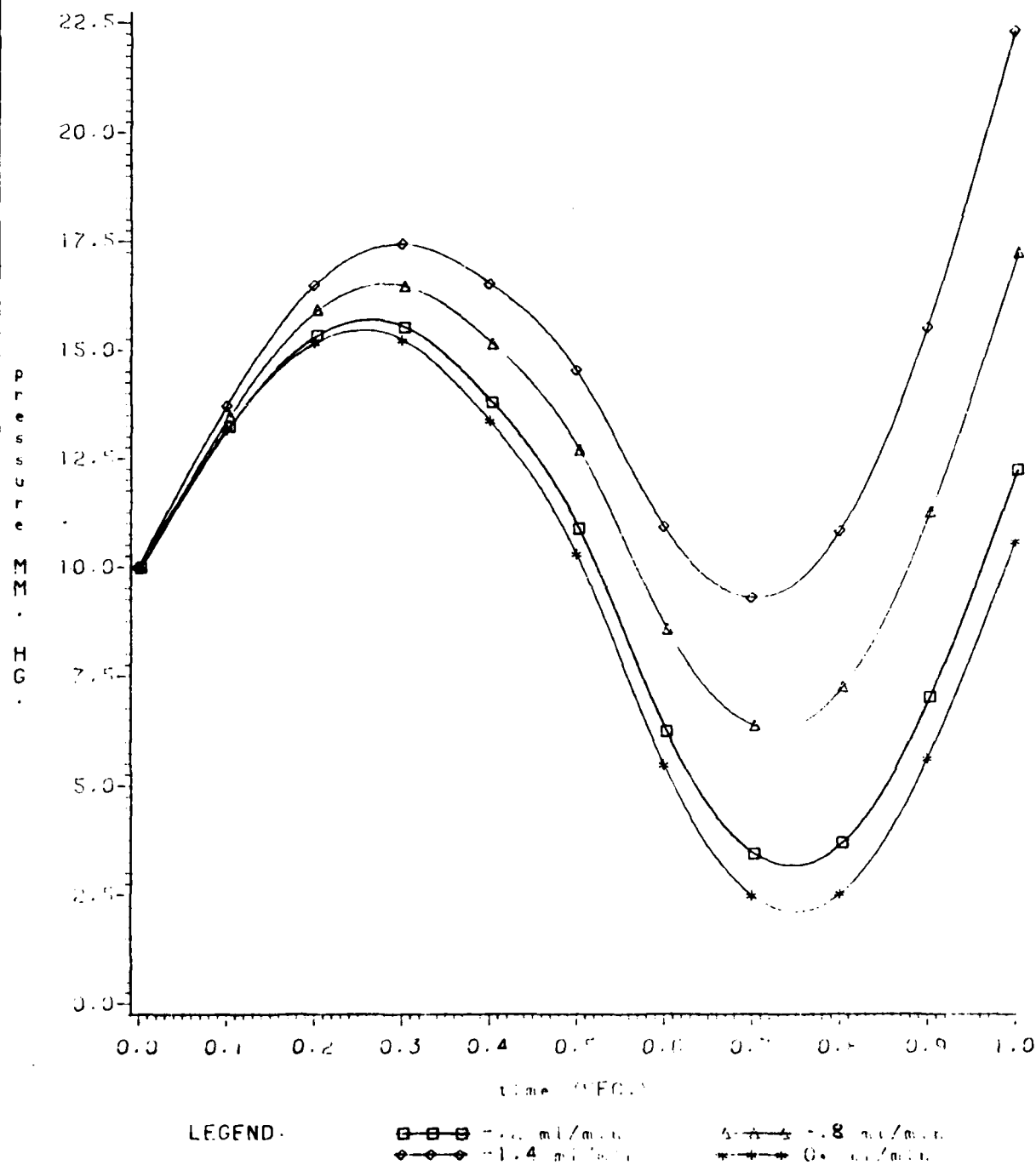


Figure 15: focusing on one cycle

mean pressures $P_a=100$ $P_c=30$ $P_b=9.5$ $P_f=10$ $P_v=9$ $P_s=5$ $P_j=2$

NON STEADY P_f PULSE WAVE constant pressure in compartment b

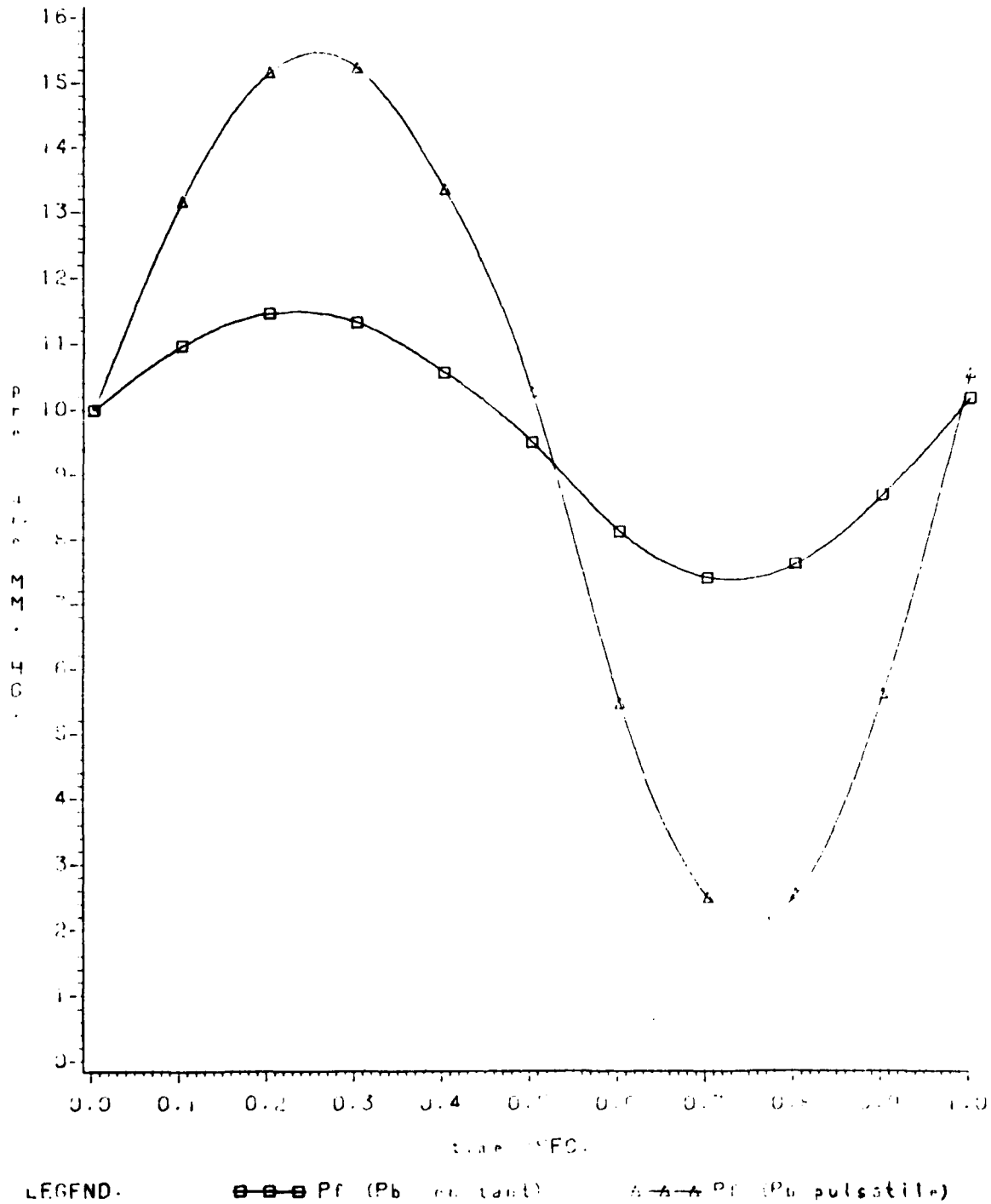


Figure 6 focusing on one cycle
mean pressures $P_a=100$ $P_v=30$ $P_b=9.5$ $P_f=10$ $P_v=9$ $P_c=5$ $P_j=2$

CAN N.P.H. BE CAUSED BY CEREBRAL SMALL VESSEL DISEASE?

A new look based on mathematical model

S. Sorek D.Sc.*, M. Feinsod M.D.** and J. Bear Ph.D.***

ABSTRACT

A novel mathematical model describing the intracranial contents as lumped interacting compartments is presented. The model predicts pressures and fluxes as function of time in the various compartments. Compartmental resistances and compliances are evaluated as step functions of mean pressures and fluxes values. According to this model, normal pressure hydrocephalus may be the result of small vessel disease that abolishes the pressure gradient between the capillaries and brain tissue. Lowering the CSF pressure as by shunting, restores the required compartmental interaction with new values for the resistances and compliances.

Keywords: normal pressure hydrocephalus, ventricular-peritoneal shunt, mathematical model, intracranial pressure, compliances, resistances, fluxes, CSF physiology, capillaries.

*Dept. of Biomedical Engineering

**Dept. of Neurosurgery

***Dept. of Civil Engineering, Technion, Israel Institute of Technology, Haifa, 32000, Israel

INTRODUCTION

The clinical features of Normal Pressure Hydrocephalus (NPH) are well known (Fisher, 1977). The mechanisms of the enlargement of ventricles in adult patients with NPH and the role of intracranial pressure is still speculative (Sorek et al. 1986a, 1986b, 1977). Various tests were suggested in order to obtain a satisfactory prediction which patient will benefit from a shunt procedure but no one gained yet the expected recognition.

In this paper we will report a patient with NPH whose clinical course could be explained by application of a mathematical model of inter relations between brain compartments (Sorek et al. 1986a).

This model may shed light on the still obscure etiology of NPH.

CASE REPORT

A.K. is a 65 year old merchant started exhibiting signs of memory loss and impaired judgement. His appearance continued to be immaculate and small talk did not reveal his deficit. CT Scan demonstrated enlarged ventricular system. The fourth ventricle seemed less involved than the others CSF pressure on lumbar puncture was $120\text{mmH}_2\text{O}$ RHISA cisternography showed rapid entrance of the isotope into the ventricles, it cleared only after more than 48 hours.

A shunting procedure was suggested but the family elected to wait. His condition slowly deteriorated, his dementia became overt and he was confined to home. Six months later another consultation was sought now because of progressive ataxia. Repeat CT revealed further enlargement of the hydrocephalus. Only 4 months later, when the patient was confined to bed due to severe ataxia, incontinence and speechlessness did the guardian permit operation. CSF pressure at that time was $115\text{mmH}_2\text{O}$.

A ventriculo-peritoneal shunt with an opening pressure of $90\text{mmH}_2\text{O}$ was installed. The postoperative course was remarkable for the rapid return of speech, memory, ambulation and continence. A month after the operation the patient returned to his business and several weeks later reported success in complicated financial considerations and decisions. CT scan demonstrated small, well drained ventricles.

Eight months later he started to deteriorate and within 3 weeks he was approaching his pre-operative condition. CT scan revealed, again, enlarged ventricles (Fig. 1). Shunt malfunction was presumed but surgical revision failed to demonstrate any

obstruction and did not alter his condition. Only after installment of a new shunt system with a low opening pressure (60mmH₂O) did the patient improve. Once again, his recuperation was remarkable; he is back in finances and doing well. CT scan (Fig. 2) is evident for well drained ventricular system.

AD-A171 483

MODELS OF CEREBRAL SYSTEM MECHANICS(U) TECHNION -
ISRAEL INST OF TECH HAIFA S SOREK ET AL 20 JUL 86
SCIENTIFIC-2 BOARD-TR-86-07 AFOSR-85-0233

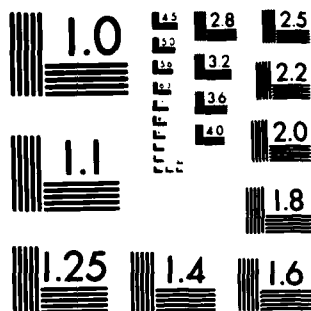
2/2

UNCLASSIFIED

F/G 6/16

NL

END
DATE
FILMED
10-86



MICROCOPY RESOLUTION TEST CHART
NATIONAL BUREAU OF STANDARDS-1963-A

DISCUSSION

In a series of recent papers (Karni et al. 1986, Sorek et al. 1986a,b,c) a model depicting the brain as an assembly of interacting compartments was put forward.

The model (Fig. 3) solves the distribution of pressures, fluxes, resistances and compliances within these compartments.

In this model we attempt to define each intracranial structure as a cell. Seven such cells - arteries (A), capillaries and choroid plexus (C), veins (V), venous sinuses, (S), ventricular cerebrospinal fluid (F), jugular bulb (J) and brain tissue (B) are lumped together and their interactions are described by a series of flux balance equations (Sorek et al. 1985a).

As an example let us consider the equation describing flux balance for the capillary compartment.

$$\frac{P_A - P_C}{R_{AC}} = \frac{P_C - P_F}{R_{CF}} + \frac{P_C - P_B}{R_{CB}} + \frac{P_C - P_V}{R_{CV}} + C_{CF} \frac{d}{dt} (P_C - P_F) \quad (1)$$

where

P_A = arterial pressure

P_C = capillary pressure

P_F = CSF pressure (ventricular)

P_B = brain tissue pressure

P_V = venous pressure

R_{AC} = resistance to flow between arteries and capillaries

R_{CF} = resistance to flow between capillaries and ventricular CSF

R_{CB} = resistance to flow between capillaries and brain tissues

R_{CV} = resistance to flow between capillaries and venous

C_{CF} = compliance factor between choroid plexus and ventricular CSF

$\frac{d}{dt}(P_C - P_F)$ = time derivative of the pressure difference between
choroid plexus and ventricular CSF

As a first approximation the resistance and compliances were considered as mean effective values i.e., constants. The overall matrix of resistances and compliances were evaluated via an inverse procedure (Sorek et al. 1986a).

Note that equation (1) describes the flux balance in steady as well as in non steady situations. The cells may be rigid giving a flux term expressed by pressure differences divided by resistance or contractile yielding a flux which is the product of compliance and time changes of pressure differences.

In the course of evaluating the resistances of the model it was shown that a situation leading to evolution of a 'normotensive' hydrocephalus may take place.

The usual accepted mechanism for development of hydrocephalus is defective absorption of CSF in the venous sinus. In our mathematical model this will be expressed by $R_{FS} = \infty$ or $Z_{FS} = 1/R_{FS} = 0$ (where R_{FS} is the resistance to flow between the ventricular CSF compartment and venous sinus compartment and where Z_{FS} stands for the conductance between these compartments).

However it was shown (Sorek et al. 1986a) that at the same time the resistance (R) between capillaries (C) and brain tissue (B) attain infinite values $R_{CB} = \infty$

In the set of equations for the solution of the model resistances we have relations between fluxes, pressure differences and coefficients α and β .

$$\alpha = \frac{R_{FB}}{R_{VS}} \quad (2)$$

$$\beta = \frac{R_{FB}}{R_{CB}} \quad (3)$$

For instance the relation for Z_{CB} (conductance between capillaries and brain tissue) and Z_{FS} (conductance between ventricular CSF and venous sinus) is as follows

$$Z_{CB} = \frac{\beta(Q_A^* - Q_F^*)}{\alpha(P_V^* - P_S^*) - (P_F^* - P_B^*)} \quad (4)$$

$$Z_{FS} = \frac{\alpha(P_V^* - P_S^*)Q_F^* - (P_F^* - P_B^*)Q_A^*}{(P_F^* - P_S^*)[\alpha(P_V^* - P_S^*) - (P_F^* - P_B^*)]} \quad (5)$$

where ()^{*} denotes mean effective values

Q_A flux entering the arterial compartment

Q_F flux entering the CSF compartment = CSF generation

Q_F may be described by

$$Q_F = \frac{P_C - P_F}{R_{CF}} \quad (6)$$

A solution of the set can be attained when we allow $\beta=0$. An accompanying condition $Z_{FS}=0$ will still yield a possible solution.

Thus the following mathematical equations now exists

$$Z_{CB}=0 \quad (R_{CB} = \infty) \quad (7)$$

$$Z_{FS}=0 \quad (R_{FS} = \infty) \quad (8)$$

$$\alpha Q_F^*(P_V^* - P_S^*) - Q_A^*(P_F^* - P_B^*) = 0 \quad (9)$$

Equation (7) is the mathematical representation of a flow impediment between the capillaries and the brain tissue. The condition $Z_{CB}=0$ may be regarded as a precondition activating the NPH situation represented by equations (8) and (9).

Conditions expressed by equations (8) and (9) indicate blockage of CSF transfer from the ventricles to the venous sinus. As this conditions do not affect production of CSF by the choroid plexus ($Q_F=0$) compartment (F) will expand. The presence of compliances C_{FB} , C_{FS} and C_{CF} (Fig. 3) allow for the expansion without increase of pressure i.e. NPH.

Thus, in a situation where the flow from capillaries to brain tissue is impaired as may be the case arteriosclerotic cerebrovascular disease and especially in small vessel disease in the aged, a NPH may develop.

In order to overcome the NPH situation one has to interfere with the balance as stated in equation (9). By lowering the CSF pressure P_F i.e. shunting procedure, the previous conductivities may change in a step fashion accommodating the new mean pressures

and fluxes as indicated by equations (4) and (5). Note that according to equation (9) such step changes may also take place when changing other factors e.g. P_v , P_s , etc. Thus removal of CSF will also yield a change in capillary to brain tissue transfer which may explain the improvement in neurological functions after shunting. It was shown that CSF drainage in hydrocephalic patients increase regional cerebral blood flow (Symon and Hingzpeter, 1977). If the small vessel disease continues, equation (9) may again prevail and a further decrease in CSF pressure is necessary in order to accomodate for the new resistances and complainces as could be the case in our patient.

ACKNOWLEDGEMENT

This paper describes research on Modelling Brain Mechanics and Chemical Processes, conducted in the Dept. of Biomedical Engineering, Technion, Israel Institute of Technology, Haifa, Israel. The research is sponsored in part by the U.S. Air Force (grant AFOSR-85-0233). The authors wish to thank the U.S.A.F., the Technion and the Fund for the Promotion of Research at the Technion for their financial support.

REFERENCES

- C.M. Fisher, The clinical picture in occult hydrocephalus. Clin. Neurosurgery, 24:270-284, 1977.
- Z. Karni, T. Bear, S. Sorek and Z. Pinczewski "A quasi-steady state compartmental model of intracranial fluid dynamics", 1986 (submitted).
- R.G. Ojeman and P.M. Black, Hydrocephalus in adults. In Neurological Surgery, Ed. J.R. Youmans, Vol. 3, Chap. 37, pp. 1423-1435, W.B. Saunders Co. 1982.
- S. Sorek, J. Bear and Z. Karni "A non-steady compartmental flow model of the cerebrovascular system", 1986a (submitted).
- S. Sorek, J. Bear and Z. Karni, "Intracranial compartmental pulse wave simulation", 1986b (submitted).
- S. Sorek, J. Bear and Z. Karni, "Compartmental resistance and compliances of the cerebrovascular fluid system" 1986c (submitted).
- L. Symon and T. Hinzpeter, The enigma of normal pressure hydrocephalus: tests to select patients for surgery and to predict shunt function. Clin. Neurosurg. 214:285-315, 1977.



FIG. 1 : ENLARGED LATERAL VENTRICLES INSPITE OF A PATENT MEDIUM PRESSURE VENTRICULO PERITONEAL SHUNT.



FIG. 2 : WELL DRAINED VENTRICLES AFTER INSTALLMENT OF LOW PRESSURE V-P SHUNT.

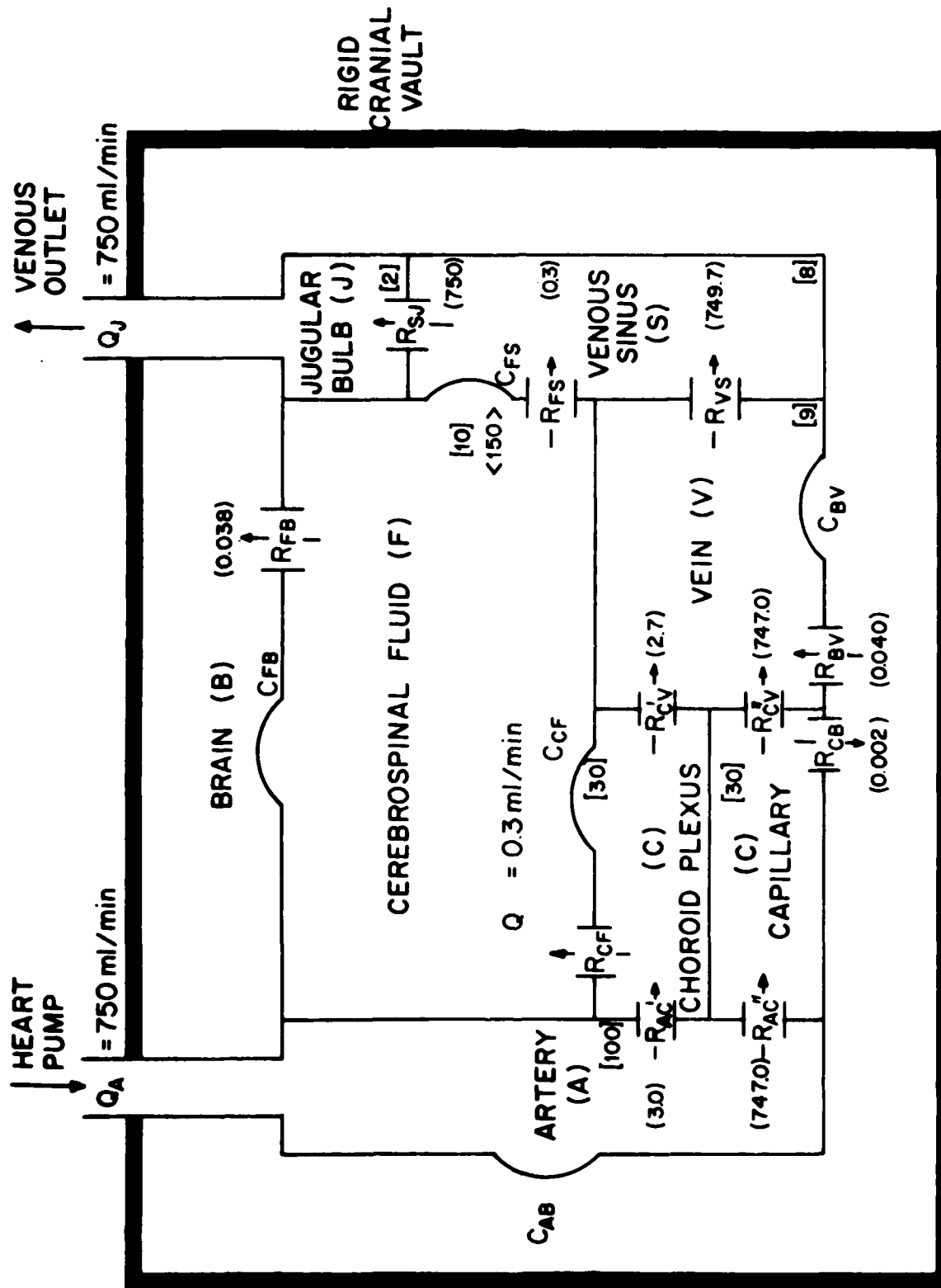


Fig. 3. Lumped-parameter, seven-compartmental model of the intracranial cerebrovascular fluid system (R -resistance, C -compliance; [] pressure (mm Hg); () flow (ml/min); < > volume (ml)).

A SIMPLE CONTINUUM MODEL OF BRAIN TISSUE DEFORMATION

by

S..Sorek*, J. Bear** and Z. Karni***

ABSTRACT

The continuum approach is employed for modelling the distribution of deformation and stress within the brain tissue visualized as the domain between two concentric ellipsoids having the same axes. Phasic pressures in the Jugular Bulb and CSF ventricles, estimated by a compartmental model, provide the conditions on the outer and inner boundaries, respectively. The simulation yields phasic stress and deformation which are consistent with clinical observations.

Keywords: brain tissue, CSF ventricles, jugular bulb, Hook's law, compartmental phasic pressures

*Dept. of Biomedical Engineering

**Dept. of Civil Engineering

***Deceased

Technion, IIT

Haifa, 32000, Israel

INTRODUCTION

Changes in pressure in both the jugular bulb and in CSF ventricles, produce stress variations, accompanied by deformation, within the brain tissue. Our objective in this paper is to obtain estimates of stress and deformation distribution within the brain. To achieve this goal, a simplified continuum model of the brain is introduced and investigated.

In the literature on the biomechanics of head impacts, much use of spherical and oblate spheroidal coordinates is made. The skull is idealized as a rigid sphere with an opening that stimulates the foramen magnum, while the spinal dura mater is idealized as a cylindrical membrane fitted to the foramen magnum (Liu, 1978). The intradural content of the central nervous system (CNS) fluid-filled continuum is regarded by some as a single-phase, quasistatic incompressible fluid in a two compartment (skull and spinal dura-mater) structure, or as a single-phase compressible elastic fluid possessing a single "averaged" bulk modulus and a sheer modulus (Pollack and Boshes, 1936; Ommaya and Hirsch, 1971; Lofgren and Zwetnow, 1973; Goldsmith, 1972; Marmarou, 1973; King and Chou, 1976). Hakim et al. (1976) stipulated the case of static equilibrium to find the stress in the brain tissue, regarding the cranial vault as a hollow sphere with ventricles in the middle. The inner and outer boundary conditions were the pressure value of CSF in the ventricles and at the subarachnoidal space.

Apart from the spherical models, other curvilinear mappings were suggested such as a truncated shell of revolution (Schumacher, 1978).

Our present attempt is to revive Leonardo da Vinci's idea, based on his anatomical sketches (Fig. 1a) (cf. Russel, 1959), and consider the domain between two ellipsoids, the inner ventricular ependyma and the outer pia mater, as an approximate geometry of the cranial vault.

The brain tissue is assumed to be a homogeneous and isotropic, single-phased material.

In an earlier work, Sorek et al. (1986a,b,c), simulated the cerebrovascular flow regime in a compartmental model cerebral system (Fig. 2). They derived the non-steady phasic pressure and flux waves associated with the artery (A), capillary and choroid plexus (C), CSF ventricles (F), veins (V), brain tissue (B), venous sinus (S), and jugular bulb (J). Here we will use the phasic pressures in the CSF ventricles and in jugular bulb obtained in that study as an inner and outer boundary conditions respectively, imposed on the considered brain tissue domain.

Clinical data show that the material comprising of this organ is deformable. However, it is not strictly elastic, since under external stresses, it exhibits also the delayed property of viscosity (Pamidi, 1976). Nevertheless, as a first approximation, we choose here an elastic stress-strain constitutive relation for this material.

ASSUMPTIONS

The following assumptions underline the constructing of the model simulating stress and deformation of the brain tissue:

1. The brain tissue configuration is approximated as a shell between two prolated spheroidal bodies (Fig. 1b). Its inner (CSF ventricles) and outer surfaces are obtained by rotating ellipses about their common major axes. The relation between a cartesian system (X,Y,Z) and the prolate spheroidal coordinate (ξ, η, ψ) system is given by

$$\bar{x} = a \sinh(\xi) \sin(\eta) \cos(\psi) \quad (1.1)$$

$$y = a \sinh(\xi) \sin(\eta) \sin(\psi) \quad (1.2)$$

$$z = a \cosh(\xi) \cos(\eta) \quad (1.3)$$

where, $\xi \geq 0$, $0 \leq \eta \leq \pi$; $0 \leq \psi < 2\pi$. The associated scale coefficients (h_ξ, h_η, h_ψ) are expressed by

$$h_\xi^2 = h_\eta^2 = a^2 [\sinh^2(\xi) + \sin^2(\eta)] \quad (2.1)$$

$$h_\psi^2 = a^2 \sinh^2(\xi) \sin^2(\eta) \quad (2.2)$$

2. The equations of the outer and inner ellipsoids are given respectively by $\xi = \xi_0 = \text{const.}$ and $\xi = \xi_1 = \text{const.}$

3. The brain tissue material is assumed isotropic, homogeneous and elastic, obeying Hook's Law, which can be expressed by

$$\epsilon_{ij} = \frac{1+\mu}{E} \sigma_{ij} - \frac{\mu}{E} \delta_{ij} \sigma_{kk} \quad (3)$$

where μ = Poisson's ratio, E =Young's Modulus, δ_{ij} =Kronecker delta, ϵ_{ij} =strain tensor, σ_{ij} =stress tensor and σ_{kk} =diagonal stress tensor.

4. The inner and outer boundaries are loaded by spatially uniform pressures in the CSF ventricles and in the jugular bulb, respectively.

5. At each point within the considered domain, we can determine the radius of curvature of the ellipsoid $\xi = \text{const.}$ passing through that point. We then assume that deformations are mainly along the radius of curvature. Also it is assumed that the organ is undergoing small deformations. The compatible relation between strain and deformation is expressed by

$$\epsilon_{ij} = \frac{1}{2} (u_{i,j} + u_{j,i}) \quad (4)$$

where u_i is the deformation in the i direction and $u_{i,j}$ is the derivative of u_i with respect to the j coordinate.

5. Bending moments and shear forces are neglected because of the symmetries involved in the assumed configuration.

6. Body forces (e.g., due to gravity) are neglected.

We may now write the force balance equation in the (ξ, η, ψ) coordinate system. Note that the prevailing stresses are normal to the surface, $\sigma_{\xi\xi}$, which is balanced by the components of the longitudinal stress, $\sigma_{\eta\eta}$, and the latitudinal stress $\sigma_{\psi\psi}$.

FORCE BALANCE EQUATION

Let us first evaluate the length of the mean semimajor and semiminor axes of the CSF ventricles visualized as a prolate spheroidal. Let a_j, b_j and c_j denote the semi-axes of the Jugular bulb and a_F, b_F, c_F denote those of the CSF ventricles. For the outer surface, we introduce the estimates. $a_j = 9\text{cm.}$; $b_j = 6\text{cm.}$

$C_J = 3\text{cm.}$ (i.e., a volume of approximately 680ml.).

The volume of the CSF ventricles is taken as
 $V_F = 150\text{cm.}^3$, i.e.,

$$V_F = \frac{4}{3} \pi a_F b_F c_F = 150 \quad (5)$$

We now assume that the inner and outer prolate spheroids are similar. This means that

$$b_F = 2c_F \quad (6)$$

$$a_F = 3c_F \quad (7)$$

Hence, by virtue of equations (5), (6) and (7) we obtain

$$a_F = 5.4\text{cm.} \quad b_F = 3.6\text{cm.} \quad c_F = 1.8\text{cm.}$$

As was stated above, the deformation is a function of the ξ coordinate only. Any volume element (Fig. 3), is subject to radial $F_{\xi\xi}$, longitudinal $F_{\eta\eta}$ and latitudinal $F_{\psi\psi}$ forces. The lengths of the volume element edges are $h_\xi d_\xi$, $h_\eta d_\eta$, and $h_\psi d_\psi$.

By writing a force balance along the radius of curvature, we obtain the resultant in that direction in the form.

$$2F_{\psi\psi} \sin\left(\frac{d\psi}{2}\right) + 2F_{\eta\eta} \sin\left(\frac{d\eta}{2}\right) = dF_{\xi\xi} \quad (8)$$

For small angles $d\psi \ll 1$ and $d\eta \ll 1$ an equivalent form of (8), written in terms of stresses is

$$\frac{d}{d\xi} (\sigma_{\xi\xi} h_{\psi} h_{\eta}) - \sigma_{\psi\psi} h_{\xi} h_{\eta} - \sigma_{\eta\eta} h_{\psi} h_{\xi} = 0 \quad (9)$$

One may obtain (9) by replacing the forces in (8) by stresses multiplied by the appropriate areas.

Equation (9) is subject to the following conditions on the external ($\xi = \xi_J$) and internal ($\xi = \xi_F$) surfaces.

$$\sigma_{\xi\xi} = -P_F \quad \text{at} \quad \xi = \xi_F \quad (10.1)$$

$$\sigma_{\xi\xi} = -P_J \quad \text{at} \quad \xi = \xi_J \quad (10.2)$$

We note that because of symmetry, the resultants in the other two directions vanish.

Recalling the assumption that the displacement u , is normal to the $\xi = \text{constant}$ surface (i.e., $u = u(\xi)$) and that these displacements are very small, we now stipulate the condition

$$u = 0 \quad \text{at} \quad \xi = 0 \quad (11)$$

In view of equations (1), (2), (4) and (11), we obtain

$$\epsilon_{\xi\xi} = \frac{du}{d\xi} \quad (12)$$

$$\epsilon_{\eta\eta} = \frac{\int_0^\pi [h_{\eta(\xi+u)} - h_{\eta(\xi)}] d\eta}{\int_0^\pi h_{\eta(\xi)} d\eta} \approx \frac{(1+du/d\xi)^2 (\xi+u)^2 - \xi^2}{\xi^2} \quad (13)$$

$$\approx 2 \frac{u}{\xi}; \quad \left(\frac{du}{d\xi} \ll 1 \right)$$

$$\epsilon_{\psi\psi} = \frac{\int_0^\pi [h_{\psi(\xi+u)} - h_{\psi(\xi)}] d\psi}{\int_0^\pi h_{\psi(\xi)} d\psi} \approx \frac{1+du/d\xi)(\xi+u)-\xi}{\xi} \approx \frac{u}{\xi} \quad (14)$$

We will relate strain to stress by Hook's constitutive law (equation (3)). By virtue of equations (3) and (12)-(14), we therefore obtain

$$\frac{du}{d\xi} = \frac{1}{E} [\sigma_{\xi\xi} - \mu(\sigma_{\eta\eta} + \sigma_{\psi\psi})] \quad (15)$$

$$2 \frac{u}{\xi} = \frac{1}{E} [\sigma_{\eta\eta} - \mu(\sigma_{\psi\psi} + \sigma_{\xi\xi})] \quad (16)$$

$$\frac{u}{\xi} = \frac{1}{E} [\sigma_{\psi\psi} - \mu(\sigma_{\xi\xi} + \sigma_{\eta\eta})] \quad (17)$$

Equating equations (16) and (17), we obtain

$$\sigma_{\psi\psi} = A\sigma_{\eta\eta} + B\sigma_{\xi\xi} \quad (18)$$

where

$$A = \frac{1+2\mu}{2+\mu} \quad (19.1)$$

$$B = \frac{\mu}{2+\mu} \quad (19.2)$$

Substituting equation (18) into (9) yields,

$$\sigma_{\eta\eta} = C \frac{d\sigma_{\xi\xi}}{d\xi} + D\sigma_{\xi\xi} \quad (20)$$

where

$$C = \frac{h_{\psi}}{h_{\psi} + Ah_{\eta}} \quad (21.1)$$

$$D = \frac{\frac{d}{d\xi} (h_\psi h_\eta) - B h_\xi h_\eta}{h_\xi (h_\psi + A h_\eta)} \quad (21.2)$$

Differentiating (16) with respect to ξ , equating the result to (15), substituting (18) and (20), we obtain

$$M \frac{d^2 \sigma_{\xi\xi}}{d\xi^2} + K \frac{d\sigma_{\xi\xi}}{d\xi} + W \sigma_{\xi\xi} = 0 \quad (22)$$

where

$$M = C \xi \quad (23.1)$$

$$K = \xi \frac{dC}{d\xi} + \frac{1+2\mu}{1-\mu} C + D - \frac{\mu}{1-\mu} \quad (23.2)$$

$$W = \xi \frac{dD}{d\xi} + \frac{1+2\mu}{1-\mu} D - \frac{2+\mu}{1-\mu} \quad (23.3)$$

We then solve equation (22) together with boundary conditions (10), for $\sigma_{\xi\xi} = \sigma_{\xi\xi}(\xi)$. With the calculated $\sigma_{\xi\xi}$, we evaluate $\sigma_{\eta\eta}$, $\sigma_{\psi\psi}$ and u as functions of ξ , using equations (20), (18) and (17) respectively. All calculations are done numerically.

IMPLEMENTATION

Employing equations (1), with the values a, b , and c of the semi-axis, of the inner and outer surfaces, we calculate $\xi_F = 0.454$, $\xi_J = 0.689$ and $\psi_F = \psi_J = 26.5^\circ$, at $\eta_F = \eta_J = 90^\circ$. We then impose the phasic pressures P_F and P_J , evaluated by Sorek et al. (1986), using compartmental modelling, as boundary conditions (equations (10)) to calculate phasic variations of stresses and deformation as distributed along .

Figure 4 depicts the mean distribution of stresses $\sigma_{\xi\xi}$, $\sigma_{\eta\eta}$, $\sigma_{\psi\psi}$ and deformation u due to mean pressures $P_F = 10 \text{ mmHg}$ and $P_J = 2 \text{ mmHg}$. Note that compression stress in $\sigma_{\xi\xi}$ result in tension in the longitudinal, $\sigma_{\eta\eta}$, and latitudinal, $\sigma_{\psi\psi}$, stresses. Also note the hyperbolic characteristic for deformation and stresses, demonstrating a decay in intensity from the CSF ventricles surface to the outer brain tissue surface. Figures 5 and 6 show $\sigma_{\xi\xi}$, and u surfaces as functions of time and location, depicting the pulsational nature of stresses and deformation. The range of deformation as described by figure 6 is consistent with reported clinical observation (Allen et al. 1983).

CONCLUSION

A continuum model was developed and employed to simulate stress and deformation in an elastic ellipsoidal shaped brain tissue. The results of a compartmental model were employed to account for phasic pressures used as boundary conditions in the model presented herewith. Although the model is basically a 1-D and simplified results, are consistent with clinical

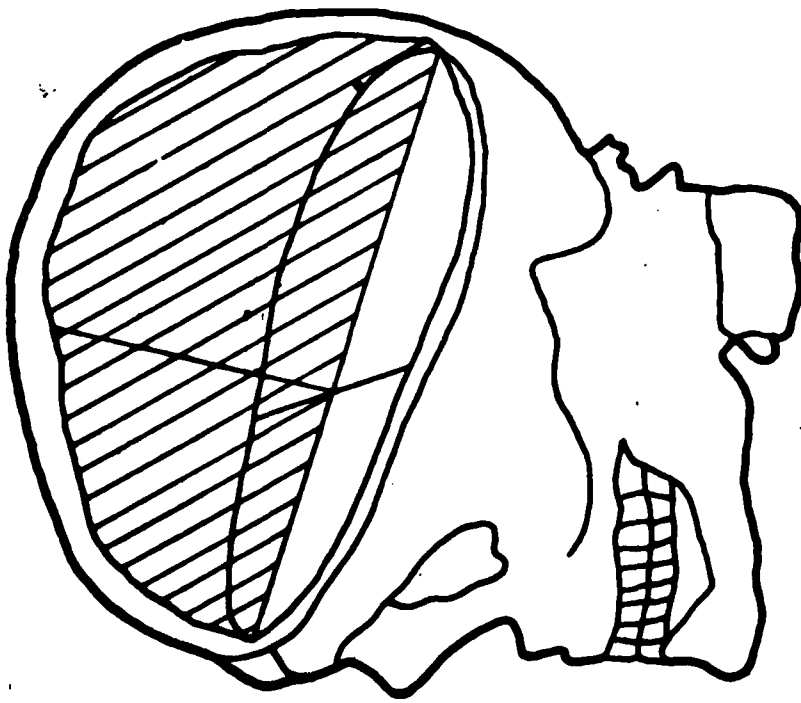
observations. Modifications such as the use of a non-elastic stress-strain constitutive law, may yield better predictions of stress and deformation distribution in time and space.

ACKNOWLEDGEMENT

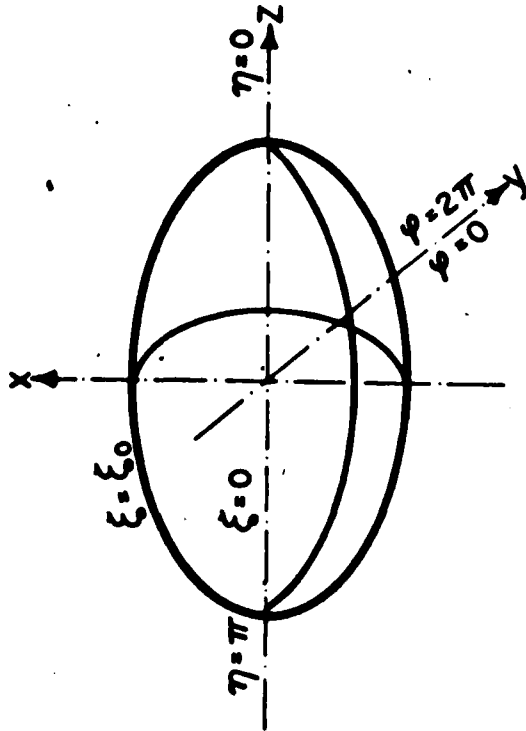
This paper describes research on Modelling Brain Mechanics and Chemical Processes, conducted in the Dept. of Biomedical Engineering, Technion, Israel Institute of Technology, Haifa, Israel. The research is sponsored in part by the U.S. Air Force (grant AFOSR-85-0233). The authors wish to thank the U.S.A.F., the Technion and the Fund for the Promotion of Research at the Technion for their financial support.

REFERENCES

- Marmarou, A. (1973) A theoretical model and experimental evaluation of the cerebrospinal fluid system. Ph.D. disseration presented to Drexel University, Phila, Pa.
- Ommaya, A.K. and Hirsch, A.E. (1971) Tolerances for cerebral concussion from head impact and whiplash in primates. *J. Biomech.* 4:13-21.
- Pamidi, M.R. and Advani, S.H. (1978) Nonlinear constitutive relations for human brain tissue. *Trans. ASME*, 100:44-48.
- Pollack, K.J. and Boshes, B. (1936) Cerebrospinal fluid pressure. *Arch. Neurol. Psych.* 36:931-974.
- Schumacher, G.H. (1978) Biomechanik des Schadels-Theoretische untersuchungen und praktische kompressionsversuche. *Folia anatomica ingoslavica*, 7:39-48.
- Sorek, S., Bear, J. and Karni, Z. (1986a) A non-steady compartmental flow model of the cerebrovascular system. Submitted for publication.
- Sorek, S., Bear, J. and Karni, Z. (1986b) Intracranial compartmental pulse wave simulation. Submitted for publication.
- Sorek, S., Bear, J. and Karni, Z. (1986c) Resistances and compliances of a cerebrovascular compartmental model. Submitted for publication.



(A)



(B)

fig. 1: A. Leonardo da Vinci sketch of the carniun.
 B. Prolate spheroidal coordinate (ξ, η, φ) system.

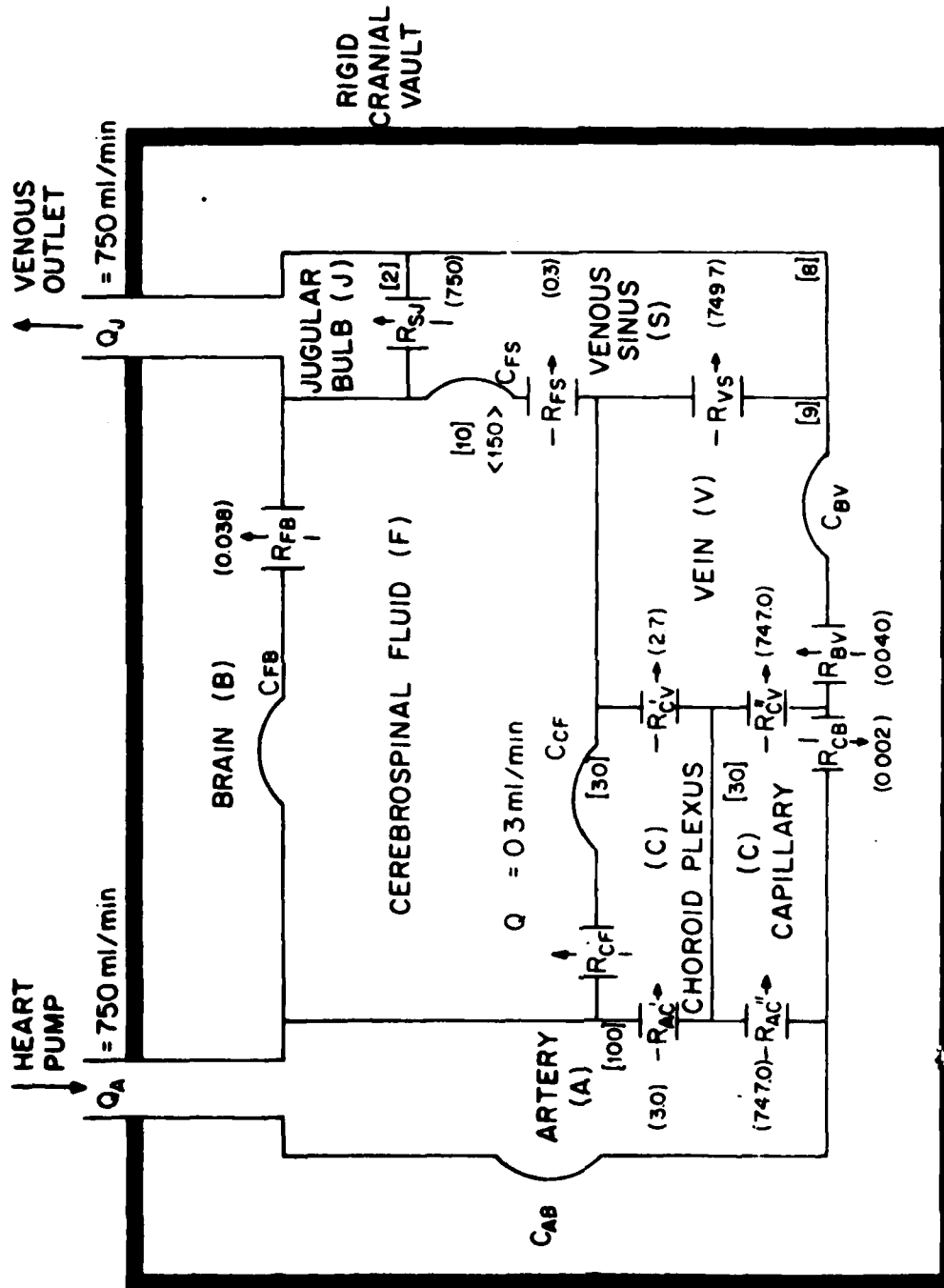


Fig. 2. Lumped-parameter, seven-compartmental model of the intracranial fluid system (R-resistance, C-compliance; [] pressure (mm Hg); () flow (ml/min); < > volume (ml)).

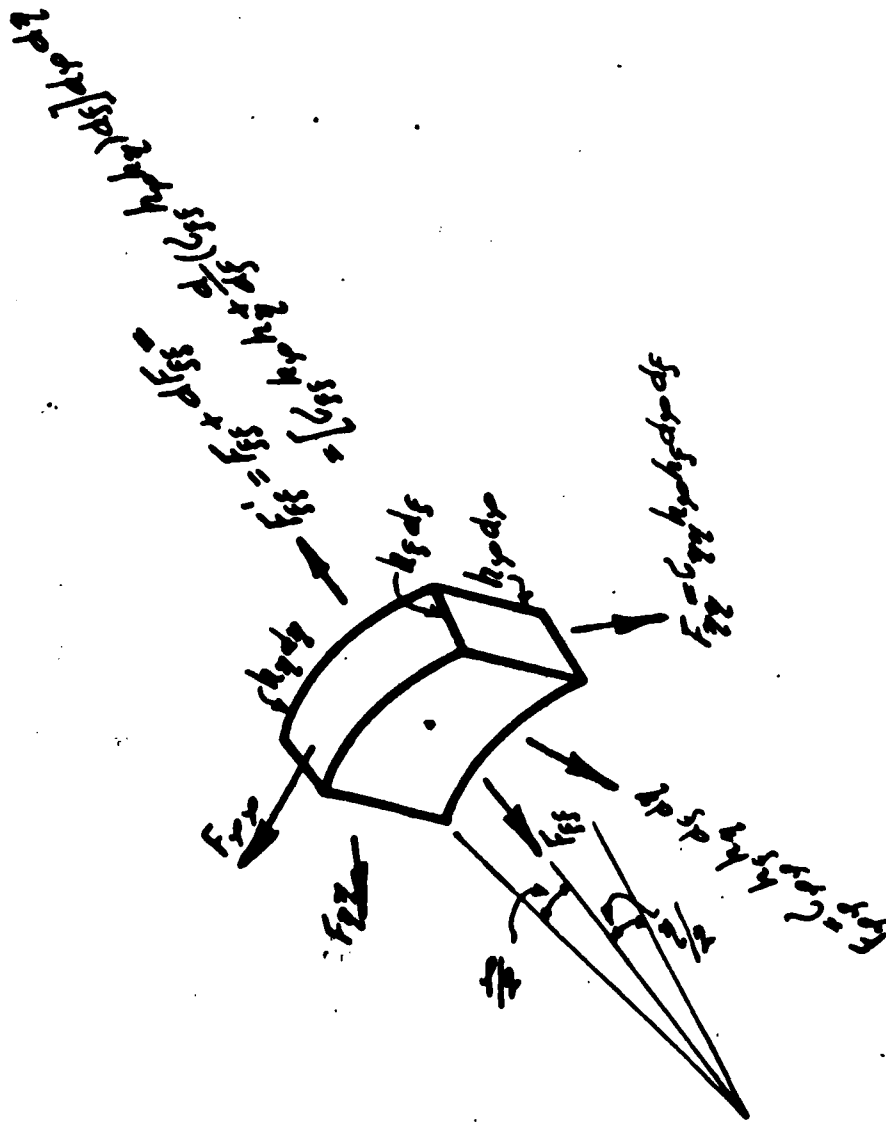


fig. 3: Internal force system acting on a volume element.

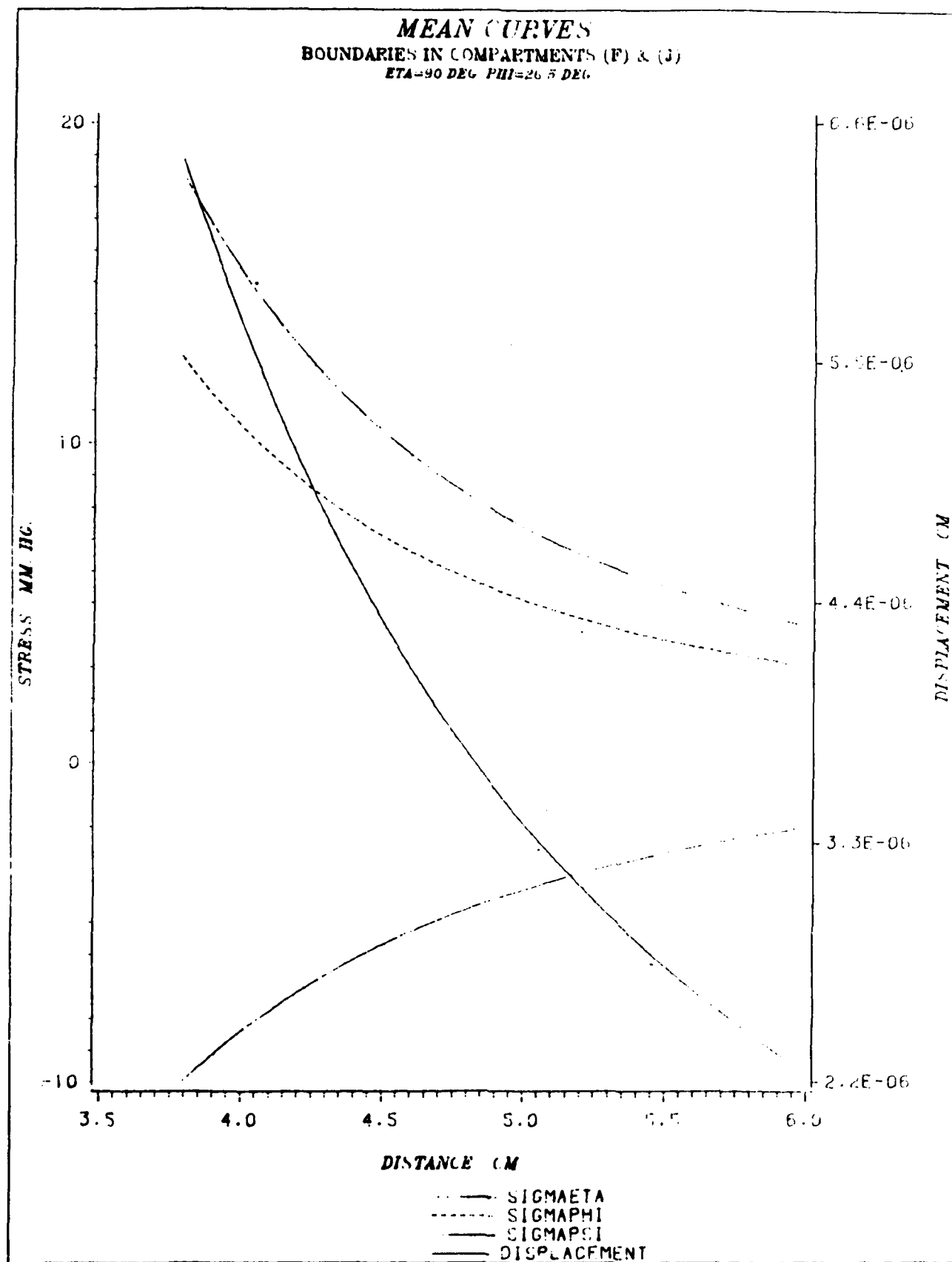
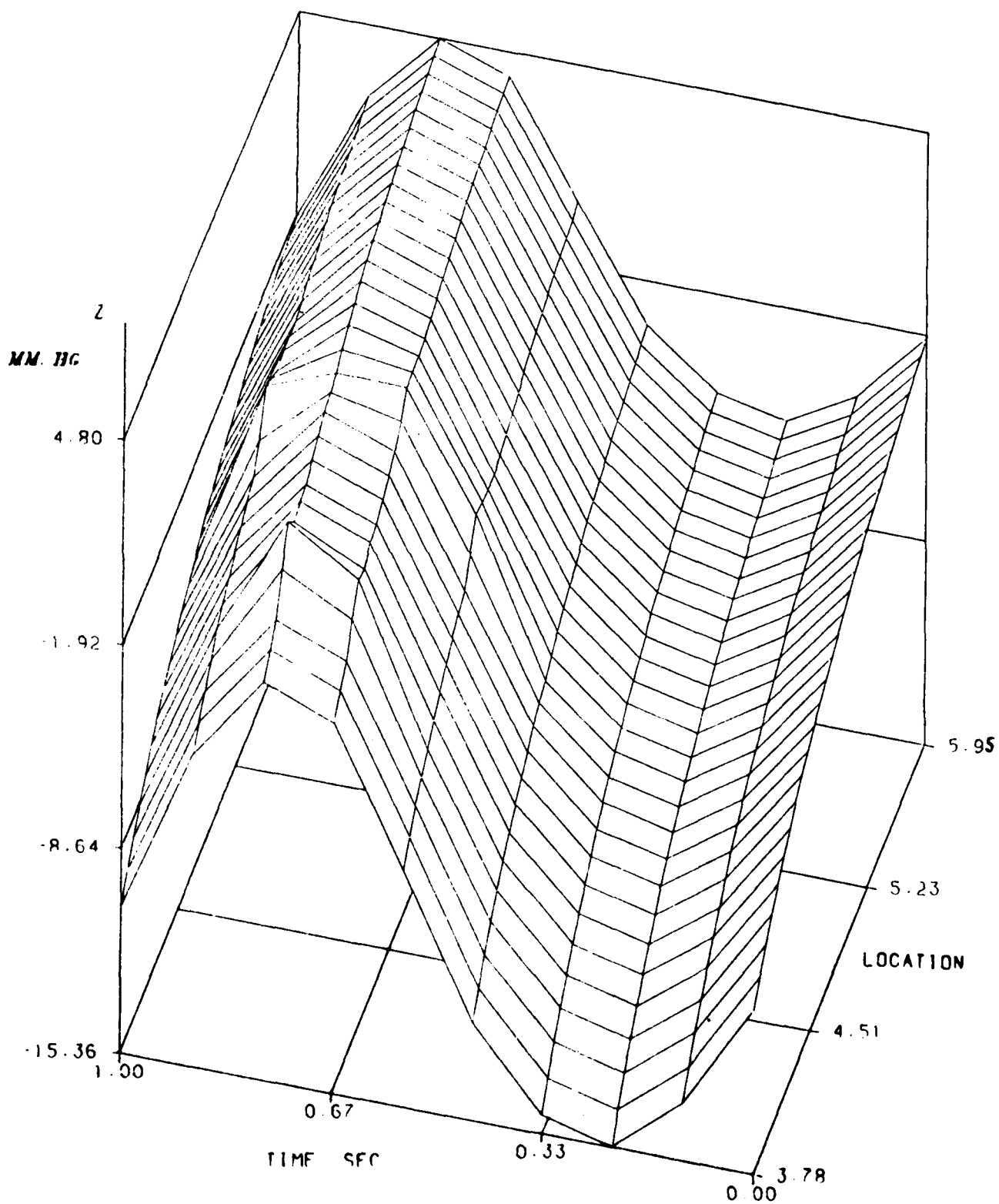
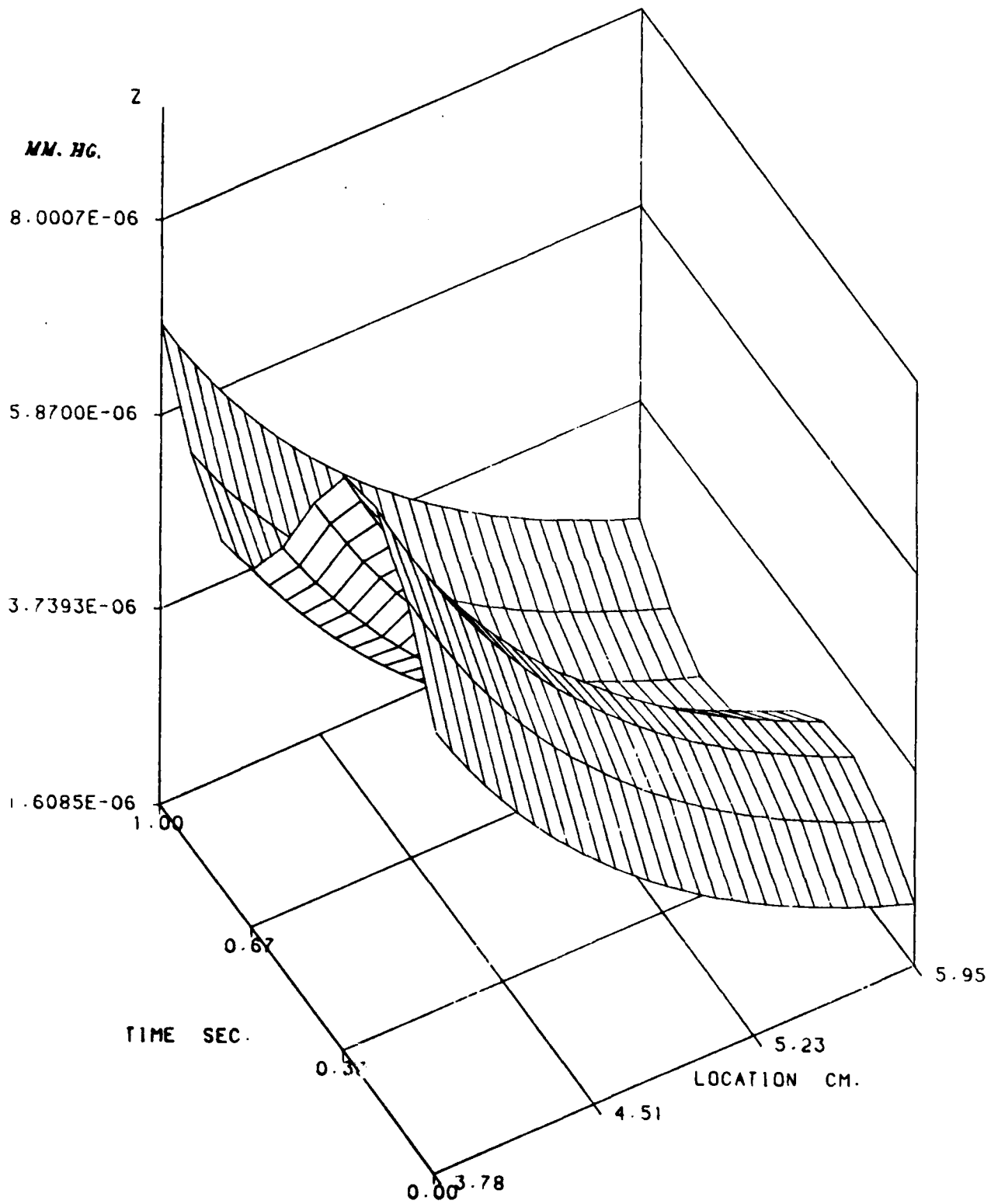


fig. 4.

SIGMAPSI SURFACE**ETA=90 DEG PHI=26 5 DEG****fig. 5.**

DISPLACEMENT SURFACE***BTA=90 DEG. PHI=26.5 DEG.*****fig. 6.**

FILMED
0-8